Signal Processing Using Frequency Domain Methods in Clifford Algebra

Master Thesis

Cognitive Systems Group
Institute of Computer Science
and Applied Mathematics
Christian–Albrechts–University of Kiel

Proposed by
Michael Felsberg (227605)

Supervisor: Thomas Bülow

October 5, 1998

Abstract

The aim of this Master Thesis is to extend the classical concepts of the Fourier transform and the cross correlation in order to create an intrinsic multi–dimensional signal analysis which is more flexible with regard to distortions. Frequency domain methods and pattern matching are two signal–theoretic approaches which are frequently applied in computer vision. By comparing one–dimensional signal processing with multi–dimensional signal theory new problems and requirements arise. Therefore, Lie groups and Clifford algebras are introduced in order to obtain new representations of signals in the frequency domain and more efficient possibilities for comparing signals. Special consideration was given to the aspects of invariance and parameter estimation. This thesis finally raises issues for future research in the field of local approaches and new spectral representations.

Contents

Acknowledgements

I am grateful to all those who contributed to this Master thesis, to my professors, especially Gerald Sommer, and other professionals who have taken the time to answer questions and forced me to ask new ones.

I particularly appreciate the professional wisdom and assistance of Thomas Bülow, the language skills of Chris Brylla and Jürgen Jonietz who helped with the final reading and after all the encouragement and moral support by my fiancée Regina Kohl.

Chapter 1

Introduction

Classical approaches in computer vision distinguish between non–linear and linear concepts. This thesis only deals with linear concepts, which comprise the Fourier transform and convolution. However, the set of linearly solvable problems is extended by these new methods, in order to cover problems which were formerly solvable only by non–linear methods.

The Fourier transform yields the spectral representation of a signal. Since frequency domain methods offer powerful possibilities for manipulating, steering and identifying signals, they belong to the most important approaches in signal processing. Therefore, one issue of investigation has been the development of fast algorithms for numerically calculating the spectrum of a signal. The best known fast Fourier transform (FFT) is the algorithm of Cooley and Tuckey (see e.g. [Bra86]).

The manipulation, steering and identification of signals can also be performed by convolutions in the spatial domain. Consequently, both concepts (the Fourier transform and the convolution) are closely related by the convolution theorem and for each application the most appropriate method can be chosen.

From a stochastical point of view, two signals are considered to be the more similar the more they correlate. In the case of stationary, ergodic signals, the cross correlation of two signals can be calculated by their convolution[1]. The systematical evaluation of the cross correlation of an unknown signal with patterns from a data base is usually referred to as *pattern matching*.

The described classical approaches behave disadvantageously with regard to specifically multi–dimensional properties and distortions in the signals. So far, the classical complex–valued Fourier transform is used exclusively to obtain the spectrum of a multi–dimensional

[1]They differ in that one signal is mirrored before the calculation.

signal. Since a complex number contains only one phase, the correspondence between the symmetry of a signal and the symmetry of its representation in the spectral domain gets worse with increasing dimension. Consequently, the Hermit theorem (the spectrum of a real, one–dimensional signal is Hermit symmetric) cannot be extended to higher dimensions in a straightforward way.

Besides the classical Fourier transform based on complex numbers there are also the quaternionic Fourier transform and its generalised version, the Clifford Fourier transform. The second chapter, therefore, deals with the generalisation of the classical Fourier transform based on complex numbers and derive the definition of the Clifford Fourier transform (CFT). In the two–dimensional case, the CFT yields the quaternionic Fourier transform (QFT) which has been developed independently by T. A. Ell and T. Bülow [Ell92, BS97a]. The QFT transforms a two–dimensional signal (e.g. an image) into a quaternionic frequency domain. This transform makes it possible to separate four cases of symmetry in the signal instead of just two, as in a complex frequency domain. T. Bülow has generalised several approaches[2] for the QFT [BS97b].

The Clifford Fourier transform (CFT) calculates the Clifford valued spectrum of a multi–dimensional signal, which is based on the proper Clifford algebra. Consequently, all cases of symmetry are covered by this transform because the algebra contains enough involutions. Furthermore, an arbitrary shifting of the signal yields a linear phase vector (CFT shift theorem). Besides these (first order) phases additional phase–terms can be defined which contain further information. Apart from the shift theorem, the convolution theorem is also stated and proved.

Based on some algorithms of V. M. Chernov [Che95] which use quaternions for calculating the complex–valued Fourier transform and based on the fast quaternionic Fourier transform [Fel97] a fast Clifford Fourier transform (FCFT) for arbitrary dimension is derived.

However, this derivation can only be formulated in a commutative algebra. Since Clifford algebras are not commutative in general, it is necessary to find a different, commutative algebra which can substitute the former. The transform formulated in the new algebra must produce the same coefficients as the original Clifford Fourier transform. Therefore, an algebra which satisfies the previous constraint for real signals is formulated. The restriction to real signals is irrelevant because of the possibility to compute spectra for Clifford signals in a component–wise fashion.

[2]in particular, instantaneous and local phase, shift theorem, convolution theorem, analytic signal, and Gabor–filters

During the investigation of the algebraical properties of the commutative algebra (which is isomorphic to the $\mathbb{C}^m$) it became obvious that the Clifford spectrum can be calculated from the complex spectrum. Consequently, every fast algorithm for the complex spectrum yields a fast algorithm for the corresponding Clifford spectrum and, in addition, the latter can be calculated with the same asymptotic complexity.

To sum up, the second chapter contains all the definitions and derivations above and is concluded by a consideration of the complexities of all presented algorithms.

In chapter three, a systematic derivation of an invariant (under some group operation) integral transform is described. Such a transform makes it possible to identify the spectrum of a signal which has been distorted by a known group. New possibilities for steering and filtering also arise, however, these are out of the scope of this thesis.

As already mentioned above, the shifting of a signal yields a linear phase in its spectrum. Rubinstein, Segman and Zeevi generalised this property (which is often referred to as *strong invariance*) by a group theoretical approach [RSZ91]. They introduced a derivation of integral transforms so that instead of translations every commutative group of transformations corresponds to a linear phase in the spectrum.

The kernel of the aspired transform can be derived systematically utilising the Lie group theory (which is introduced in chapter three), because the Lie algebra of the considered group induces a canonical coordinate transform. The sequential execution of the canonical transform and the Clifford Fourier transform yields the invariant integral transform. This general approach is illustrated by some examples and experiments which show that the resulting transform satisfies the former condition of strong invariance. The latter is fulfilled even if the signal has been distorted by a mapping which is only locally similar to the group.

In the fourth chapter, the classical concept of pattern matching is resumed. If signals (distorted by a known group) are to be identified, the following method has been used in classical pattern matching so far: the patterns in the data base are transformed by the considered group for some specific parameters (sampling of the parameter space). Subsequently, the unknown signal is cross correlated with every instance of each pattern. The over–all maximum indicates the best matching pattern and the parameter of the instance is the estimated parameter of the distortion.

Instead, by application of the Lie theory it is possible to obtain a much more elegant approach which is less time and memory consuming. Just as the Fourier transform, the cross correlation can be combined with the approach of canonical coordinates. This method has already been suggested by Segman and Zeevi but they have not considered it in more detail [SZ93].

The latter concept is referred to as *cross group correlation* in this thesis. A generalised correlation theorem is stated and proved; the theoretical results are verified by experiments.

The stability of the cross (group) correlation can be enhanced by introducing the approach of *phase only matched filtering* (POMF [HG84]). A further advantage of this method is that, in addition, the results become more noise resistant. Consequently, signals distorted by arbitrary group operations can be compared and the parameters of the distortions can be extracted reliably. Corresponding experiments underpin the applicability of the proposed concept. Furthermore, symmetrical phase only matched filtering is compared to its non–symmetrical instance.

To end this chapter, the parameter space of the cross (group) correlation is extended to higher dimensions. This extension makes it possible to compare two signals which are distorted by non–commutative groups. In addition, the number of parameters can be higher than the dimension of the signal.

A correlation theorem for this double parametric cross group correlation is stated and proved. In this theorem, a signal independent term appears which shows some interesting properties: a) by use of this term it becomes possible to obtain the spectrum of a signal directly from its own invariant spectrum; b) the Fourier transform of this term yields the characteristic function of the monge patch of the canonical coordinate transform. Experiments illustrate the theoretical results.

To conclude, the fifth chapter once again reviews all the results as well as the chosen solutions and approaches. The critical discussion of the limitations and inadequacies of the presented methods leads to suggestions for further development.

Chapter 2

Multidimensional Signal Analysis

In this chapter, the algebraic and algorithmetic bases which are needed for an intrinsic multidimensional signal analysis are presented.

To begin with, the generalisation of complex numbers, the hyper–complex numbers and some special algebras namely the Clifford algebras and the corresponding commutative hyper–complex algebras which are isomorphic to the $\mathbb{C}^m$ for fitting m are introduced.

In the second part the Clifford Fourier Transform and some fundamental theorems are formulated by use of the former terms. Two algorithms are proposed: a fast algorithm which is based on one–dimensional FFTs and an intrinsic fast algorithm which is constructed following the ideas of Cooley and Tuckey.

In the last part of this chapter the possibilities for a further increase of speed of the calculation are considered. Connections between the classical complex Fourier transform and the Clifford Fourier transform are drawn. The complexities of all presented algorithms are estimated and compared.

2.1 Hyper–Complex Algebras

In the following sections the algebraic bases of the Clifford Fourier transform are formulated. We introduce hyper–complex numbers, a specific subset of Clifford algebras (CA) and other, commutative hyper–complex algebras, abbreviated HCA. We prove that CA corresponds to HCA (the meaning of "corresponds" is explained in section 2.1.5), especially for the Fourier kernels. Due to the isomorphism between HCA and the $\mathbb{C}^m$ (which is also proved), we automatically obtain a correspondence between Clifford spectra and Complex spectra which will be utilised in the last part of this chapter.

2.1.1 Hyper–Complex Numbers

In this section hyper–complex numbers are defined. The notation and main theorems are taken from Kantor, chapter 5 ([Sol89]).

Definition 1 (Hyper–Complex numbers) *A hyper–complex number of dimension $n+1$ is an expression of the form*

$$a_0 + a_1 i_1 + a_2 i_2 + \ldots + a_n i_n \tag{2.1}$$

where $a_j \in \mathbb{R}$ for all $j \in \{0, \ldots, n\}$ and i_j ($j \in \{1, \ldots, n\}$) are symbols (often called imaginary units). Two hyper–complex numbers $\boldsymbol{a} = a_0 + a_1 i_1 + \ldots + a_n i_n$ and $\boldsymbol{b} = b_0 + b_1 i_1 + \ldots + b_n i_n$ are equal if and only if $a_j = b_j$ for all $j \in \{0, \ldots, n\}$.

Examples: The complex numbers are hyper–complex numbers of dimension two and quaternions are hyper–complex numbers of dimension four.

Definition 2 (Addition, subtraction, and multiplication) *The addition of two hyper–complex numbers $\boldsymbol{a}$ and $\boldsymbol{b}$ is defined by*

$$\begin{aligned}(a_0 + a_1 i_1 + \ldots + a_n i_n) &+ (b_0 + b_1 i_1 + \ldots + b_n i_n) \\ &= (a_0 + b_0) + (a_1 + b_1) i_1 + \ldots + (a_n + b_n) i_n\end{aligned} \tag{2.2}$$

and their subtraction is defined by

$$\begin{aligned}(a_0 + a_1 i_1 + \ldots + a_n i_n) &- (b_0 + b_1 i_1 + \ldots + b_n i_n) \\ &= (a_0 - b_0) + (a_1 - b_1) i_1 + \ldots + (a_n - b_n) i_n.\end{aligned} \tag{2.3}$$

The multiplication of two hyper–complex numbers is defined by an $n \times n$ multiplication table with the entries

$$i_\alpha i_\beta = p_0^{\alpha\beta} + p_1^{\alpha\beta} i_1 + \ldots + p_n^{\alpha\beta} i_n \tag{2.4}$$

where $\alpha, \beta \in \{1, \ldots, n\}$. The product

$$(a_0 + a_1 i_1 + \ldots + a_n i_n)(b_0 + b_1 i_1 + \ldots + b_n i_n) \tag{2.5}$$

is evaluated by using the distributive law and the multiplication table.

Example: The multiplication table for quaternions is represented in table 2.1.1:

	i	j	k
i	-1	k	$-j$
j	$-k$	-1	i
k	j	$-i$	-1

Table 2.1: Multiplication table for quaternions

A *hyper–complex number system* of dimension n consists of all numbers of the form (2.1) of dimension n and the operations which are defined in (2.2),(2.3), and (2.5).

Theorem 1 (Properties of hyper–complex number systems) *All hyper–complex number systems fulfil the following properties:*

$\mathcal{HC}$*1: The product of a hyper–complex number* $\boldsymbol{b}$ *by a real number* a *is obtained through multiplication of each coefficient of* $\boldsymbol{b}$ *by* a*:*

$$a\boldsymbol{b} = ab_0 + ab_1 i_1 + \ldots + ab_n i_n = \boldsymbol{b}a. \tag{2.6}$$

$\mathcal{HC}$*2: If* $\boldsymbol{u}, \boldsymbol{v}$ *are hyper–complex numbers and* $a, b \in \mathbb{R}$ *then*

$$(a\boldsymbol{u})(b\boldsymbol{v}) = (ab)(\boldsymbol{u}\boldsymbol{v}) \tag{2.7}$$

is satisfied.

$\mathcal{HC}$*3: The left and right distributive laws hold true:*

$$\begin{aligned} \boldsymbol{u}(\boldsymbol{v}+\boldsymbol{w}) &= \boldsymbol{u}\boldsymbol{v} + \boldsymbol{u}\boldsymbol{w} \\ (\boldsymbol{v}+\boldsymbol{w})\boldsymbol{u} &= \boldsymbol{v}\boldsymbol{u} + \boldsymbol{w}\boldsymbol{u} \end{aligned} \tag{2.8}$$

where $\boldsymbol{u}, \boldsymbol{v}, \boldsymbol{w}$ *are hyper–complex numbers.*

Proof:

The theorem is proved by elementary calculations using definition 2.

$\square$

Definition 3 (Commutative, associative, and division systems) *Let* $\boldsymbol{u}, \boldsymbol{v}, \boldsymbol{w}$ *be arbitrary elements of a hyper–complex number system.*

If

$$\boldsymbol{u}\boldsymbol{v} = \boldsymbol{v}\boldsymbol{u} \tag{2.9}$$

holds true, it is called a commutative system*,*

if

$$(\boldsymbol{u}\boldsymbol{v})\boldsymbol{w} = \boldsymbol{u}(\boldsymbol{v}\boldsymbol{w}) \tag{2.10}$$

holds true, it is called an associative system*,*

and if both

$$\boldsymbol{v}\boldsymbol{x} = \boldsymbol{u} \tag{2.11}$$

and

$$\boldsymbol{x}\boldsymbol{v} = \boldsymbol{u} \tag{2.12}$$

have unique solutions $\boldsymbol{x}$*, it is called a* division system*.*

Note that (2.9) is fulfilled if and only if the multiplication table is symmetric about the principal diagonal.

Examples: The complex number system is commutative, associative and a division system; the quaternions are associative and a division system but not commutative.

Note that every hyper–complex number system is an algebra of the same dimension (see [Sol89], chapter 7). Hence, we need not distinguish between hyper–complex number systems and hyper–complex algebras in the sequel.

2.1.2 Clifford Algebras

In contrast to the common way of defining Clifford algebras (e.g. [Por95, GM91]) we do not use a quadratic space which induces the Clifford algebra. The reason for this is that only a subset of all Clifford algebras is needed[1] and the specific properties of all these algebras are clearer if they are defined in a constructive way as it is done below. Similar construction rules are proved to be correct in [GM91]. Note that only this specific subset is considered if the notion Clifford algebra is used in the following.

A Clifford algebra is isomorphic to a special hyper–complex number system. An element c of the 2^n–dimensional Clifford algebra is defined as a 2^n–tuple of real numbers $c := (r_1, \ldots, r_{2^n})$. The first component is called the real part and the other components are called the imaginary parts. Consequently, the algebra contains $2^n - 1$ imaginary units. In contrast to the complex numbers, not all of the imaginary units square to -1, due to the specific construction of Clifford algebras:

- take n imaginary units $i_1, \ldots, i_n$ which square to -1

- create $\sum_{i=1}^{n-1} i = (n-1)\frac{n}{2} = \binom{n}{2}$ different second order units $i_{12}, \ldots, i_{(n-1)n}$ where $i_{ab} = i_a i_b = -i_b i_a$ (anti–commutative, $a \neq b$)

- create $\binom{n}{m}$ different units of order $m = 3 \ldots n$ by multiplying one unit of order $m-1$ by one of order 1

- this procedure yields $\sum_{m=1}^{n} \binom{n}{m} = 2^n - 1$ imaginary units and the square of each unit can easily be calculated by using $i_1^2 = \ldots = i_n^2 = -1$ and the rule $i_a i_b = -i_b i_a$ ($a \neq b$).

Example: In table 2.2 the multiplication table obtained by these rules is calculated for the case $n = 3$.

Obviously, the Clifford algebra is not commutative in general, but associative (due to its construction rules). In the case of $n = 0, 1, 2$ (real numbers, complex numbers, quaternions) the Clifford algebra is a division algebra. In the sequel, Clifford algebra will be referred to as CA.

[1] The specific property of the considered Clifford algebras is that their corresponding n–dimensional vector space has an Euclidean inner product.

	1	i_1	i_2	i_3	i_{23}	i_{13}	i_{12}	i_{123}
1	1	i_1	i_2	i_3	i_{23}	i_{13}	i_{12}	i_{123}
i_1	i_1	-1	i_{12}	i_{13}	i_{123}	$-i_3$	$-i_2$	$-i_{23}$
i_2	i_2	$-i_{12}$	-1	i_{23}	$-i_3$	$-i_{123}$	i_1	i_{13}
i_3	i_3	$-i_{13}$	$-i_{23}$	-1	i_2	i_1	i_{123}	$-i_{12}$
i_{23}	i_{23}	i_{123}	i_3	$-i_2$	-1	$-i_{12}$	i_{13}	$-i_1$
i_{13}	i_{13}	i_3	$-i_{123}$	$-i_1$	i_{12}	-1	$-i_{23}$	i_2
i_{12}	i_{12}	i_2	$-i_1$	i_{123}	$-i_{13}$	i_{23}	-1	$-i_3$
i_{123}	i_{123}	$-i_{23}$	i_{13}	$-i_{12}$	$-i_1$	i_2	$-i_3$	1

Table 2.2: Multiplication table of the eight–dimensional Clifford algebra

2.1.3 Commutative Hyper–Complex Algebras

In this section, a new algebra is introduced which is very similar to the Clifford algebra. The aim is to construct an algebra which a) is commutative and b) has an isomorphic 2^n–dimensional vector space to that of the CA. Further demands are put on the product which has to be identical for sorted imaginary units. The reason for this specification will be explained in section 2.2.

The idea of a commutative algebra is not unknown in mathematics, e.g., T. A. Ell used this possibility to simplify some theorems in his Phd. thesis [Ell92].

In order to create such an algebra the construction rules of CA are slightly modified:

- take n imaginary units $i_1, \ldots, i_n$ which square to -1
- create $\sum_{i=1}^{n-1} i = (n-1)\frac{n}{2} = \binom{n}{2}$ different second order units $i_{12}, \ldots, i_{(n-1)n}$ where $i_{ab} = i_a i_b = i_b i_a$ (commutative, $a \neq b$)
- create $\binom{n}{m}$ different units of order $m = 3 \ldots n$ by multiplying one unit of order $m-1$ by one of order 1
- this procedure yields $\sum_{m=1}^{n} \binom{n}{m} = 2^n - 1$ imaginary units and the square of each unit can easily be calculated by using $i_1^2 = \ldots = i_n^2 = -1$ and the rule $i_a i_b = i_b i_a$ $(a \neq b)$.

Example: In table 2.3 the multiplication table obtained by these rules is calculated for the case $n = 3$. Note the similarity to table 2.2.

The algebra created by these rules is abbreviated by *HCA* in the sequel. It is a commutative and associative hyper–complex algebra with no division defined on it for $n \geq 2$.

	1	i_1	i_2	i_3	i_{23}	i_{13}	i_{12}	i_{123}
1	1	i_1	i_2	i_3	i_{23}	i_{13}	i_{12}	i_{123}
i_1	i_1	-1	i_{12}	i_{13}	i_{123}	$-i_3$	$-i_2$	$-i_{23}$
i_2	i_2	i_{12}	-1	i_{23}	$-i_3$	i_{123}	$-i_1$	$-i_{13}$
i_3	i_3	i_{13}	i_{23}	-1	$-i_2$	$-i_1$	i_{123}	$-i_{12}$
i_{23}	i_{23}	i_{123}	$-i_3$	$-i_2$	1	$-i_{12}$	$-i_{13}$	i_1
i_{13}	i_{13}	$-i_3$	i_{123}	$-i_1$	$-i_{12}$	1	$-i_{23}$	i_2
i_{12}	i_{12}	$-i_2$	$-i_1$	i_{123}	$-i_{13}$	$-i_{23}$	1	i_3
i_{123}	i_{123}	$-i_{23}$	$-i_{13}$	$-i_{12}$	i_1	i_2	i_3	-1

Table 2.3: Multiplication table of the eight–dimensional commutative algebra

The only way to define a division is to restrict the divisor on a subalgebra. Consider, for example, the four–dimensional HCA. Let i_1, i_2, i_{12} be the imaginary units. Then, the equation

$$(1 + i_{12})x = 2 + 2i_{12} \tag{2.13}$$

has more than one solution for x, e.g. $x = 2$ or $x = 1 + i_{12}$. This is a general problem if there are imaginary units which square to $+1$. In the eight–dimensional CA the same problem occurs if we want to solve

$$(1 + i_{123})x = 2 + 2i_{123}. \tag{2.14}$$

Considering the Clifford Fourier transform (see section 2.2), there is no problem concerning the division, because we only multiply by factors which do not have imaginary parts of higher order than one — each kernel factor is the element of a subalgebra of CA/HCA isomorphic to the complex numbers. In order to treat this subject more in detail let k be an arbitrary element of HCA, $w = a + bi_j$ and $w^* = a - bi_j$ for an arbitrary $j \in 1, \ldots, n$ and $a^2 + b^2 = 1$. The following equation is fulfilled

$$(kw)w^* \stackrel{associativity}{=} k(ww^*) = k. \tag{2.15}$$

This equation only holds true since w^* and w are elements of a subalgebra isomorphic to the complex numbers. Consequently, it is not necessary to have a division algebra in order to obtain an arbitrary algebra element from a product with such a restricted element. This informal argumentation can be treated as the sketch of a proof.

2.1.4 Isomorphism between HCA and $\mathbb{C}^m$

C. M. Davenport proposed in [Dav96] that the HCA of dimension four is isomorphic to the ring $\mathbb{C}^2$. In this section we elaborate an isomorphism for 2^n–dimensional HCAs.

Theorem 2 (Isomorphism between HCA and $\mathbb{C}^m$) *The 2^n–dimensional HCA is isomorphic to $\mathbb{C}^{2^{n-1}}$. Let k be an arbitrary element of the 2^n–dimensional HCA and let $z_1, \ldots, z_{2^{n-1}}$ be the representation of k in $\mathbb{C}^{2^{n-1}}$. Then, the isomorphism is denoted as*

$$\begin{aligned} \boldsymbol{\eta}(k) &= (z_1, \ldots, z_{2^{n-1}}) \qquad \textit{with} \\ z_i &= \eta_i(k). \end{aligned} \tag{2.16}$$

Proof:

In order to construct the isomorphism, we inductively define a matrix representation of the HCA of dimension 2^n. For the sake of short writing, the indices are sometimes denoted as sets in the sequel (e.g. $i_{123} = i_{\{1,2,3\}}$). In addition, let $\mathcal{P}(M)$ be the set of all subsets of M in the following. An arbitrary element of the HCA of dimension 2^n is denoted $k = \sum_{j \in \mathcal{P}(\{1,\ldots,n\})} k_j i_j$, where $k_j i_j$ is the real part if $j = \emptyset$.

Consider the two matrices

$$X(A) = \begin{bmatrix} A & 0 \\ 0 & A \end{bmatrix} \qquad \text{and} \qquad Y(A) = \begin{bmatrix} 0 & -A \\ A & 0 \end{bmatrix} \tag{2.17}$$

where A is an arbitrary $m \times m$ matrix ($m \geq 1$). Utilising these two matrices, we can construct matrix representations for the imaginary units of every HCA:

1. $n = 1$: (Complex numbers $k_\emptyset 1 + k_1 i_1$) Let be $A = 1$ then we get $1 \to X(1) = A_\emptyset$ and $i_1 \to Y(1) = A_1$.

2. $n = 2$: (Like in [Dav96] $k_\emptyset 1 + k_1 i_1 + k_2 i_2 + k_{12} i_{12}$) We have $A'_\emptyset$ and A'_1 from the first step. If $A = A'_\emptyset$ we obtain $1 \to X(A'_\emptyset) = A_\emptyset$ and $i_2 \to Y(A'_\emptyset) = A_2$ and if $A = A'_1$ we get $i_1 \to X(A'_1) = A_1$ and $i_{12} \to Y(A'_1) = A_{12}$.

3. $n > 2$: We have 2^{n-1} matrices $A'_1, \ldots, A'_{1\ldots n}$ from the step $n-1$ and we create for each of those matrices A'_j, $j \in \mathcal{P}(\{1, \ldots, n-1\})$ two matrices $A_j = X(A'_j)$ and $A_{j\cup\{n\}} = Y(A'_j)$ so that $i_j \to X(A'_j)$ and $i_{j\cup\{n\}} \to Y(A'_j)$.

So far, we have constructed a vector space isomorphism from HCA onto the vector space spanned by the matrices A_j, denoted as $\chi : \text{HCA} \longrightarrow K \subseteq Gl(2^n, \mathbb{R})$. In order to prove that this mapping is an algebra isomorphism, we still have to show that

$$\chi(i_{j_1} i_{j_2}) = \chi(i_{j_1})\chi(i_{j_2}) \qquad \text{with } i_{j_1}, i_{j_2} \in \mathcal{P}(\{1, \ldots, n\}). \tag{2.18}$$

We prove this by induction over n. In order to distinguish between the isomorphisms, they are indicated by their dimension.

IB: Let be $n = 1$. The matrix representation of complex numbers reads $\chi^1(1) = X(1)$ and $\chi^1(i) = Y(1)$ and we have $\chi^1(1)\chi^1(i) = X(1)Y(1) = Y(1)X(1) = Y(1) = \chi^1(i)$, $\chi^1(i)\chi^1(i) = Y(1)Y(1) = -X(1) = \chi^1(i^2)$ and $\chi^1(1)\chi^1(1) = X(1)X(1) = X(1) = \chi^1(1)$.

IS: Let be $n > 1$. The induction assumption reads:

$$\chi^{n-1}(i_{j_1} i_{j_2}) = \chi^{n-1}(i_{j_1})\chi^{n-1}(i_{j_2}) \tag{2.19}$$

with $i_{j_1}, i_{j_2} \in \mathcal{P}(\{1, \dots, n-1\})$. Consequently, we obtain for the 2^n–dimensional HCA the matrices $\chi^n(i_j) = X(\chi^{n-1}(i_j))$ and $\chi^n(i_{j\cup\{n\}}) = \chi^n(i_j i_{\{n\}}) = Y(\chi^{n-1}(i_j))$ (for all $j \in \mathcal{P}(\{1, \dots, n-1\})$) and their matrix product yields four cases:

$$\begin{aligned}
\chi^n(i_{j_1})\chi^n(i_{j_2}) &= X(\chi^{n-1}(i_{j_1}))X(\chi^{n-1}(i_{j_2})) = X(\chi^{n-1}(i_{j_1})\chi^{n-1}(i_{j_2})) \\
&\overset{(2.19)}{=} X(\chi^{n-1}(i_{j_1} i_{j_2})) = \chi^n(i_{j_1} i_{j_2}) \\
\chi^n(i_{j_1\cup\{n\}})\chi^n(i_{j_2}) &= Y(\chi^{n-1}(i_{j_1}))X(\chi^{n-1}(i_{j_2})) = Y(\chi^{n-1}(i_{j_1})\chi^{n-1}(i_{j_2})) \\
&\overset{(2.19)}{=} Y(\chi^{n-1}(i_{j_1} i_{j_2})) = \chi^n(i_{\{n\}} i_{j_1} i_{j_2}) = \chi^n(i_{j_1\cup\{n\}} i_{j_2}) \\
\chi^n(i_{j_1})\chi^n(i_{j_2\cup\{n\}}) &= X(\chi^{n-1}(i_{j_1}))Y(\chi^{n-1}(i_{j_2})) = Y(\chi^{n-1}(i_{j_1})\chi^{n-1}(i_{j_2})) \\
&\overset{(2.19)}{=} Y(\chi^{n-1}(i_{j_1} i_{j_2})) = \chi^n(i_{\{n\}} i_{j_1} i_{j_2}) = \chi^n(i_{j_1} i_{j_2\cup\{n\}}) \\
\chi^n(i_{j_1\cup\{n\}})\chi^n(i_{j_2\cup\{n\}}) &= Y(\chi^{n-1}(i_{j_1}))Y(\chi^{n-1}(i_{j_2})) = -X(\chi^{n-1}(i_{j_1})\chi^{n-1}(i_{j_2})) \\
&\overset{(2.19)}{=} X(-\chi^{n-1}(i_{j_1} i_{j_2})) = \chi^n(i_{\{n\}}^2 i_{j_1} i_{j_2}) = \chi^n(i_{j_1\cup\{n\}} i_{j_2\cup\{n\}})
\end{aligned} \tag{2.20}$$

Consequently, equation (2.18) is satisfied.

Now, we must proof that $\mathbb{C}^m$ is isomorphic to K. However, since this isomorphism is obtained by an eigenvalue transform of K, we only have to prove the existance of a method (with constant coefficients) which transforms a matrix of K into a diagonal matrix. Since the elements of K consist of block–matrices of the form $X(A)$ and $Y(A)$, we only need to state matrices which transform $Y(A)$ into a block–diagonal form:

$$\frac{1}{2}\begin{bmatrix} \mathrm{Id} & -i_1\,\mathrm{Id} \\ \mathrm{Id} & i_1\,\mathrm{Id} \end{bmatrix} \begin{bmatrix} 0 & -A \\ A & 0 \end{bmatrix} \begin{bmatrix} \mathrm{Id} & \mathrm{Id} \\ i_1\,\mathrm{Id} & -i_1\,\mathrm{Id} \end{bmatrix} = \begin{bmatrix} -i_1 A & 0 \\ 0 & i_1 A \end{bmatrix} \tag{2.21}$$

The remaining transforms follow by induction and the successive application of them yields a method for obtaining the diagonal matrix. Consequently, the components of the isomorphism $\eta_1 \dots \eta_{2^{n-1}}$ (and their conjugates $\eta_1^* \dots \eta_{2^{n-1}}^*$) are obtained by calculating the eigenvalues of the matrix representation of a general HCA element.

□

Example: The isomorphisms for $n = 1, 2, 3$ is constructed. For $n = 1$ the isomorphism is trivial. We have $A_\emptyset = \begin{bmatrix} 1 & 0 \\ 0 & 1 \end{bmatrix}$ and $A_1 = \begin{bmatrix} 0 & -1 \\ 1 & 0 \end{bmatrix}$. Consequently, a general complex number is represented by $\begin{bmatrix} k_\emptyset & -k_1 \\ k_1 & k_\emptyset \end{bmatrix}$ and the eigenvalues are $\eta_1 = k_\emptyset \pm i_1 k_1$.

For $n = 2$ we have

$$A_\emptyset = \begin{bmatrix} 1 & 0 & 0 & 0 \\ 0 & 1 & 0 & 0 \\ 0 & 0 & 1 & 0 \\ 0 & 0 & 0 & 1 \end{bmatrix} A_1 = \begin{bmatrix} 0 & -1 & 0 & 0 \\ 1 & 0 & 0 & 0 \\ 0 & 0 & 0 & -1 \\ 0 & 0 & 1 & 0 \end{bmatrix} A_2 = \begin{bmatrix} 0 & 0 & -1 & 0 \\ 0 & 0 & 0 & -1 \\ 1 & 0 & 0 & 0 \\ 0 & 1 & 0 & 0 \end{bmatrix} A_{12} = \begin{bmatrix} 0 & 0 & 0 & 1 \\ 0 & 0 & -1 & 0 \\ 0 & -1 & 0 & 0 \\ 1 & 0 & 0 & 0 \end{bmatrix} \tag{2.22}$$

and a general HCA element is represented by

$$\begin{bmatrix} k_\emptyset & -k_1 & -k_2 & k_{12} \\ k_1 & k_\emptyset & -k_{12} & -k_2 \\ k_2 & -k_{12} & k_\emptyset & -k_1 \\ k_{12} & k_2 & k_1 & k_\emptyset \end{bmatrix}. \tag{2.23}$$

The eigenvalues and eigenvectors read

$$\begin{aligned} \eta_1 &= (k_\emptyset - k_{12}) + i_1(k_1 + k_2) \\ \eta_1^* &= (k_\emptyset - k_{12}) - i_1(k_1 + k_2) \\ \eta_2 &= (k_\emptyset + k_{12}) + i_1(k_1 - k_2) \\ \eta_2^* &= (k_\emptyset + k_{12}) - i_1(k_1 - k_2) \qquad \text{and} \end{aligned}$$
$$\boldsymbol{e}_1 = \begin{bmatrix} 1 \\ -i_1 \\ -i_1 \\ -1 \end{bmatrix} \quad \boldsymbol{e}_2 = \begin{bmatrix} 1 \\ i_1 \\ i_1 \\ -1 \end{bmatrix} \quad \boldsymbol{e}_3 = \begin{bmatrix} 1 \\ -i_1 \\ i_1 \\ 1 \end{bmatrix} \quad \boldsymbol{e}_4 = \begin{bmatrix} 1 \\ i_1 \\ -i_1 \\ 1 \end{bmatrix} \tag{2.24}$$

respectively and we obtain

$$\begin{bmatrix} k_\emptyset \\ k_1 \\ k_2 \\ k_{12} \end{bmatrix} = \frac{1}{4} \begin{bmatrix} \boldsymbol{e}_1 & \boldsymbol{e}_2 & \boldsymbol{e}_3 & \boldsymbol{e}_4 \end{bmatrix} \begin{bmatrix} \eta_1 \\ \eta_1^* \\ \eta_2 \\ \eta_2^* \end{bmatrix} \tag{2.25}$$

or $k = \eta_1 \frac{1-i_{12}}{2} + \eta_2 \frac{1+i_{12}}{2}$.

For $n = 3$ we only state the eigenvalues and eigenvectors:

$$\eta_1 = (k_\emptyset - k_{12} - k_{13} - k_{23}) + i_1(k_1 + k_2 + k_3 - k_{123})$$
$$\eta_2 = (k_\emptyset - k_{12} + k_{13} + k_{23}) + i_1(k_1 + k_2 - k_3 + k_{123})$$
$$\eta_3 = (k_\emptyset + k_{12} - k_{13} + k_{23}) + i_1(k_1 - k_2 + k_3 + k_{123})$$
$$\eta_4 = (k_\emptyset + k_{12} + k_{13} - k_{23}) + i_1(k_1 - k_2 - k_3 - k_{123})$$

$$\boldsymbol{e}_1 = \begin{bmatrix} 1 \\ -i_1 \\ -i_1 \\ -1 \\ -i_1 \\ -1 \\ -1 \\ i_1 \end{bmatrix} \quad \boldsymbol{e}_2 = \begin{bmatrix} 1 \\ i_1 \\ i_1 \\ -1 \\ i_1 \\ -1 \\ -1 \\ -i_1 \end{bmatrix} \quad \boldsymbol{e}_3 = \begin{bmatrix} 1 \\ -i_1 \\ -i_1 \\ -1 \\ i_1 \\ 1 \\ 1 \\ -i_1 \end{bmatrix} \quad \boldsymbol{e}_4 = \begin{bmatrix} 1 \\ i_1 \\ i_1 \\ -1 \\ -i_1 \\ 1 \\ 1 \\ i_1 \end{bmatrix}$$
$$\boldsymbol{e}_5 = \begin{bmatrix} 1 \\ -i_1 \\ i_1 \\ 1 \\ -i_1 \\ -1 \\ 1 \\ -i_1 \end{bmatrix} \quad \boldsymbol{e}_6 = \begin{bmatrix} 1 \\ i_1 \\ -i_1 \\ 1 \\ i_1 \\ -1 \\ 1 \\ i_1 \end{bmatrix} \quad \boldsymbol{e}_7 = \begin{bmatrix} 1 \\ -i_1 \\ i_1 \\ 1 \\ i_1 \\ 1 \\ -1 \\ i_1 \end{bmatrix} \quad \boldsymbol{e}_8 = \begin{bmatrix} 1 \\ i_1 \\ -i_1 \\ 1 \\ -i_1 \\ 1 \\ -1 \\ -i_1 \end{bmatrix} \tag{2.26}$$

The original HCA element is obtained by

$$\begin{bmatrix} k_\emptyset \\ k_1 \\ k_2 \\ k_{12} \\ k_3 \\ k_{13} \\ k_{23} \\ k_{123} \end{bmatrix} = \frac{1}{8} \begin{bmatrix} \boldsymbol{e}_1 & \boldsymbol{e}_2 & \boldsymbol{e}_3 & \boldsymbol{e}_4 & \boldsymbol{e}_5 & \boldsymbol{e}_6 & \boldsymbol{e}_7 & \boldsymbol{e}_8 \end{bmatrix} \begin{bmatrix} \eta_1 \\ \eta_1^* \\ \eta_2 \\ \eta_2^* \\ \eta_3 \\ \eta_3^* \\ \eta_4 \\ \eta_4^* \end{bmatrix} . \tag{2.27}$$

Note that the order of the components is given by the positions of the non–zero entries in the first column of the matrix representation of the imaginary units (e.g., we find the non–zero entry of $A_3 \begin{bmatrix} 1 & 0 & 0 & 0 & 0 & 0 & 0 & 0 \end{bmatrix}^T$ at the fifth position). In the sequel, we set $m = 2^{n-1}$ if we refer to $\mathbb{C}^m$ as the isomorphic algebra of HCA (of dimension 2^n).

2.1.5 Main Theorems

For the sake of short writing the indices are sometimes denoted as sets in this section (e.g. $i_{123} = i_{\{1,2,3\}}$). Additionally, let $\mathcal{P}(M)$ be the set of all subsets of M in the following.

Consider the division problem on page 15 again. Let v be an arbitrary algebra element and let w be an element isomorphic to a complex number with magnitude 1.0. The inverse of the multiplication of v by w is obtained from the multiplication of v by the conjugate of w in which the conjugate is derived as in the complex number system. This negation of the first order imaginary units induces $2^n - 1$ non trivial mappings:

Definition 4 (α–mappings of HCA) *Let $k = \sum_{j\in\mathcal{P}(\{1,\dots,n\})} k_j i_j$ be an arbitrary element of the HCA, where $k_j i_j$ is the real part if $j = \emptyset$. The $2^n - 1$ α–mappings are defined by:*

$$
\begin{aligned}
\alpha_1(k) &= \sum_{j\in\mathcal{P}(\{2,\dots,n\})} k_j i_j - \sum_{j\in\mathcal{P}(\{2,\dots,n\})} k_{\{1\}\cup j} i_{\{1\}\cup j}\\
&\vdots\\
\alpha_n(k) &= \sum_{j\in\mathcal{P}(\{1,\dots,n-1\})} k_j i_j - \sum_{j\in\mathcal{P}(\{1,\dots,n-1\})} k_{\{n\}\cup j} i_{\{n\}\cup j}\\
\alpha_{12}(k) &= \alpha_1(\alpha_2(k))\\
&\vdots\\
\alpha_{1\dots n}(k) &= \alpha_1(\dots(\alpha_n(k))\dots)
\end{aligned}
\tag{2.28}
$$

In order to clarify the meaning of this definition two examples are considered. Firstly, let $n = 1$ (complex numbers). Using the notion introduced in the preceeding definition, we denote an arbitrary complex number $k = k_\emptyset + i_1 k_1$ and we obtain one mapping $\alpha_1(k) = k_\emptyset - i_1 k_1$ which is the non trivial involution of the complex numbers.

Secondly, consider the case $n = 3$. An arbitrary element is denoted as $k = k_\emptyset + i_1k_1 + i_2k_2 + i_3k_3 + i_{12}k_{12} + i_{13}k_{13} + i_{23}k_{23} + i_{123}k_{123}$. So, there are seven α–mappings:

$$
\begin{aligned}
\alpha_1(k) &= k_\emptyset - i_1k_1 + i_2k_2 + i_3k_3 - i_{12}k_{12} - i_{13}k_{13} + i_{23}k_{23} - i_{123}k_{123}\\
\alpha_2(k) &= k_\emptyset + i_1k_1 - i_2k_2 + i_3k_3 - i_{12}k_{12} + i_{13}k_{13} - i_{23}k_{23} - i_{123}k_{123}\\
\alpha_3(k) &= k_\emptyset + i_1k_1 + i_2k_2 - i_3k_3 + i_{12}k_{12} - i_{13}k_{13} - i_{23}k_{23} - i_{123}k_{123}\\
\alpha_{12}(k) &= k_\emptyset - i_1k_1 - i_2k_2 + i_3k_3 + i_{12}k_{12} - i_{13}k_{13} - i_{23}k_{23} + i_{123}k_{123}\\
\alpha_{13}(k) &= k_\emptyset - i_1k_1 + i_2k_2 - i_3k_3 - i_{12}k_{12} + i_{13}k_{13} - i_{23}k_{23} + i_{123}k_{123}\\
\alpha_{23}(k) &= k_\emptyset + i_1k_1 - i_2k_2 - i_3k_3 - i_{12}k_{12} - i_{13}k_{13} + i_{23}k_{23} + i_{123}k_{123}\\
\alpha_{123}(k) &= k_\emptyset - i_1k_1 - i_2k_2 - i_3k_3 + i_{12}k_{12} + i_{13}k_{13} + i_{23}k_{23} - i_{123}k_{123}
\end{aligned}
\tag{2.29}
$$

Note that the α–mappings obtained from the definition above are the same mappings as the non trivial involutions of the Clifford algebra of the same size.

In the following theorem we prove that the α–mappings are non trivial involutions of the considered algebra:

Theorem 3 (Involutions of HCA) *The mappings $\alpha_1, \ldots, \alpha_{1\ldots n}$ are non trivial involutions of HCA.*

Proof:

To start with, we prove that the α–mappings are automorphisms by showing that for arbitrary k_1, k_2 and $j \in \mathcal{P}(\{1, \ldots, n\}) \setminus \emptyset$ the following equation holds true:

$$\alpha_j(k_1)\alpha_j(k_2) = \alpha_j(k_1 k_2) \tag{2.30}$$

Firstly, let $j \in \{\{1\}, \ldots, \{n\}\}$ (i.e. i_j is of first order). The replacement of the imaginary units of higher order by products of imaginary units of first order simplifies the verification of (2.30). The consideration of an arbitrary component $(k_1 k_2)_l$ of $k_1 k_2$ yields two cases:

1. If i_j is a factor of the imaginary unit of the component $(k_1 k_2)_l$, α_j negates it. This is correct because the component $(k_1 k_2)_l$ is evaluated by a sum of products. Each product consists of one component of k_1 multiplied by one component of k_2. Since i_j appears in the product of two components, either the first or the second factor must contain i_j. Consequently, either the first or the second factor is negated by α_j.

2. The unit i_j is not a factor of the imaginary unit of the component $(k_1 k_2)_l$ and therefore, α_j does not negate it. If we consider the factors in the summation again, two possibilities arise: a) the unit i_j does not appear if both factors contain i_j or b) none of them contains i_j. In the first case, both factors are negated by α_j; in the second case both remain unchanged. In any case the product is not negated.

Consequently, (2.30) is satisfied if $j \in \{\{1\}, \ldots, \{n\}\}$.

Secondly, let i_j be of higher order. Using the definition of the α_j–mappings and the first part of this proof, the remaining proofs simply follow by induction:

$$\alpha_{j_1}(\alpha_{j_2}(k_1))\alpha_{j_1}(\alpha_{j_2}(k_2)) = \alpha_{j_1}(\alpha_{j_2}(k_1)\alpha_{j_2}(k_2)) = \alpha_{j_1}(\alpha_{j_2}(k_1 k_2)). \tag{2.31}$$

So (2.30) is satisfied for all $j \in \mathcal{P}(\{1, \ldots, n\}) \setminus \emptyset$.

Based on the automorphism proof and in order to show that the α–mappings are involutions, we now have to prove that

$$\alpha_j(\alpha_j(k)) = k \qquad \forall j \in \mathcal{P}(\{1,\dots,n\}). \tag{2.32}$$

Firstly, we prove the condition (2.32) for $j \in \{1,\dots,n\}$:

$$\begin{aligned}
\alpha_j(\alpha_j(k)) =& \alpha_j\left(\sum_{l\in\mathcal{P}(\{1,\dots,n\}\setminus\{j\})} k_l i_l - \sum_{l\in\mathcal{P}(\{1,\dots,n\}\setminus\{j\})} k_{\{j\}\cup l} i_{\{j\}\cup l}\right)\\
=& \sum_{l\in\mathcal{P}(\{1,\dots,n\}\setminus\{j\})} k_l i_l - \left(-\sum_{l\in\mathcal{P}(\{1,\dots,n\}\setminus\{j\})} k_{\{j\}\cup l} i_{\{j\}\cup l}\right)\\
=& \sum_{l\in\mathcal{P}(\{1,\dots,n\})} k_l i_l\\
=& k
\end{aligned} \tag{2.33}$$

The other cases simply follow by induction, because the α–mappings are commutative:

$$\alpha_{j_1}(\alpha_{j_2}(\alpha_{j_1}(\alpha_{j_2}(k)))) = \alpha_{j_1}(\alpha_{j_1}(\alpha_{j_2}(\alpha_{j_2}(k)))) = \alpha_{j_2}(\alpha_{j_2}(k)) = k. \tag{2.34}$$

□

The subsequent definition can be used to refer to the components of an HCA element.

Definition 5 (Component selection) *Let* $k = \sum_{j\in\mathcal{P}(\{1,\dots,n\})} k_j i_j$ *be an arbitrary element of HCA. Then, the component selection functions are defined in the following way:*

$$\begin{aligned}
\Re(k) &= k_\emptyset\\
\Im_j(k) &= k_j \qquad \forall j \in \mathcal{P}(\{1,\dots,n\}) \setminus \emptyset
\end{aligned} \tag{2.35}$$

Example: If $n = 1$ definition 5 yields the well known functions which return real and imaginary parts of a complex number respectively.

In order to distinguish between CA and HCA, the imaginary units of the CA are denoted in a different typeface: $\mathfrak{i}_j$ instead of i_j. The correspondence between two terms in CA and HCA is expressed by a linear mapping $\kappa : \mathrm{CA} \longrightarrow \mathrm{HCA}$. The first order imaginary units and the real units correspond accordingly: $\kappa(\mathfrak{i}_j) = i_j$ and $\kappa(1) = 1$. Hence, all products of first order imaginary units with *ascending* index correspond as well ($\kappa(\mathfrak{i}_j\mathfrak{i}_k) = i_j i_k$, $j < k$). An additional correspondence needed in section 2.2 is stated by the following theorem.

Theorem 4 (Kernel correspondence) *Let* $\varphi_j \in \mathbb{R}\ \forall j \in \{1,\dots,n\}$. *Then, the following equation holds true:*

$$\kappa\left(\prod_{j=1}^{n} e^{\mathfrak{i}_j\varphi_j}\right) = e^{\sum_{j=1}^{n} i_j\varphi_j} \tag{2.36}$$

Proof:

The kernel correspondence theorem is proved by induction over n.

IB: Let be $n = 1$. In this case theorem 4 yields

$$\kappa\left(e^{\mathfrak{i}_1\varphi_1}\right) \overset{\kappa \text{ is linear}}{=} \kappa(1)\cos\varphi_1 + \kappa(\mathfrak{i}_1)\sin\varphi_1 = \cos\varphi_1 + i_1\sin\varphi_1 = e^{i_1\varphi_1} \tag{2.37}$$

and, hence equation (2.36) holds true if $n = 1$.

IS: Let be $n > 1$. The induction assumption reads:

$$\kappa\left(\prod_{j=1}^{n-1} e^{\mathfrak{i}_j\varphi_j}\right) = e^{\sum_{j=1}^{n-1} i_j\varphi_j}. \tag{2.38}$$

Assuming that (2.38) holds true we have to show that (2.36) is satisfied likewise.

$$\begin{aligned}
\kappa\left(\prod_{j=1}^{n} e^{\mathfrak{i}_j\varphi_j}\right) &= \kappa\left(\left(\prod_{j=1}^{n-1} e^{\mathfrak{i}_j\varphi_j}\right) e^{\mathfrak{i}_n\varphi_n}\right) \\
&= \kappa\left(\left(\prod_{j=1}^{n-1} e^{\mathfrak{i}_j\varphi_j}\right)\cos\varphi_n\right) + \kappa\left(\left(\prod_{j=1}^{n-1} e^{\mathfrak{i}_j\varphi_j}\right)\mathfrak{i}_n\sin\varphi_n\right) \\
&\overset{(2.38) \text{ and } n>j}{=} \left(e^{\sum_{j=1}^{n-1} i_j\varphi_j}\right)(\cos\varphi_n + i_n\sin\varphi_n) \\
&\overset{\text{commutativity}}{=} e^{\sum_{j=1}^{n} i_j\varphi_j}
\end{aligned} \tag{2.39}$$

Since both the induction beginning and the induction step hold true theorem 4 is proved to be correct.

□

Example: Consider the case $n = 2$. Starting with the quaternionic kernel we obtain the following derivation:

$$\begin{aligned}
\kappa\left(e^{\mathfrak{i}_1\varphi_1}e^{\mathfrak{i}_2\varphi_2}\right) &= \kappa((\cos\varphi_1 + \mathfrak{i}_1\sin\varphi_1)(\cos\varphi_2 + \mathfrak{i}_2\sin\varphi_2)) \\
&= \cos\varphi_1\cos\varphi_2 + \kappa(\mathfrak{i}_1)\sin\varphi_1\cos\varphi_2 + \kappa(\mathfrak{i}_2)\cos\varphi_1\sin\varphi_2 + \kappa(\mathfrak{i}_1\mathfrak{i}_2)\sin\varphi_1\sin\varphi_2 \\
&= \cos\varphi_1\cos\varphi_2 + i_1\sin\varphi_1\cos\varphi_2 + i_2\cos\varphi_1\sin\varphi_2 + i_1 i_2\sin\varphi_1\sin\varphi_2 \\
&= (\cos\varphi_1 + i_1\sin\varphi_1)(\cos\varphi_2 + i_2\sin\varphi_2) \\
&= e^{i_1\varphi_1}e^{i_2\varphi_2} = e^{i_1\varphi_1 + i_2\varphi_2}
\end{aligned} \tag{2.40}$$

2.2 The n–dimensional Clifford Fourier Transform

This section starts with the definition of the n–dimensional Clifford Fourier transform (CFT) which is the generalisation of the quaternionic Fourier transform (QFT) proposed by T. A. Ell and T. Bülow [Ell92, BS97a]. Due to the correspondence of the kernels in CA and HCA the following theorems and algorithms are not based on the Clifford algebra but on the corresponding commutative hyper–complex algebra.

Using the definition of the CFT we adapt the shift theorem and the convolution theorem for it and prove them. This is necessary because we utilise the theorems in the rest of the thesis.

In the following two sub–sections, we propose algorithms for calculating the CFT numerically. The first one uses cascaded one–dimensional FFTs to calculate the Clifford spectrum and the second one is the systematical extension of the radix 2 algorithm of Cooley and Tuckey.

2.2.1 Transform and Inverse Transform

We begin with the definition of the Clifford Fourier transform.

Definition 6 (Clifford Fourier transform) *The Clifford Fourier transform $V(\boldsymbol{u})$ of an n–dimensional signal $v(\boldsymbol{x})$ is defined by*

$$V(\boldsymbol{u}) = \int_{\mathbb{R}^n} v(\boldsymbol{x}) \prod_{j=1}^{n} e^{-\mathrm{i}_j 2\pi u_j x_j} d\boldsymbol{x} \tag{2.41}$$

where $\boldsymbol{u} = (u_1, u_2, \dots, u_n)$ and $\boldsymbol{x} = (x_1, x_2, \dots, x_n)$. The spectral values are elements of the 2^n–dimensional Clifford algebra.

Example: If $n = 1$ equation (2.41) yields the classical Fourier transform and if $n = 2$ it yields the quaternionic Fourier transform. In the sequel we denote the CFT of a signal $v(\boldsymbol{x})$ $\mathcal{F}\{v(\boldsymbol{x})\} = V(\boldsymbol{u})$.

Note that the CFT of a real signal which is mirrored concerning the jth coordinate is mapped by the involution α_j $(j = 1, \dots, n)$, e.g.

$$\mathcal{F}\{v(x_1, \dots, x_{j-1}, -x_j, x_{j+1}, \dots, x_n)\} = \alpha_j(V(\boldsymbol{u})). \tag{2.42}$$

In the one–dimensional case this property is called *Hermitian symmetry.*

Theorem 5 (Inverse Clifford Fourier transform) *The inverse Clifford Fourier transform is obtained by*

$$v(\boldsymbol{x}) = \int_{\mathbb{R}^n} V(\boldsymbol{u}) \prod_{j=n}^{1} e^{\mathrm{i}_j 2\pi u_j x_j} d\boldsymbol{u}. \tag{2.43}$$

Proof:

Inserting term (2.41) into the formula (2.43) yields

$$\begin{aligned}
&\int_{\mathbb{R}^n}\int_{\mathbb{R}^n} v(\boldsymbol{x}') \prod_{j=1}^{n} e^{-\mathrm{i}_j 2\pi u_j x'_j} d\boldsymbol{x}' \prod_{j=n}^{1} e^{\mathrm{i}_j 2\pi u_j x_j} d\boldsymbol{u} \\
=&\int_{\mathbb{R}^n}\int_{\mathbb{R}^n} v(\boldsymbol{x}') \prod_{j=1}^{n-1} e^{-\mathrm{i}_j 2\pi u_j x'_j} e^{-\mathrm{i}_n 2\pi u_n x'_n} e^{\mathrm{i}_n 2\pi u_n x_n} d\boldsymbol{x}' \prod_{j=n-1}^{1} e^{\mathrm{i}_j 2\pi u_j x_j} d\boldsymbol{u}
\end{aligned}$$

drawing on the fact that the harmonic exponential functions are orthogonal

$$\begin{aligned}
=&\int_{\mathbb{R}^{n-1}}\int_{\mathbb{R}^n} v(\boldsymbol{x}')\delta_0(x_n - x'_n) \prod_{j=1}^{n-1} e^{-\mathrm{i}_j 2\pi u_j x'_j} d\boldsymbol{x}' \prod_{j=n-1}^{1} e^{\mathrm{i}_j 2\pi u_j x_j} d\boldsymbol{u} \qquad (2.44)\\
&\vdots \\
=&\int_{\mathbb{R}^n} v(\boldsymbol{x}')\delta_0(\boldsymbol{x} - \boldsymbol{x}') d\boldsymbol{x}' \\
=&v(\boldsymbol{x}),
\end{aligned}$$

i.e., the original signal is obtained.

$\square$

The Clifford Fourier transform has already been applied in several tasks. Especially the quaternionic Fourier transform is used as an extension of the classical complex valued Fourier transform in order to create more powerful Gabor filters (see [Bül98]). Furthermore, colour images can be transformed by taking the basic colours as a vector mapped on the imaginary parts of a quaternion (see [San96]).

In the sequel, we formulate the CFT in terms of the commutative algebra HCA, because the proof of (2.43) already demonstrates that the non commutativity of the Clifford algebra is troublesome. Consequently, the commutative algebra HCA will be used instead of the Clifford algebra.

Theorem 6 (Correspondence of the transforms) *The coefficients of the spectrum of a real signal calculated by (2.41) are the same if the commutative algebra HCA is used:*

$$\kappa(V(\boldsymbol{u})) = \int_{\mathbb{R}^n} v(\boldsymbol{x}) e^{-2\pi \sum_{j=1}^{n} i_j u_j x_j} d\boldsymbol{x} \tag{2.45}$$

and if

$$I_n = \begin{bmatrix} i_1 & 0 & \dots & 0 \\ 0 & i_2 & \ddots & \vdots \\ \vdots & \ddots & \ddots & 0 \\ 0 & \dots & 0 & i_n \end{bmatrix} \tag{2.46}$$

formula (2.45) yields

$$\kappa(V(\boldsymbol{u})) = \int_{\mathbb{R}^n} v(\boldsymbol{x}) e^{-2\pi \boldsymbol{x} I_n \boldsymbol{u}^T} d\boldsymbol{x}. \tag{2.47}$$

The inverse transform is calculated by

$$v(\boldsymbol{x}) = \int_{\mathbb{R}^n} \kappa(V(\boldsymbol{u})) e^{2\pi \boldsymbol{x} I_n \boldsymbol{u}^T} d\boldsymbol{u}. \tag{2.48}$$

Proof:

The proof follows directly from theorem 4 and the linearity of κ.

□

Due to the equivalence of the components of the spectra $\kappa(V(\boldsymbol{u}))$ and $V(\boldsymbol{u})$, the latter denotes both spectra in the sequel.

The definition of the discrete transform of an n–dimensional signal of the size N^n is derived directly from (2.47) by sampling:

$$V_{\boldsymbol{u}} = \sum_{\boldsymbol{x} \in \{0,\dots,N-1\}^n} v_{\boldsymbol{x}} e^{-2\pi \boldsymbol{x} I_n \boldsymbol{u}^T N^{-1}}. \tag{2.49}$$

The discrete inverse transform analogously reads:

$$v_{\boldsymbol{x}} = \frac{1}{N^n} \sum_{\boldsymbol{u} \in \{0,\dots,N-1\}^n} V_{\boldsymbol{u}} e^{2\pi \boldsymbol{x} I_n \boldsymbol{u}^T N^{-1}}. \tag{2.50}$$

Note that the discrete transforms are constructed similarly to the discrete version of the classical Fourier transform.

2.2.2 Main Theorems

In this section some important theorems concerning the Clifford Fourier transform are proposed. In the one–dimensional case, the following theorems yield the classical shift theorem and convolution theorem, respectively.

Theorem 7 (Shift theorem) *The spectrum of a shifted signal is equal to the modulated spectrum of the original signal.*

$$\mathcal{F}\{v(\boldsymbol{x}-\boldsymbol{x}_0)\} = e^{-2\pi \boldsymbol{x}_0 I_n \boldsymbol{u}^T} V(\boldsymbol{u}) \tag{2.51}$$

Proof:

$$\begin{aligned}
\mathcal{F}\{v(\boldsymbol{x}-\boldsymbol{x}_0)\} &= \int_{\mathbb{R}^n} v(\boldsymbol{x}-\boldsymbol{x}_0) e^{-2\pi \boldsymbol{x} I_n \boldsymbol{u}^T} d\boldsymbol{x} \\
&= \int_{\mathbb{R}^n} v(\boldsymbol{x}-\boldsymbol{x}_0) e^{-2\pi(\boldsymbol{x}-\boldsymbol{x}_0) I_n \boldsymbol{u}^T} e^{-2\pi \boldsymbol{x}_0 I_n \boldsymbol{u}^T} d\boldsymbol{x} \\
&\overset{\boldsymbol{y}=\boldsymbol{x}-\boldsymbol{x}_0}{=} \int_{\mathbb{R}^n} v(\boldsymbol{y}) e^{-2\pi \boldsymbol{y} I_n \boldsymbol{u}^T} e^{-2\pi \boldsymbol{x}_0 I_n \boldsymbol{u}^T} d\boldsymbol{y} \\
&\overset{\boldsymbol{x}=\boldsymbol{y}}{=} e^{-2\pi \boldsymbol{x}_0 I_n \boldsymbol{u}^T} \int_{\mathbb{R}^n} v(\boldsymbol{x}) e^{-2\pi \boldsymbol{x} I_n \boldsymbol{u}^T} d\boldsymbol{x} \\
&= e^{-2\pi \boldsymbol{x}_0 I_n \boldsymbol{u}^T} V(\boldsymbol{u})
\end{aligned} \tag{2.52}$$

Hence, equation (2.51) is proved to be true.

□

The discrete pendant analogously reads

$$\mathcal{F}\{v_{\boldsymbol{x}-\boldsymbol{x}_0}\} = e^{-2\pi \boldsymbol{x}_0 I_n \boldsymbol{u}^T N^{-1}} V_{\boldsymbol{u}}. \tag{2.53}$$

Definition 7 (n–dimensional convolution) *Let v, w be two n–dimensional signals. The n–dimensional convolution $v * w$ is defined as:*

$$v(\boldsymbol{x}) * w(\boldsymbol{x}) = \int_{\mathbb{R}^n} v(\boldsymbol{\xi}) w(\boldsymbol{x}-\boldsymbol{\xi}) d\boldsymbol{\xi}. \tag{2.54}$$

The discrete pendant is defined analogously:

$$v_{\boldsymbol{x}} * w_{\boldsymbol{x}} = \sum_{\boldsymbol{\xi} \in \{0,\ldots,N-1\}} v_{\boldsymbol{\xi}} w_{\boldsymbol{x}-\boldsymbol{\xi}} \tag{2.55}$$

Note that one has to distinguish between the linear and cyclic convolution like in the one–dimensional case.

Theorem 8 (Convolution theorem) *Let v, w be two $n-$dimensional signals. The Clifford Fourier transform of $v(\boldsymbol{x}) * w(\boldsymbol{x})$ is equal to the product of the Clifford Fourier transforms of v and w:*
Let $V(\boldsymbol{u}) = \int_{\mathbb{R}^n} v(\boldsymbol{x}) e^{-2\pi \boldsymbol{x} I_n \boldsymbol{u}^T} d\boldsymbol{x}$ and $W(\boldsymbol{u}) = \int_{\mathbb{R}^n} w(\boldsymbol{x}) e^{-2\pi \boldsymbol{x} I_n \boldsymbol{u}^T} d\boldsymbol{x}$. Thus, the following equation is satisfied:

$$\mathcal{F}\{v(\boldsymbol{x}) * w(\boldsymbol{x})\} = V(\boldsymbol{u}) W(\boldsymbol{u}). \tag{2.56}$$

Proof:

$$\begin{aligned}
\mathcal{F}\{v(\boldsymbol{x}) * w(\boldsymbol{x})\} &= \int_{\mathbb{R}^n} v(\boldsymbol{x}) * w(\boldsymbol{x}) e^{-2\pi \boldsymbol{x} I_n \boldsymbol{u}^T} d\boldsymbol{x} \\
&= \int_{\mathbb{R}^n} \int_{\mathbb{R}^n} v(\boldsymbol{\xi}) w(\boldsymbol{x} - \boldsymbol{\xi}) d\boldsymbol{\xi} e^{-2\pi \boldsymbol{x} I_n \boldsymbol{u}^T} d\boldsymbol{x} \\
&\overset{\boldsymbol{y}=\boldsymbol{x}-\boldsymbol{\xi}}{=} \int_{\mathbb{R}^n} \int_{\mathbb{R}^n} v(\boldsymbol{\xi}) w(\boldsymbol{y}) e^{-2\pi \boldsymbol{\xi} I_n \boldsymbol{u}^T} e^{-2\pi \boldsymbol{y} I_n \boldsymbol{u}^T} d\boldsymbol{\xi} d\boldsymbol{y} \\
&= V(\boldsymbol{u}) W(\boldsymbol{u})
\end{aligned} \tag{2.57}$$

So equation (2.56) is proved true.

□

The discrete pendant analogously reads

$$\mathcal{F}\{v_{\boldsymbol{x}} * w_{\boldsymbol{x}}\} = V_{\boldsymbol{u}} W_{\boldsymbol{u}} \tag{2.58}$$

where $v_{\boldsymbol{x}} * w_{\boldsymbol{x}}$ must be the cyclic convolution.

2.2.3 CFT calculated by cascaded FFTs

In this section the algebraically simplest way to build a fast algorithm for the Clifford Fourier transform is described. The spectrum of an n–dimensional signal is calculated by applying FFTs on each of the n coordinates separately. The transform following this concept is called FCFTa in the sequel. Let $v(\boldsymbol{x}) = v(x_1, x_2, \ldots, x_n)$ be an n–dimensional signal of the size N^n and let FFT(i_j) be the FFT–algorithm using the imaginary unit i_j instead of i. The algorithm starts with the choice of one coordinate (e.g. the first) and applies the FFT(i_1)–algorithm, assuming the other coordinates to be constant. Hence, N^{n-1} runs of the FFT have to be performed. The result is the complex–valued (with imaginary unit i_1) spectrum of first order, denoted ${}^1v(p_1(\boldsymbol{u}, \boldsymbol{x}))$, where p_j is defined by

$$p_j(\boldsymbol{u}, \boldsymbol{x}) = (u_1, \ldots, u_j, x_{j+1}, \ldots, x_n). \tag{2.59}$$

This procedure is repeated for the other coordinates as well. Since the signal is n–dimensional, it is repeated n times. The FFT always uses the corresponding imaginary unit i_j for the coordinate j. Hence, we obtain

$${}^jv(p_j(\boldsymbol{u}, \boldsymbol{x})) = \mathrm{FFT}(i_j)({}^{j-1}v(p_{j-1}(\boldsymbol{u}, \boldsymbol{x}))) \tag{2.60}$$

and $V(\boldsymbol{u}) = {}^nv(p_n(\boldsymbol{u}, \boldsymbol{x}))$.
The implementation of the cascaded FFTs must transform each part (the real part and the imaginary parts) of ${}^jv$ separately.
This yields a high constant in the complexity of the FCFTa, which can be calculated in the following way (provided that $\mathcal{C}(\mathrm{FFT}) = c_1 N \operatorname{ld}(N) + c_2 N$ and c_1, c_2 are constants):

$$\begin{aligned} & N^{n-1}\mathcal{C}(\mathrm{FFT}) + N^{n-1}2\mathcal{C}(\mathrm{FFT}) + N^{n-1}4\mathcal{C}(\mathrm{FFT}) + \ldots + N^{n-1}2^{n-1}\mathcal{C}(\mathrm{FFT}) \\ &= N^{n-1}(2^n - 1)\mathcal{C}(\mathrm{FFT}) \\ &= c_1\left((2N)^n - N^n\right)\operatorname{ld}(N) + c_2\left((2N)^n - N^n\right) \end{aligned} \tag{2.61}$$

Example: Let us consider the quaternionic Fourier transform: the FQFT1 algorithm transforms the N rows of the two–dimensional signal (e.g. image). The real parts of these first spectra are transformed in a column–wise fashion. The real parts of the resulting spectra are the real parts of the quaternionic spectrum and the imaginary parts are the i_2–imaginary parts. The imaginary parts from the first N transforms taken as real numbers are transformed in a column–wise way as well. The resulting real parts are the i_1–imaginary parts and the resulting imaginary parts are the i_{12}–imaginary parts of the quaternionic spectrum.

2.2.4 Fast n–dimensional Clifford Fourier Transform

The main reason for formulating the Clifford Fourier Transform in the algebra HCA is the possibility to formulate a fast algorithm in that algebra. The resulting spectrum has the same coefficients as the spectrum calculated by the transform (2.41). Figure 2.1 illustrates this approach.

$$\begin{tikzcd}
\boxed{\text{real signal}} \arrow[r, "\text{Clifford Fourier transform}"] \arrow[d, "\text{sorting and/or}"', "\text{overlapping (see next section)}"] & \boxed{\text{spectrum in CA}} \\
\boxed{\text{modified signal}} \arrow[r, "\text{fast algorithm in HCA}"] & \boxed{\text{spectrum in HCA}} \arrow[u, "\kappa^{-1}"']
\end{tikzcd}$$

Figure 2.1: Obtaining the Clifford spectrum via HCA fast algorithm

Let v be a real, n–dimensional, discrete, finite signal of the length $N^n = 2^{kn}$ and V its discrete and periodic Clifford spectrum. Let be $\boldsymbol{x} = (x_1, \dots, x_n)$, $\boldsymbol{u} = (u_1, \dots, u_n)$ and the matrix I_n defined as in (2.46).

As it has been shown in section 2.2 V is evaluated by

$$V_{\boldsymbol{u}} = \sum_{\substack{x_l=0 \\ 1\le l\le n}}^{N-1} v_{\boldsymbol{x}} e^{-2\pi \boldsymbol{x} I_n \boldsymbol{u}^T 2^{-k}}. \tag{2.62}$$

In order to reduce the complexity, a recursive formula must be found, which divides the problem into 2^n parts in each step of recursion (divide and conquer). Therefore, the used frequency domains must be of the size $(\frac{N}{2})^n = 2^{(k-1)n}$ and the frequency vector must be substituted in each component:

$$\begin{aligned}
u_i &= u_{i0} + 2^{k-1} u_{i1} \qquad \forall i \in \{1, \dots, n\} \\
\boldsymbol{u} &= \boldsymbol{u}_0 + 2^{k-1}\boldsymbol{u}_1 \begin{cases} \boldsymbol{u}_0 & = (u_{10}, \dots, u_{n0}) \\ \boldsymbol{u}_1 & = (u_{11}, \dots, u_{n1}) \end{cases}
\end{aligned} \tag{2.63}$$

As $\boldsymbol{x}$ is reciprocal to $\boldsymbol{u}$, $\boldsymbol{x}$ is substituted as well:

$$\begin{aligned}
x_i &= x_{i0} + 2x_{i1} \qquad \forall i \in \{1, \dots, n\} \\
\boldsymbol{x} &= \boldsymbol{x}_0 + 2\boldsymbol{x}_1 \begin{cases} \boldsymbol{x}_0 & = (x_{10}, \dots, x_{n0}) \\ \boldsymbol{x}_1 & = (x_{11}, \dots, x_{n1}) \end{cases}
\end{aligned} \tag{2.64}$$

For the sake of short writing we define $w = e^{-2\pi 2^{-k}}$ and $m = 2^{k-1} - 1$. By applying (2.63) and (2.64), formula (2.62) yields the following derivation:

$$\begin{aligned} V_{\boldsymbol{u}} &= \sum_{\substack{x_{l0}=0 \\ 1\le l\le n}}^{1} \sum_{\substack{x_{l1}=0 \\ 1\le l\le n}}^{m} v_{2\boldsymbol{x}_1+\boldsymbol{x}_0} w^{(\boldsymbol{x}_0+2\boldsymbol{x}_1)I_n(\boldsymbol{u}_0+2^{k-1}\boldsymbol{u}_1)^T} \\ &= \sum_{\substack{x_{l0}=0 \\ 1\le l\le n}}^{1} \sum_{\substack{x_{l1}=0 \\ 1\le l\le n}}^{m} v_{2\boldsymbol{x}_1+\boldsymbol{x}_0} w^{2\boldsymbol{x}_1 I_n \boldsymbol{u}_0} w^{\boldsymbol{x}_0 I_n \boldsymbol{u}} w^{2^k \boldsymbol{x}_1 I_n \boldsymbol{u}_1} \\ &= \sum_{\substack{x_{l0}=0 \\ 1\le l\le n}}^{1} \left(\sum_{\substack{x_{l1}=0 \\ 1\le l\le n}}^{m} v_{2\boldsymbol{x}_1+\boldsymbol{x}_0} w^{2\boldsymbol{x}_1 I_n \boldsymbol{u}_0} \right) w^{\boldsymbol{x}_0 I_n \boldsymbol{u}} \cdot 1 \end{aligned} \tag{2.65}$$

(Note that $w^{2^k \boldsymbol{x}_1 I_n \boldsymbol{u}_1} = e^{-2\pi \boldsymbol{x}_1 I_n \boldsymbol{u}_1} \equiv 1$ because x_{j1} and u_{j1} are integers for all j.)
In order to make the recursion in (2.65) evident we define

$$V_{\boldsymbol{x}_0 \boldsymbol{u}_0} = \sum_{\substack{x_{l1}=0 \\ 1\le l\le n}}^{m} v_{2\boldsymbol{x}_1+\boldsymbol{x}_0} w^{2\boldsymbol{x}_1 I_n \boldsymbol{u}_0}. \tag{2.66}$$

These 2^n sub–spectra $V_{\boldsymbol{x}_0 \boldsymbol{u}_0}$ are of the size $(\frac{N}{2})^n = 2^{(k-1)n}$. $V_{\boldsymbol{x}_0 \boldsymbol{u}_0}$ is the spectrum of a partial signal $v_{\boldsymbol{x}_0} : \boldsymbol{x}_1 \longrightarrow v_{2\boldsymbol{x}_1+\boldsymbol{x}_0}$ of $v_{\boldsymbol{x}}$, i.e. of those positions $\boldsymbol{x}$ where $\boldsymbol{x} \bmod 2 = \boldsymbol{x}_0$ (even/odd corresponding to the components). Thus, formula (2.65) yields

$$V_{\boldsymbol{u}} = \sum_{\substack{x_{l0}=0 \\ 1\le l\le n}}^{1} V_{\boldsymbol{x}_0 \boldsymbol{u}_0} w^{\boldsymbol{x}_0 I_n \boldsymbol{u}} \tag{2.67}$$

by use of the former terms.

We can determine $\boldsymbol{u}_0$ from $\boldsymbol{u}$ by using

$$u_{i0} = u_i \bmod 2^{k-1} \qquad \forall i \in \{1, \dots, n\}. \tag{2.68}$$

Note that $\boldsymbol{u}_0$ does not need to be calculated explicitly, because spectra of discrete signals are periodic ones.

Finally, a recursive definition of the FCFTb algorithm results from (2.67), assuming that $V_{\boldsymbol{x}_0} = \mathrm{FCFTb}(v_{\boldsymbol{x}_0})$ if $k > 0$:

$$\mathrm{FCFTb}(v) = \sum_{\substack{x_{l0}=0 \\ 1\le l\le n}}^{1} \mathrm{FCFTb}(v_{\boldsymbol{x}_0}) w^{\boldsymbol{x}_0 I_n \boldsymbol{u}} \tag{2.69}$$

If $k=0$, the recursion is terminated and the transform is equivalent to the identity.

Example: Consider the case $n=2$. We obtain a fast algorithm for the quaternionic Fourier transform by the following formula:

$$\mathrm{FQFT2}(v) = \mathrm{FQFT2}(v_{ee}) + \mathrm{FQFT2}(v_{oe})w^{i_1 u_1} + \mathrm{FQFT2}(v_{eo})w^{i_2 u_2} + \mathrm{FQFT2}(v_{oo})w^{i_1 u_1 + i_2 u_2} \tag{2.70}$$

where the index e or o indicates whether the signal is even or odd corresponding to the first or second coordinate, respectively.

In order to prevent copying the data at each step, the data must be sorted once at the beginning. The order is the same as for the FFT, but applied to each coordinate. The common formula (called *bit–change–rule*) changes the indices in the following way:

$$v_{\sum_{i=0}^{k} a_i 2^i} = v_{\sum_{i=0}^{k} a_i 2^{k-i}} \tag{2.71}$$

where v is a signal of the length 2^{k+1} and $a_i \in \{0,1\}$ for all i.

The recursive calls stop after k steps because the domain is divided into 2^n parts in each recursive step. The spectrum has to be calculated for each frequency, thus 2^{kn} values have to be determined for each recursive step. The exact complexities of both algorithms (FCFTa and FCFTb) have to be calculated in order to decide which one is faster.

Note that it would not be possible to formulate such a simple recursive formula as (2.69) if we used Clifford algebras instead of the commutative hyper–complex algebras because the commutativity is necessary to separate the terms in the derivation (2.65). Furthermore, a simple recursive formula can be implemented in a faster algorithm.

So far, there are no investigations whether the Clifford spectrum or the HCA spectrum yield a more powerful multidimensional signal analysis. Since the Clifford spectrum is more common at the moment we also provide an algorithm to calculate the CFT of a Clifford valued signal. The method is rather simple because each component has to be transformed separately (2^n CFTs of real signals) and afterwards the spectra have to be combined in the Clifford algebra.

Example: Consider the three–dimensional signal

$$v = v_{\emptyset} + i_1 v_1 + i_2 v_2 + i_3 v_3 + i_{23} v_{23} + i_{13} v_{13} + i_{12} v_{12} + i_{123} v_{123} \tag{2.72}$$

and let V_j be the CFTs of the (real) signals v_j, $j \in (\{1,2,3\})$. Due to the correspondence of spectra of real signals we can write V_j as an element of the eight–dimensional CA, denoted V_j'. Then, we obtain the CFT of v V by the formula

$$V = V_{\emptyset}' + \mathrm{i}_1 V_1' + \mathrm{i}_2 V_2' + \mathrm{i}_3 V_3' + \mathrm{i}_{23} V_{23}' + \mathrm{i}_{13} V_{13}' + \mathrm{i}_{12} V_{12}' + \mathrm{i}_{123} V_{123}'. \tag{2.73}$$

2.3 Optimised Algorithms and their Complexities

In the last part of this chapter we consider some possibilities of increasing the speed of the fast algorithms which have been presented in the previous part of this chapter.

The first approach is called *overlapping* and utilises the redundancy which is contained in the spectrum of a real signal. Overlapping has been proposed in [Che95] and [CP97] for the two–dimensional case. Due to the isomorphism of HCA and $\mathbb{C}^m$ we can use the overlapping algorithm for complex spectra, too. The algorithm uses the FCFT except for the last step. This has been the original application of overlapping in [CP97].

The following algorithm uses the isomorphism the other way round: the Clifford spectrum is derived from the complex spectrum. Hence, a classical complex valued fast algorithm can be used to calculate the CFT, too. In the last section of this chapter we estimate the complexities of the previous algorithms and compare them in order to show which one is the fastest.

2.3.1 Overlapping

The complexity of the computation of the FCFTb can be decreased by a method called *overlapping* (see [CP97]). It implicitly uses the redundancy which is contained in spectra of real signals (see also [Che95, Fel97]). At the beginning, the data is not only sorted according to (2.71) but also mapped onto a Clifford valued signal of the size $\left(\frac{N}{2}\right)^n$. For the sake of better understanding, every formula for the n–dimensional case is supplemented by the three–dimensional case as an example.

Firstly, the domain of the signal $v_{\boldsymbol{x}}$ of the size N^n is divided into 2^n parts by the substitution $\boldsymbol{x} = 2\boldsymbol{x}_1 + \boldsymbol{x}_0$ where $x_{0j} = x_j \bmod 2$ and $x_{1j} = \lfloor x_j/2 \rfloor$. The signal value $v_{2\boldsymbol{x}_1+\boldsymbol{x}_0}$ is mapped onto one component of $\bar{v}_{\boldsymbol{x}_1}$. Which value is mapped onto which component is determined by $\boldsymbol{x}_0$:
We define a coding function

$$\boldsymbol{C} : \mathcal{P}(\{1, \dots, n\}) \longrightarrow \{0,1\}^n$$

with

$$C_k(j) = \begin{cases} 1 & \text{if} \quad k \in j \\ 0 & \text{else} \end{cases} \tag{2.74}$$

and use the following mapping:

$$\Im_j(\bar{v}_{\boldsymbol{x}_1}) = v_{2\boldsymbol{x}_1+\boldsymbol{C}(j)} \tag{2.75}$$

for all $j \in \mathcal{P}(\{1, \ldots, n\}) \setminus \emptyset$ and

$$\Re(\bar{v}_{\boldsymbol{x}_1}) = v_{2\boldsymbol{x}_1}. \tag{2.75'}$$

In the three–dimensional case the coding reads:

$$\begin{aligned} \boldsymbol{C}(\emptyset) &= (0,0,0) \\ \boldsymbol{C}(\{1\}) &= (1,0,0) \\ \boldsymbol{C}(\{2\}) &= (0,1,0) \\ \boldsymbol{C}(\{3\}) &= (0,0,1) \\ \boldsymbol{C}(\{1,2\}) &= (1,1,0) \\ \boldsymbol{C}(\{1,3\}) &= (1,0,1) \\ \boldsymbol{C}(\{2,3\}) &= (0,1,1) \\ \boldsymbol{C}(\{1,2,3\}) &= (1,1,1) \end{aligned} \tag{2.76}$$

and $\bar{v}_{\boldsymbol{x}_1}$ is constructed by

$$\begin{aligned} \bar{v}_{\boldsymbol{x}_1} = v_{2\boldsymbol{x}_1} + v_{2\boldsymbol{x}_1+(1,0,0)} i_1 + v_{2\boldsymbol{x}_1+(0,1,0)} i_2 + v_{2\boldsymbol{x}_1+(0,0,1)} i_3 + v_{2\boldsymbol{x}_1+(1,1,0)} i_{12} \\ + v_{2\boldsymbol{x}_1+(1,0,1)} i_{13} + v_{2\boldsymbol{x}_1+(0,1,1)} i_{23} + v_{2\boldsymbol{x}_1+(1,1,1)} i_{123}. \end{aligned} \tag{2.77}$$

Consequently, a value at a position which is odd with respect to coordinate k is mapped onto an imaginary part which contains i_k. This procedure is illustrated in the figure 2.2 for the case $n = 2$. The 8×8 real signal is mapped onto a 4×4 quaternionic signal. The imaginary units i_1, i_2, and i_{12} are abbreviated by i, j, and k respectively. The real part is denoted by r.

Calculating the spectrum of $\bar{v}_{\boldsymbol{x}_1}$ yields

$$\bar{V}_{\boldsymbol{u}_0} = \sum_{j \in \mathcal{P}(\{1,\ldots,n\})} i_j V_{\boldsymbol{C}(j)\boldsymbol{u}_0} \tag{2.78}$$

where $V_{\boldsymbol{x}_0 \boldsymbol{u}_0}$ are the sub–spectra from (2.66).

Hence, in the three–dimensional case we get:

$$\begin{aligned} \bar{V}_{\boldsymbol{u}_0} = V_{(0,0,0)\boldsymbol{u}_0} + i_1 V_{(1,0,0)\boldsymbol{u}_0} + i_2 V_{(0,1,0)\boldsymbol{u}_0} + i_3 V_{(0,0,1)\boldsymbol{u}_0} + i_{12} V_{(1,1,0)\boldsymbol{u}_0} \\ + i_{13} V_{(1,0,1)\boldsymbol{u}_0} + i_{23} V_{(0,1,1)\boldsymbol{u}_0} + i_{123} V_{(1,1,1)\boldsymbol{u}_0} \end{aligned} \tag{2.79}$$

The sub–spectra can be extracted from (2.78) by inverting the involutions (2.28):

$$2^n i_j V_{\boldsymbol{C}(j)\boldsymbol{u}_0} = \sum_{k \in \mathcal{P}(\{1,\ldots,n\})} \alpha_k(\bar{V}_{\boldsymbol{u}_0^k})(-1)^{\mathrm{card}(j \cap k)} \tag{2.80}$$

		0		1		2		3	
		0	1	2	3	4	5	6	7
0	0	r	i	r	i	r	i	r	i
	1	j	k	j	k	j	k	j	k
1	2	r	i	r	i	r	i	r	i
	3	j	k	j	k	j	k	j	k
2	4	r	i	r	i	r	i	r	i
	5	j	k	j	k	j	k	j	k
3	6	r	i	r	i	r	i	r	i
	7	j	k	j	k	j	k	j	k

Figure 2.2: A two–dimensional real signal is mapped onto a quaternionic signal

where $u_{0i}^k = \begin{cases} -u_{0i} & \text{if } i \in k \\ u_{0i} & \text{else} \end{cases}$ and $\mathrm{card}(M)$ is the cardinality of M.

Considering the three–dimensional case, the sub–spectra are extracted by:

$$\begin{aligned}
\bar{V}^{1}_{\boldsymbol{u}_0} &= \alpha_1(\bar{V}_{(-u_{01},u_{02},u_{03})}) \\
\bar{V}^{2}_{\boldsymbol{u}_0} &= \alpha_2(\bar{V}_{(u_{01},-u_{02},u_{03})}) \\
\bar{V}^{3}_{\boldsymbol{u}_0} &= \alpha_3(\bar{V}_{(u_{01},u_{02},-u_{03})}) \\
\bar{V}^{12}_{\boldsymbol{u}_0} &= \alpha_{12}(\bar{V}_{(-u_{01},-u_{02},u_{03})}) \\
\bar{V}^{13}_{\boldsymbol{u}_0} &= \alpha_{13}(\bar{V}_{(-u_{01},u_{02},-u_{03})}) \\
\bar{V}^{23}_{\boldsymbol{u}_0} &= \alpha_{23}(\bar{V}_{(u_{01},-u_{02},-u_{03})}) \\
\bar{V}^{123}_{\boldsymbol{u}_0} &= \alpha_{123}(\bar{V}_{(-u_{01},-u_{02},-u_{03})}) \\
8V_{(0,0,0)\boldsymbol{u}_0} &= \bar{V}_{\boldsymbol{u}_0} + \bar{V}^{1}_{\boldsymbol{u}_0} + \bar{V}^{2}_{\boldsymbol{u}_0} + \bar{V}^{3}_{\boldsymbol{u}_0} + \bar{V}^{12}_{\boldsymbol{u}_0} + \bar{V}^{13}_{\boldsymbol{u}_0} + \bar{V}^{23}_{\boldsymbol{u}_0} + \bar{V}^{123}_{\boldsymbol{u}_0} \qquad (2.81) \\
8i_1V_{(1,0,0)\boldsymbol{u}_0} &= \bar{V}_{\boldsymbol{u}_0} - \bar{V}^{1}_{\boldsymbol{u}_0} + \bar{V}^{2}_{\boldsymbol{u}_0} + \bar{V}^{3}_{\boldsymbol{u}_0} - \bar{V}^{12}_{\boldsymbol{u}_0} - \bar{V}^{13}_{\boldsymbol{u}_0} + \bar{V}^{23}_{\boldsymbol{u}_0} - \bar{V}^{123}_{\boldsymbol{u}_0} \\
8i_2V_{(0,1,0)\boldsymbol{u}_0} &= \bar{V}_{\boldsymbol{u}_0} + \bar{V}^{1}_{\boldsymbol{u}_0} - \bar{V}^{2}_{\boldsymbol{u}_0} + \bar{V}^{3}_{\boldsymbol{u}_0} - \bar{V}^{12}_{\boldsymbol{u}_0} + \bar{V}^{13}_{\boldsymbol{u}_0} - \bar{V}^{23}_{\boldsymbol{u}_0} - \bar{V}^{123}_{\boldsymbol{u}_0} \\
8i_3V_{(0,0,1)\boldsymbol{u}_0} &= \bar{V}_{\boldsymbol{u}_0} + \bar{V}^{1}_{\boldsymbol{u}_0} + \bar{V}^{2}_{\boldsymbol{u}_0} - \bar{V}^{3}_{\boldsymbol{u}_0} + \bar{V}^{12}_{\boldsymbol{u}_0} - \bar{V}^{13}_{\boldsymbol{u}_0} - \bar{V}^{23}_{\boldsymbol{u}_0} - \bar{V}^{123}_{\boldsymbol{u}_0} \\
8i_{12}V_{(1,1,0)\boldsymbol{u}_0} &= \bar{V}_{\boldsymbol{u}_0} - \bar{V}^{1}_{\boldsymbol{u}_0} - \bar{V}^{2}_{\boldsymbol{u}_0} + \bar{V}^{3}_{\boldsymbol{u}_0} + \bar{V}^{12}_{\boldsymbol{u}_0} - \bar{V}^{13}_{\boldsymbol{u}_0} - \bar{V}^{23}_{\boldsymbol{u}_0} + \bar{V}^{123}_{\boldsymbol{u}_0} \\
8i_{13}V_{(1,0,1)\boldsymbol{u}_0} &= \bar{V}_{\boldsymbol{u}_0} - \bar{V}^{1}_{\boldsymbol{u}_0} + \bar{V}^{2}_{\boldsymbol{u}_0} - \bar{V}^{3}_{\boldsymbol{u}_0} - \bar{V}^{12}_{\boldsymbol{u}_0} + \bar{V}^{13}_{\boldsymbol{u}_0} - \bar{V}^{23}_{\boldsymbol{u}_0} + \bar{V}^{123}_{\boldsymbol{u}_0} \\
8i_{23}V_{(0,1,1)\boldsymbol{u}_0} &= \bar{V}_{\boldsymbol{u}_0} + \bar{V}^{1}_{\boldsymbol{u}_0} - \bar{V}^{2}_{\boldsymbol{u}_0} - \bar{V}^{3}_{\boldsymbol{u}_0} - \bar{V}^{12}_{\boldsymbol{u}_0} - \bar{V}^{13}_{\boldsymbol{u}_0} + \bar{V}^{23}_{\boldsymbol{u}_0} + \bar{V}^{123}_{\boldsymbol{u}_0} \\
8i_{123}V_{(1,1,1)\boldsymbol{u}_0} &= \bar{V}_{\boldsymbol{u}_0} - \bar{V}^{1}_{\boldsymbol{u}_0} - \bar{V}^{2}_{\boldsymbol{u}_0} - \bar{V}^{3}_{\boldsymbol{u}_0} + \bar{V}^{12}_{\boldsymbol{u}_0} + \bar{V}^{13}_{\boldsymbol{u}_0} + \bar{V}^{23}_{\boldsymbol{u}_0} - \bar{V}^{123}_{\boldsymbol{u}_0}
\end{aligned}$$

Finally, the spectrum $V_{\boldsymbol{u}}$ is calculated by use of formula (2.67).

2.3.2 Calculating the Complex Spectrum

The classical complex–valued Fourier transform of an n–dimensional signal can be obtained from the FCFTb, too. We only need to change the reconstructed sub–spectra derived from formula (2.80). The only effect of taking the Clifford–valued transform is the speed up of the calculation due to overlapping (see also [Che95]).

In order to obtain the complex sub–spectra we only need to apply the isomorphism between the 2^n–dimensional HCA and $\mathbb{C}^{2^{n-1}}$. There always is one eigenvalue η_j so that the real part of η_j contains all imaginary components of degree $4k$ ($0 \leq k \leq \lfloor \frac{n}{4} \rfloor$) with positive signs and all imaginary components of degree $2(2k+1)$ with negative signs. The imaginary part consists of all imaginary units of degree $4k+1$ with positive signs and of all imaginary units of degree $2(2k+1)+1$ with negative signs. We obtain this eigenvalue if we set all imaginary units of first order equal to i ($i_1 = \ldots = i_n = i$). Exactly this is done if we calculate the complex valued Fourier transform instead of the CFT: we use the kernel $e^{-i2\pi \boldsymbol{x}\boldsymbol{u}^T}$ instead of $e^{-2\pi \boldsymbol{x} I_n \boldsymbol{u}^T}$.

Consequently, we obtain the complex sub–spectra from

$$V^{\mathbb{C}}_{\boldsymbol{x}_0\boldsymbol{u}_0} = \eta_j(V_{\boldsymbol{x}_0\boldsymbol{u}_0}) \tag{2.82}$$

and the whole spectrum is calculated by using

$$V^{\mathbb{C}}_{\boldsymbol{u}} = \sum_{\substack{x_{l0}=0 \\ 1\leq l\leq n}}^{1} V^{\mathbb{C}}_{\boldsymbol{x}_0\boldsymbol{u}_0} w^{i\boldsymbol{x}_0\boldsymbol{u}}. \tag{2.83}$$

Example: In the three–dimensional case, we obtain the complex sub–spectra from

$$\begin{aligned} V^{\mathbb{C}}_{\boldsymbol{x}_0\boldsymbol{u}_0} = {} & (\Re(V_{\boldsymbol{x}_0\boldsymbol{u}_0}) - \Im_{23}(V_{\boldsymbol{x}_0\boldsymbol{u}_0}) - \Im_{13}(V_{\boldsymbol{x}_0\boldsymbol{u}_0}) - \Im_{12}(V_{\boldsymbol{x}_0\boldsymbol{u}_0})) \\ & + i(\Im_1(V_{\boldsymbol{x}_0\boldsymbol{u}_0}) + \Im_2(V_{\boldsymbol{x}_0\boldsymbol{u}_0}) + \Im_3(V_{\boldsymbol{x}_0\boldsymbol{u}_0}) - \Im_{123}(V_{\boldsymbol{x}_0\boldsymbol{u}_0})) \end{aligned} \tag{2.84}$$

and thus the whole spectrum reads

$$\begin{aligned} V^{\mathbb{C}}_{\boldsymbol{u}} = {} & V^{\mathbb{C}}_{(0,0,0)\boldsymbol{u}_0} + V^{\mathbb{C}}_{(1,0,0)\boldsymbol{u}_0} w^{i\boldsymbol{u}_1} + V^{\mathbb{C}}_{(0,1,0)\boldsymbol{u}_0} w^{i\boldsymbol{u}_2} + V^{\mathbb{C}}_{(0,0,1)\boldsymbol{u}_0} w^{i\boldsymbol{u}_3} + V^{\mathbb{C}}_{(0,1,1)\boldsymbol{u}_0} w^{i(\boldsymbol{u}_2+\boldsymbol{u}_3)} \\ & + V^{\mathbb{C}}_{(1,0,1)\boldsymbol{u}_0} w^{i(\boldsymbol{u}_1+\boldsymbol{u}_3)} + V^{\mathbb{C}}_{(1,1,0)\boldsymbol{u}_0} w^{i(\boldsymbol{u}_1+\boldsymbol{u}_2)} + V^{\mathbb{C}}_{(1,1,1)\boldsymbol{u}_0} w^{i(\boldsymbol{u}_1+\boldsymbol{u}_2+\boldsymbol{u}_3)}. \end{aligned} \tag{2.85}$$

2.3.3 Calculating the CFT by Complex n–D FFTs

As in the previous section, we use the isomorphism between the 2^n–dimensional HCA and $\mathbb{C}^{2^{n-1}}$ in order to obtain the spectrum. Firstly, we extract the CFT of a real signal from its complex–valued FT.

We know that the values of the complex FT are one eigenvalue of the CFT values. Since the spectrum of a real signal is Hermitian in the extended meaning (i.e. concerning the $2^n - 1$ involutions) we obtain the other eigenvalues and their conjugates by mirroring the spectrum with respect to each coordinate and all combinations of all coordinates. Therefore, we can evaluate the CFT by the inverse isomorphism without additional multiplications.

Example: Consider the complex–valued Fourier transform $V^{\mathbb{C}}$ of a three–dimensional real signal v. If V is the Clifford spectrum of v we have

$$V^{\mathbb{C}}_{\boldsymbol{u}_1\boldsymbol{u}_2\boldsymbol{u}_3} = (\Re(V) - \Im_{23}(V) - \Im_{13}(V) - \Im_{12}(V)) + i(\Im_1(V) + \Im_2(V) + \Im_3(V) - \Im_{123}(V)). \tag{2.86}$$

If we mirror the spectrum with respect to the coordinates $\boldsymbol{u}_3$, $\boldsymbol{u}_2$ and the combination of both, denoted $\boldsymbol{u}_1\boldsymbol{u}_2\bar{\boldsymbol{u}}_3$, $\boldsymbol{u}_1\bar{\boldsymbol{u}}_2\boldsymbol{u}_3$, and $\boldsymbol{u}_1\bar{\boldsymbol{u}}_2\bar{\boldsymbol{u}}_3$, respectively, we obtain

$$\begin{aligned} V^{\mathbb{C}}_{\boldsymbol{u}_1\boldsymbol{u}_2\bar{\boldsymbol{u}}_3} &= (\Re(V) + \Im_{23}(V) + \Im_{13}(V) - \Im_{12}(V)) + i(\Im_1(V) + \Im_2(V) - \Im_3(V) + \Im_{123}(V)) \\ V^{\mathbb{C}}_{\boldsymbol{u}_1\bar{\boldsymbol{u}}_2\boldsymbol{u}_3} &= (\Re(V) + \Im_{23}(V) - \Im_{13}(V) + \Im_{12}(V)) + i(\Im_1(V) - \Im_2(V) + \Im_3(V) + \Im_{123}(V)) \\ V^{\mathbb{C}}_{\boldsymbol{u}_1\bar{\boldsymbol{u}}_2\bar{\boldsymbol{u}}_3} &= (\Re(V) - \Im_{23}(V) + \Im_{13}(V) + \Im_{12}(V)) + i(\Im_1(V) - \Im_2(V) - \Im_3(V) - \Im_{123}(V)) \end{aligned} \tag{2.87}$$

which are all eigenvalues (except for their conjugates). The Clifford spectrum can be constructed by use of formula (2.27) where the matrix vector multiplication eventually yields a summation of components.

Consider secondly the CFT of a Clifford valued signal v. In this case we must calculate the representation of v in $\mathbb{C}^m$ by the isomorphisms $\eta_1, \ldots, \eta_m$. Note that the new representation is isomorphic to the HCA element with the same coefficients as v and not to v itself ! The same applies with the kernel of the CFT. Therefore, the product of v and the kernel does not correspond to their multiplication in HCA or in $\mathbb{C}^m$. We can only calculate the HCA spectrum of such a signal if we use the FCFTb or m complex FTs in $\mathbb{C}^m$. Nevertheless, we can easily compute the CFT of such a signal v by calculating the spectra of its (real) components and combining their spectra as in formula (2.73).

2.3.4 Complexities

In this section the complexities of the cascaded FFTs (n-dimensional) and of the fast algorithms for the 2^n–dimensional Clifford transform using overlapping are calculated. We assume that standard multiplication is used. So we obtain the following complexity–table for addition and multiplication (table 2.4). Note that the complexities are lower than

addition	real multiplications	real additions
complex	0	2
quaternion	0	4
8–dim. CA	0	8
2^n–dim. CA	0	2^n
multiplication		
complex	4	2
quaternion	8	4
8–dim. CA	16	8
2^n–dim. CA	2^{n+1}	2^n

Table 2.4: Complexities of the basic operations in the different algebras

those of the standard algebra multiplications because one factor is always restricted to a subalgebra. This subalgebra is isomorphic to the complex algebra. Consequently, that factor comprises only two non–zero elements.

The number of arithmetic operations per sub–spectrum can be extracted directly from the recursive formulas (2.69) (the sub–spectra are of the size N^n where $N = 2^{k-i-1}$ in the ith recursive step). They are represented in table 2.5.

algorithm	multiplications	additions
FFT	$\frac{1}{2}N$	N
FQFT	N^2	$3N^2$
3–dim. FCFT	$\frac{3}{2}N^3$	$7N^3$
n–dim. FCFT	$\frac{n}{2}N^n$	$(2^n-1)N^n$

Table 2.5: Number of operations from the recursive formulas 2.69

Calculating the numbers of arithmetic operations for $k-1$ recursive calls yields the subsequent table 2.6.

algorithm	multiplications
FFT	$\frac{1}{4}kN - \frac{1}{4}N$
FQFT	$\frac{1}{4}kN^2 - \frac{1}{4}N^2$
3–dim. FCFT	$\frac{3}{16}kN^3 - \frac{3}{16}N^3$
n–dim. FCFT	$\frac{n}{2}2^{-n}kN^n - \frac{n}{2}2^{-n}N^n$
	additions
FFT	$\frac{1}{2}kN - \frac{1}{2}N$
FQFT	$\frac{3}{4}kN^2 - \frac{3}{4}N^2$
3–dim. FCFT	$\frac{7}{8}kN^3 - \frac{7}{8}N^3$
n–dim. FCFT	$(1-2^{-n})kN^n - (1-2^{-n})N^n$

Table 2.6: Operations for the whole calculation

Note that the considered signal is of the size $N_0 = 2^k$ for each dimension, but due to overlapping, the spectra which must be calculated are only of the size $N = \frac{N_0}{2}$ for each dimension.

Replacement of the arithmetic operations by the equivalent number of real operations from table 2.4 yields the complexities in table 2.7.

algorithm	multiplications	additions
FFT	$kN - N$	$\frac{3}{2}kN - \frac{3}{2}N$
FQFT	$2kN^2 - 2N^2$	$4kN^2 - 4N^2$
3–dim. FCFT	$3kN^3 - 3N^3$	$\frac{17}{2}kN^3 - \frac{17}{2}N^3$
n–dim. FCFT	$nkN^n - nN^n$	$\left(\frac{n}{2} + 2^n - 1\right)kN^n - \left(\frac{n}{2} + 2^n - 1\right)N^n$

Table 2.7: Number of real operations

We assume that sorting and mapping the data before starting the algorithm does not last longer than sorting in itself, so its complexity is the same for overlapping and cascaded transforms. The complexities of the extraction of the original spectrum from the overlapped spectrum can be found in table 2.8.

algorithm	multiplications	additions
FFT	$3N$	$5N$
FQFT	$9N^2$	$28N^2$
3–dim. FCFT	$25N^3$	$124N^3$
n–dim. FCFT	$(n2^n+1)N^n$	$(2(2^n-1)2^n+n2^{n-1})N^n$

Table 2.8: Number of operations for extracting the original spectrum

Obviously, for additions there is a great increase of complexity. Note that the computational effort of the reconstruction could be reduced if the hermite symmetry of the spectrum were used. In that case, all complexities are decreased by a factor of 2^{-n}. This concept is considered in the sequel as well, although the increase of the programming code length for utilising the hermite symmetry is enormous.

The complexity of the whole algorithm (without hermite symmetries) is represented in table 2.9.

algorithm	multiplications	additions
FFT	$kN+2N$	$\frac{3}{2}kN+\frac{7}{2}N$
FQFT	$2kN^2+7N^2$	$4kN^2+24N^2$
3–D FCFT	$3kN^3+22N^3$	$\frac{17}{2}kN^3+\frac{231}{2}N^3$
n–D FCFT	$nkN^n+(n2^n-n+1)N^n$	$(\frac{n}{2}+2^n-1)kN^n+(2^n-1)(2^n2-1+\frac{n}{2})N^n$

Table 2.9: Number of operations for the whole algorithm

In order to compare the algorithms, the complexities for the cascaded transforms are calculated using equation (2.61). The results are indicated in table 2.10

algorithm	multiplications	additions
FFT	$kN+2N$	$\frac{3}{2}kN+\frac{7}{2}N$
FFTs for QFT	$3kN^2+6N^2$	$\frac{9}{2}kN^2+\frac{21}{2}N^2$
FFTs for 3–dim. CFT	$7kN^3+14N^3$	$\frac{21}{2}kN^3+\frac{49}{2}N^3$
FFTs for n–dim. CFT	$(2^n-1)kN^n+2(2^n-1)N^n$	$\frac{3(2^n-1)}{2}kN^n+\frac{7(2^n-1)}{2}N^n$

Table 2.10: Number of operation for the cascaded algorithms

Comparing the FCFT using overlapping to the cascaded FFTs it becomes evident that the multiplicative and additive complexities are asymptotically better for the FCFTb. If finite signal sizes are considered the FCFT with overlapping is faster than the cascaded FFTs only if k is greater than a boundary k_0. Using the formulas from table 2.9 and table 2.10 k_0 can be estimated. For the multiplications k_0 is evaluated by

$$k_0 = \frac{2^n(n-2) - n + 3}{2^n - 1 - n} \tag{2.88}$$

and for the additions by

$$k_0 = \frac{(2^n - 1)(2^n 2 - 1 + \frac{n-7}{2})}{\frac{1}{2}(2^n - 1) - \frac{n}{2}}. \tag{2.89}$$

In the following table 2.11 some values of k_0 are represented. In the third column a "total" k_0 is calculated assuming that the used processor calculates additions four times faster than multiplications.

dimension	k_0 (mult.)	k_0 (add.)	k_0 ("total")
2	1	27	4
3	2	46	7
4	3	81	12

Table 2.11: Boundaries for selecting the algorithm

In this context we consider the memory complexity for some signals. If we have a three–dimensional signal with $k = k_0$ it is of the size 2^{7*3}. By assuming that the type `double` (8 byte) is employed and that the corresponding spectrum uses all components of the 2^3–dimensional CA, we obtain a memory complexity of $2^{7*3} * 8 * 2^3$ byte = 128 megabyte. If we have a four–dimensional signal with $k = k_0$ we obtain a spectrum of the approximate size of 10^{17} byte by a similar calculation.

The following figures 2.3(a)–(c) illustrate all (time–)complexities for the three–dimensional case where the complexities are divided by N^3 in order to display the point of intersection quite clearly.

Consider the transforms utilising hermite symmetry which are denoted FCFTc. The complexity decreases by a factor of 2^{-n} by the hermite symmetry. Considering further that the summands at the frequencies $\pm\pi$ are equal except for the signs, only 4^{-n} of the multiplications need to be performed. Take, for example, $n = 2$. In figure 2.4 an 8×8 domain is illustrated which shows the effects explained above. For a more detailed explanation see [Fel97]. Note that the effect of the signs is already utilised in the FCFTb algorithm.

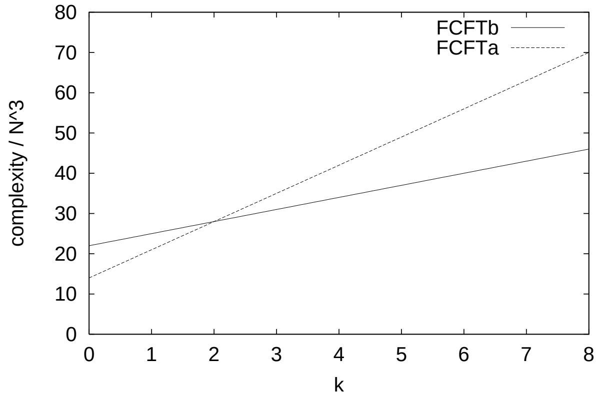

(a) Multiplications

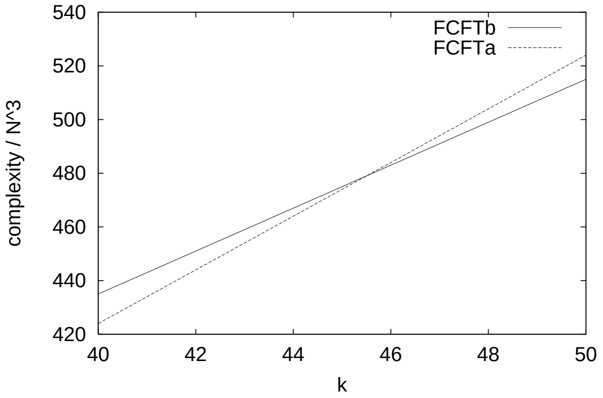

(b) Additions

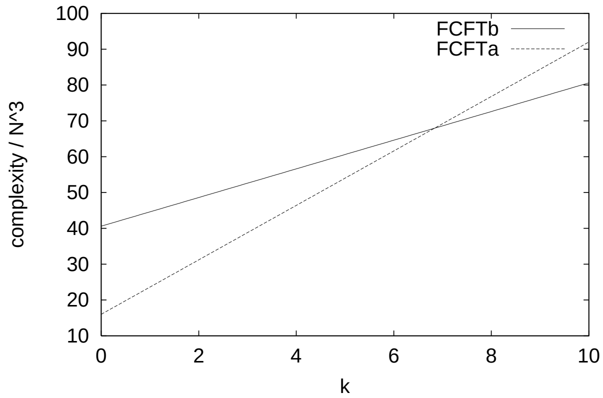

(c) Total

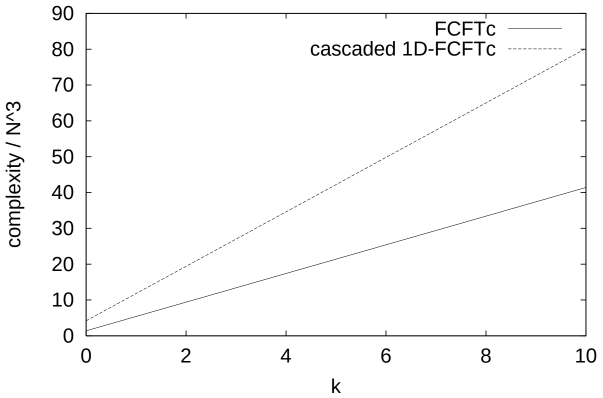

(d) Hermit

Figure 2.3: Complexities for the 3D case

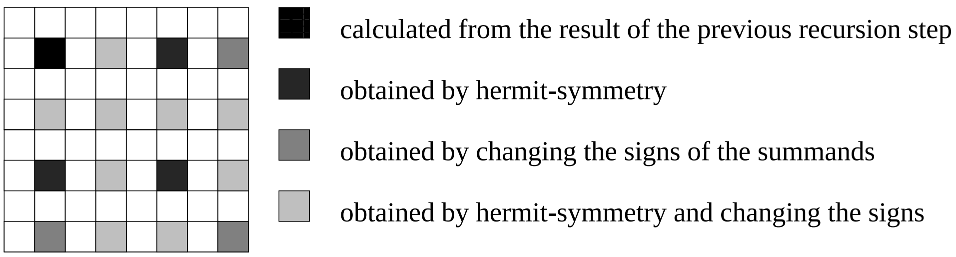

Figure 2.4: Two effects speed up the calculation of the spectrum

The following table 2.12 shows the complexities for the n–dimensional FCFTc which can be compared to the last row in the former tables 2.8, 2.9, and 2.10. In figure 2.3(d) the

	multiplications	additions
extracting	$(n+2^{-n})N^n$	$(2(2^n-1)+\frac{n}{2})N^n$
algorithm	$nkN^n+2^{-n}N^n$	$(\frac{n}{2}+2^n-1)kN^n+(2^n-1)N^n$
cascaded	$(2^n-1)kN^n+\frac{2^n-1}{2}N^n$	$\frac{3(2^n-1)}{2}kN^n+(2^n-1)N^n$

Table 2.12: Complexities utilising the hermite symmetry

complexities for the three–dimensional case utilising hermite symmetry are represented.

The complexity of the cascaded algorithm is obviously always higher than the one of the FCFTc algorithm. However, the implementation of the algorithm which profits from the hermite symmetry is rather complex. Therefore, the implementation of the n–dimensional FCFTc algorithm ($n>3$) is not profitable if scarcely used.

Although the time–complexity of the FCFTb/c algorithms in itself gives no reason to implement them, there is another fact which renders these algorithms interesting. For special signal sizes and particular computer configurations it is decisive whether the algorithm only uses local data or whether it accesses the whole data set all the time.

Consider again a three–dimensional signal of the size 2^{7*3} (128 megabyte) and a computer which can handle 32 megabyte of data without swapping (i.e. writing the data to hard–disc). Obviously, the data of the signal spectrum do not fit into the memory. Since the FCFTa algorithm performs seven runs on the whole dataset, the data is swapped seven times. The FCFTb algorithm calculates the sub–spectra of only $\frac{1}{8}$ of the data (16 megabyte). This part fits into the main memory and thus, the spectra can be calculated with one swapping of the whole data. In the last recursive step all the data is accessed one more time so that the whole FCFTb algorithm must swap the data two times. Since the processor can perform thousands of operations at the time needed by the hard–disc to deliver one byte, the arithmetic complexity is less important than the handling of the data in this case.

Apart from all these considerations, there still remains one more possibility to calculate the CFT (see section 2.3.3). So, if one has access to a fast algorithm for the complex–valued n–D FFT with a complexity which is less than that in table 2.12 (it should be faster by at least $2^{2n-1}N^n$ additions) it is recommended to use the isomorphisms to obtain the Clifford spectrum from the complex spectrum. Many of these algorithms have been published in the last few years (e.g.[Che95, CP97]).

Chapter 3

Invariants under Group Operations

In this chapter, the derivation of a kernel for a (Clifford) Fourier transform which is invariant under group operations is described.

Again we begin with mathematical bases. For the derivation of invariant kernels the Lie algebras of the involved groups are needed. Therefore, the concepts of manifolds, Lie groups and algebras are introduced.

The second part of this chapter concerns the approach of Rubinstein, Segman and Zeevi ([RSZ91]). The derivation of invariant kernels for one– and n–dimensional groups is described. For the sake of better understanding an example is considered (Fourier–Mellin transform).

The last part of this chapter contains the first experiments of this thesis. The concept of the invariant kernels is applied to a mapping which is not a group itself. However, the mapping is approximated by a group. The derivation and the results are presented. In the last section, the problems which occur with invariant kernels are discussed in order to lead to the fourth chapter.

3.1 Lie Algebras

The mathematical bases for this chapter are stated in this part. The aim is to introduce the concept of Lie algebras. However, in order to define them on a solid basis some more terms are needed. So we define *manifolds*, and *Lie groups* which are based on them, before we can introduce the term *Lie algebra*. These definitions can originally be found in Gilmore [Gil74], chapter 3 and 4. For the sake of better understanding the Lie algebra of a frequently used group is derived in the last section.

3.1.1 Manifolds

The definition of Lie groups is based on manifolds, which are specific Hausdorff spaces.

Definition 8 (Hausdorff space) *A Hausdorff space $(T, \mathcal{T})$ consists of a set of points T and a topology $\mathcal{T}$ which is defined on T. The topology $\mathcal{T}$ is a set of subsets $S_1, S_2, \ldots$ of T, so that the following axioms hold true:*

$\mathcal{T}$*1: The empty set $\emptyset$ and the space T are contained in $\mathcal{T}$: $\emptyset \in \mathcal{T}$, $T \in \mathcal{T}$.*

$\mathcal{T}$*2: Finite intersections of elements in $\mathcal{T}$ are in $\mathcal{T}$: $\bigcap_{i=1}^{n} S_i \in \mathcal{T} \quad n$ finite.*

$\mathcal{T}$*3: Arbitrary unions of elements in $\mathcal{T}$ are in $\mathcal{T}$: $\bigcup_{i=1}^{n} S_i \in \mathcal{T} \quad n$ finite or infinite.*

$\mathcal{T}$*4: If $p \in T, q \in T, p \neq q$, then there are $S_p \in \mathcal{T}, S_q \in \mathcal{T}$ with the property: $p \in S_p, q \in S_q, S_p \cap S_q = \emptyset$.*

Consequently, the specific property of a topological (or Hausdorff) space is that the notion of a continuous function can be introduced (i.e. a continuous function maps an open subset into an open subset). Some typical examples of Hausdorff spaces are the Euclidean space and its subspaces (e.g. spheres). Mappings like $A(\alpha, \beta)(t) = e^{\alpha}t + \beta$ are Hausdorff spaces as well.

A manifold arises from a Hausdorff space by introducing a set of mappings.

Definition 9 (Manifold) *A differentiable manifold $\mathcal{M}$ consists of*

1. *a Hausdorff space $(T, \mathcal{T})$ and*
2. *a set Φ of mappings $\phi_p \in \Phi: \quad \phi_p : T \longrightarrow \mathbb{R}^n \quad p \in T$, so that the following properties hold true:*

   $\mathcal{M}$*1: ϕ_p is a 1–1 mapping of an open subset $T_p\,(p \in T_p)$ into an open subset $U_p \subset \mathbb{R}^n$.*

   $\mathcal{M}$*2: $\bigcup_{p \in T} T_p = T$*

   $\mathcal{M}$*3: If $T_p \cap T_q \neq \emptyset$, $\phi_p(T_p \cap T_q)$ and $\phi_q(T_p \cap T_q)$ are different open subsets in $\mathbb{R}^n$. The mapping $\phi_p \circ \phi_q^{-1}$ must be continuous and differentiable.*

   $\mathcal{M}$*4: $\phi_p \circ \phi_q^{-1}$ and $\phi_q \circ \phi_p^{-1}$ are mappings of an open subset $U \subset \mathbb{R}^n$ into an open subset $U' \subset \mathbb{R}^n$.*

These mappings enable the creation of local Euclidean coordinate systems in the environment of each element of the manifold. In many cases the topological space itself is a subspace of the Euclidean space.

Example: Consider a sphere in the three–dimensional Euclidean space. The environment of each point of the sphere can be mapped into the plane. Since this procedure is very similar to the production of maps of our planet the local coordinate systems are sometimes called *maps*, with the set of all maps being named *atlas*. In figure 3.1, the earth with two maps having the North Pole and the South Pole as reference points, respectively, is illustrated.

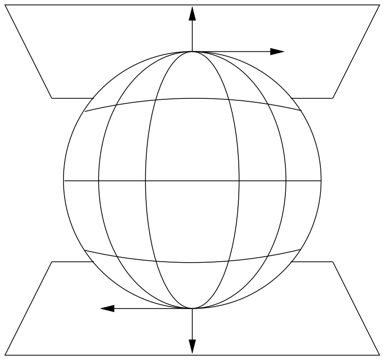

Figure 3.1: Earth with two maps

Definition 10 (Lebesgue–measure) *Let $(\mathcal{T}, T)$ be a topology (or manifold). The mapping $\mu : \mathcal{T} \longrightarrow \mathbb{R}$ is called (Lebesgue–) measure, if it obeys to the following properties $(A, B \in \mathcal{T})$:*

$\mathcal{L}$*1:* $\mu(A) \geq 0,$

$\mathcal{L}$*2:* $\mu(A \cup B) = \mu(A) + \mu(B) \qquad$ *if* $A \cap B = \emptyset,$

$\mathcal{L}$*3:* $\mu(\emptyset) = 0.$

Example: The Euclidean norm is a Lebesgue–measure.

Definition 11 (Geometric space) *A space on which a Lebesgue–measure is defined, is called geometric space.*

Example: The Euclidean space is a geometric space (even a metric space).

Note that the triangle inequality does not need to hold true for a Lebesgue–measure. Consequently, a metric space is a specific geometric space. All manifolds which are needed in the subsequent sections are either matrices or subsets of the Euclidean space; the geometric spaces are Euclidean spaces.

3.1.2 Lie Groups

The definition of Lie groups is based on some more terms which will be introduced in the sequel.

Definition 12 (Group) *A group consists of a set $\mathcal{M}$ and an operation (group multiplication) $\circ : \mathcal{M} \times \mathcal{M} \longrightarrow \mathcal{M}$, which obeys to the following axioms ($a, b, c \in \mathcal{M}$):*

$\mathcal{G}1$: $a \circ b \in \mathcal{M}$ (closure)

$\mathcal{G}2$: $(a \circ b) \circ c = a \circ (b \circ c)$ (associativity)

$\mathcal{G}3$: there is one element $0 \in \mathcal{M}$, so that for all $a \in \mathcal{M}$ $\;a \circ 0 = a$ holds true (identity)

$\mathcal{G}4$: for all $a \in \mathcal{M}$ there is one element $a^{-1} \in \mathcal{M}$, so that $a \circ a^{-1} = 0$ holds true (inverse)

A group is called an *Abelian group* if its product is commutative ($a \circ b = b \circ a$).

Examples: The quaternions $q \in \mathbb{H} \backslash \{0\}$ and the quaternion multiplication form a group. The neutral element is 1 and the inverse of q is obtained by $\frac{1}{q}$. The real numbers $n \in \mathbb{N}$ and the summation form an Abelian group. The neutral element is 0 and the inverse of n is obtained from $-n$.

Definition 13 (Topological / continuous group) *A topological or continuous group is based on an η–dimensional manifold $\mathcal{M}$ and an operation ϕ, which maps each pair (β, α) of points into a point γ in the manifold. The functions*
$\phi : \beta \times \alpha \longrightarrow \gamma = \beta\alpha$ (composition function) and
$\psi : \alpha \longrightarrow \alpha^{-1}$
must be continuous. Furthermore, ϕ must obey to the axioms of a group multiplication (algebraic closure, associativity, identity and inverse).

Examples: See above.

Definition 14 (Continuous group of transformations) *A continuous group which also contains*

1. *a geometric space G_N, which is an N–dimensional manifold and*

2. *a mapping $f : \mathcal{T} \times G_N \longrightarrow G_N$, which is continuous and obeys to the axioms of a group multiplication*

is called a continuous group of transformations.

Example: The group SO(2) (rotations in the plane) is a continuous group of transformations. The terms of definition 13 and 14 can be identified in the following way:

$$
\begin{aligned}
\mathcal{M} &= \mathbb{R}\ (\mathrm{mod}\ 2\pi) \cong S^1 \\
\phi(\alpha, \beta) &= \alpha + \beta \\
\psi(\alpha) &= -\alpha \\
G_N &= \mathbb{R}^2 \\
f(\alpha, (x, y)) &= (x \cos\alpha - y \sin\alpha, x \sin\alpha + y \cos\alpha)
\end{aligned}
\tag{3.1}
$$

The second property of definition 14 must be explained in more detail. The four properties of a group multiplication slightly differ for the mapping f:

$$
\begin{aligned}
f(\alpha, x) &\in G_N && \text{(Closure)} \\
f(\alpha, f(\beta, x)) &= f(\phi(\alpha, \beta), x) && \text{(Associativity)} \\
f(0, x) &= x && \text{(Identity)} \\
f(\alpha^{-1}, f(\alpha, x)) &= x && \text{(Inverse)}
\end{aligned}
$$

where $\alpha, \beta, 0 \in \mathcal{M}$ and $x \in G_N$.

Lie groups can be defined now by using the former terms:

Definition 15 (Lie group) *A Lie group is the connected component of a continuous group in which the composition function ϕ is an analytic function on its whole domain of definition.*

The term "*the* connected component" is justified by the fact that only one component contains the identity. Consequently, the other components are no groups.

Example: Consider the orthogonal 2×2 matrices with determinant ± 1. These matrices and matrix multiplication form the group O(2) (rotations and reflections in the plane). This group consists of two components: the set of matrices with determinant $+1$ and the set of those with determinant -1. Obviously, the identity matrix is not included in the latter set.

Lie groups of transformations are defined analogously. In the following, we use the term *Lie group* instead of *Lie group of transformations*.

Lie groups are a mathematical concept which involves both, group theory and differential geometry.

3.1.3 Lie Algebras

The principle of infinitesimal generators is introduced in the sequel considering only one–parameter groups, which is justified by the fact that most n–parameter groups can easily be constructed from n one–parameter groups. The generalised case can be found in Gilmore [Gil74].

Let p denote a point in the Euclidean space with the coordinate representation $\boldsymbol{x}(p) = (x^1(p), x^2(p), \ldots, x^N(p)) \in \mathbb{R}^N$. The movement of p in the coordinate system can be described by the application of a transformation, which is an element of the considered Lie group. The new coordinates of p can be evaluated using the notion of definition 14 by $x'^j(p) = f^j[-\alpha, \boldsymbol{x}(p)]$.

Consider a function F which is to be expressed in terms of the new coordinates. The aspired function F' is defined by $F'(\boldsymbol{x}'(p)) := F(\boldsymbol{x}(p))$. Consequently, the mapping $x'^j(p) = f^j[-\alpha, \boldsymbol{x}(p)]$ must be inverted.

With respect to practical aspects consider a transformation close to the identity:

$$\begin{aligned} x^j(p) &= f^j[(-\delta\alpha)^{-1}, \boldsymbol{x}'(p)] = f^j[\delta\alpha, \boldsymbol{x}'(p)] \\ &= f^j[\mathrm{Id}, \boldsymbol{x}'(p)] + \left.\frac{\partial f^j[\beta, \boldsymbol{x}'(p)]}{\partial\beta}\right|_{\beta=0} (\delta\alpha) + \ldots \\ &\cong x'^j(p) + \delta\alpha \left.\frac{\partial f^j[\beta, \boldsymbol{x}'(p)]}{\partial\beta}\right|_{\beta=0} \end{aligned} \tag{3.2}$$

(truncated Taylor series expansion).

Applying (3.2) to F, F' can be expressed as a truncated Taylor series expansion, too:

$$\begin{aligned} F'[\boldsymbol{x}'(p)] &= F \begin{bmatrix} x'^1(p) + \delta\alpha \left.\frac{\partial f^1[\beta, \boldsymbol{x}'(p)]}{\partial\beta}\right|_{\beta=0} \\ \vdots \\ x'^N(p) + \delta\alpha \left.\frac{\partial f^N[\beta, \boldsymbol{x}'(p)]}{\partial\beta}\right|_{\beta=0} \end{bmatrix} \\ &\cong F[\boldsymbol{x}'(p)] + \delta\alpha \sum_{j=1}^{N} \left.\frac{\partial f^j[\beta, \boldsymbol{x}'(p)]}{\partial\beta}\right|_{\beta=0} \frac{\partial}{\partial x'^j} F[\boldsymbol{x}'(p)]. \end{aligned} \tag{3.3}$$

The infinitesimal generator can be defined using this expression:

Definition 16 (Infinitesimal generator) *The quantity*

$$X(\boldsymbol{x}'(p)) = \sum_{j=1}^{N} \left. \frac{\partial f^j[\beta, \boldsymbol{x}'(p)]}{\partial \beta} \right|_{\beta=0} \frac{\partial}{\partial x'^j} \tag{3.4}$$

is called infinitesimal generator (of transformations).

Note that $\frac{\partial}{\partial x}$ is usually abbreviated as ∂_x.

Applying the last definition, formula (3.3) becomes

$$F[\boldsymbol{x}(p)] - F[\boldsymbol{x}'(p)] = \delta\alpha X(\boldsymbol{x}'(p)) F(\boldsymbol{x}'(p)). \tag{3.5}$$

Example: Consider the group of one–dimensional translations. A group operation with the parameter t on the coordinate x is expressed by $x' = f(t, x) = x + t$. Consequently, we obtain the infinitesimal generator $X(x) = \frac{\partial(x+t)}{\partial t}\partial_x = \partial_x$.

We obtain only one generator because we have considered only one–parameter groups. As mentioned above, from n one–parameter groups arise n infinitesimal generators which span a vector space for which a new product can be defined. This product is called the Lie bracket.

Definition 17 (Lie bracket) *Let V be a vector space. The mapping $[\cdot,\cdot] : V \times V \longrightarrow V$ is called Lie bracket of V, if it obeys to the following axioms:*

L1: $[c\boldsymbol{u} + d\boldsymbol{v}, \boldsymbol{w}] = c[\boldsymbol{u}, \boldsymbol{w}] + d[\boldsymbol{v}, \boldsymbol{w}]$, $\quad [\boldsymbol{u}, c\boldsymbol{v} + d\boldsymbol{w}] = c[\boldsymbol{u}, \boldsymbol{v}] + d[\boldsymbol{u}, \boldsymbol{w}]$
for all $c, d \in \mathbb{R}$ (bilinear),

L2: $[\boldsymbol{v}, \boldsymbol{w}] = -[\boldsymbol{w}, \boldsymbol{v}]$ *(anti–commutative),*

L3: $[\boldsymbol{u}, [\boldsymbol{v}, \boldsymbol{w}]] + [\boldsymbol{w}, [\boldsymbol{u}, \boldsymbol{v}]] + [\boldsymbol{v}, [\boldsymbol{w}, \boldsymbol{u}]] = 0$ *(Jacobi identity),*

for all $\boldsymbol{u}, \boldsymbol{v}, \boldsymbol{w} \in V$.

Let $\boldsymbol{a} = \sum_i a_i \frac{\partial}{\partial x^i}, \boldsymbol{b} = \sum_j b_j \frac{\partial}{\partial x^j} \in V$ and $\boldsymbol{v}^j$ be the jth component of $\boldsymbol{v}$. Then, we obtain

$$[\boldsymbol{a}, \boldsymbol{b}]^j = \sum_i \left(a_i \frac{\partial b_j}{\partial x^i} - b_i \frac{\partial a_j}{\partial x^i} \right) \partial_{x^j}. \tag{3.6}$$

If V is the vector space of $n \times n$ matrices, the Lie bracket is identical to the matrix commutator $[A, B] \equiv AB - BA$.

The Lie bracket is needed for the definition of the Lie algebra:

Definition 18 (Lie algebra) *The Lie algebra (of a group) contains the vector space which is spanned by the infinitesimal generators of the Lie group and the Lie bracket as a product.*

The generators are obtained by calculating all partial derivatives of the group at the identity. Thus, from a graphical point of view the Lie algebra is the local tangent to the group (see figure 3.2).

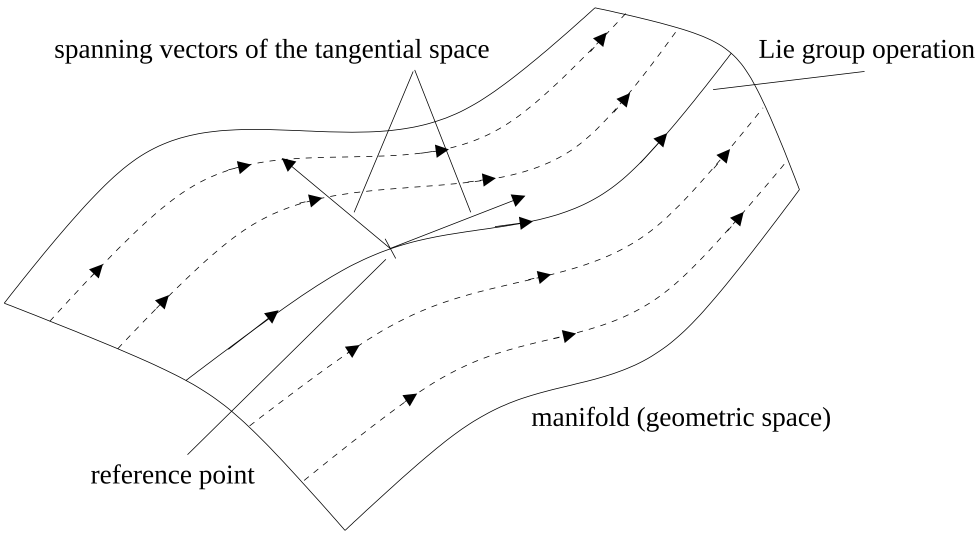

Figure 3.2: Lie algebra as tangent to the group

In practical applications it is often more interesting to derive the group from the algebra, because systems of differential equations can be solved in this way. How to obtain the group from the algebra can be derived formally by a Taylor series expansion (see [Olv86]). However, in this thesis, only the result is presented.

Consider the exponential function in its general formulation:

Definition 19 (Exponential function) *The exponential function* $\exp(\cdot)$ *is defined by:*

$$\exp(X) := \sum_{i=0}^{\infty} \frac{X^i}{i!} \tag{3.7}$$

where X is an element of an arbitrary algebra.

The question whether the series converges (or not) has been considered in several mathematical publications (for example [Nee91]), but it is out of the scope of this thesis.

Let X be a matrix. Obviously, tX ($t \in \mathbb{R}$) is a matrix, too. Consider the derivative of $\exp(tX)$:

$$\frac{d\exp(tX)}{dt} = \frac{d}{dt}\sum_{i=0}^{\infty}\frac{X^i}{i!} = \sum_{i=0}^{\infty}\frac{it^{i-1}X^i}{i!} = X\exp(tX) \tag{3.8}$$

Consequently, the derivative of $\exp(tX)$ at the identity ($t = 0$) is equivalent to X. Therefore, X is the generator of $\exp(tX)$.

The following figure 3.3 illustrates the connection between the group and the algebra:

$$\begin{tikzcd}
\boxed{\text{element of Lie group}} \arrow[r, "\text{group multiplication, summation}", "\text{and scalar multiplication}"'] \arrow[d, "\text{derivative}"', "\text{at the identity}"] & \boxed{\text{new element of Lie group}} \\
\boxed{\text{element of Lie algebra}} \arrow[r, "\text{Lie bracket, summation}", "\text{and scalar multiplication}"'] & \boxed{\text{new element of Lie algebra}} \arrow[u, "\text{exponential}", "\text{function}"']
\end{tikzcd}$$

Figure 3.3: The connection of a Lie group with its algebra

The exponential function can be interpreted as a curve in the group. Each term in the series expansion extends the curve by an infinitesimal amount (the element of the Lie algebra).

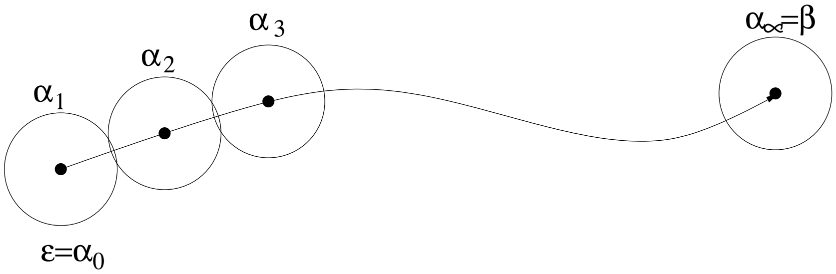

Figure 3.4: Series expansion at ε to the element of the group β

The exponential function can be graphically interpreted as a curve in the group from the identity ε to the element of the group β. Obviously, a disconnected group cannot be obtained by series expansion of its Lie algebra because starting from the identity only the (corresponding) Lie group can be reached.

In most cases, there are more than one corresponding Lie group for a Lie algebra, but all these groups must be analytically isomorphic to each other. The exponential function creates one element of this equivalence class.

One example for a group of transformations (see [Olv86]) is derived in order to verify the former theorems.
Consider the rotations in the plane $f(t,(x,y)) = (x\cos t - y\sin t, x\sin t + y\cos t)$. We obtain the infinitesimal generator $\boldsymbol{v} = -y\frac{\partial}{\partial x} + x\frac{\partial}{\partial y}$ which can be written as a matrix:

$$V := \begin{pmatrix} 0 & -1 \\ 1 & 0 \end{pmatrix}.$$

The exponential series $\exp(tV)$ starts with the terms

$$\exp(tV) = \begin{pmatrix} 1 & 0 \\ 0 & 1 \end{pmatrix} + t\begin{pmatrix} 0 & -1 \\ 1 & 0 \end{pmatrix} + \frac{t^2}{2!}\begin{pmatrix} -1 & 0 \\ 0 & -1 \end{pmatrix} + \frac{t^3}{3!}\begin{pmatrix} 0 & 1 \\ -1 & 0 \end{pmatrix} + \dots$$

which yields

$$\exp(tV)\begin{pmatrix} x \\ y \end{pmatrix} =(x\cos t - y\sin t, x\sin t + y\cos t) = f(t,(x,y)). \tag{3.9}$$

If we consider the orthogonal 2×2 matrices with determinant ± 1 (i.e. $\mathrm{O}(2)$) again, we obtain the same Lie algebra as above and consequently, the group $\mathrm{O}(2)$ cannot arise from the exponential series of its Lie algebra.

3.2 Invariant Fourier Transforms

In the following sections, the approach from J. Rubinstein, J. Segman and Y. Zeevi for creating kernels which are invariant under the operation of a group is described [RSZ91, SRZ92] (see also [GMPO95, FC94]).

Firstly, the concept of deriving invariant kernels for one–parameter groups is presented. In the next section the concept is extended to n–parameter groups. In the third section of this part the presented concept is applied to an example group and the Fourier–Mellin transform is derived.

3.2.1 Invariant Kernels for one–Parameter Groups

To start with, consider the Clifford Fourier transform. It has been shown that the Clifford spectrum of a shifted signal is equivalent to the spectrum of the non–shifted signal concerning the magnitude (2.51). There is only one additional exponential term, the linear phase which changes the phase of the spectrum. From the linear phase the shift vector can be extracted easily.

The aim of this chapter is to develop a kernel $K(\boldsymbol{x}, \boldsymbol{u})$ for a group G so that the equation

$$\left| \int f(\boldsymbol{x}) K(\boldsymbol{x}, \boldsymbol{u}) d\boldsymbol{x} \right| = \left| \int f_G(\boldsymbol{x}) K(\boldsymbol{x}, \boldsymbol{u}) d\boldsymbol{x} \right| \tag{3.10}$$

holds true. The signal f_G denotes the signal f deformed under a group operation of G. The parameter of the group operation should result in a linear phase. This condition is sometimes referred to as *strong invariance* [FC94] in contrast to the *weak invariance* of e.g. Gauß curvature where the parameter cannot be reconstructed (see [GMPO95]). The integrals of (3.10) are abbreviated in the sequel by

$$\mathcal{T}_K\{f\}(\boldsymbol{u}) = \int f(\boldsymbol{x}) K(\boldsymbol{x}, \boldsymbol{u}) d\boldsymbol{x}. \tag{3.11}$$

Consider now an arbitrary one–parameter group G and its generator L. In order to derive a kernel which satisfies the condition (3.10) a transformation of coordinates is needed so that in the new coordinate system the group operations act as translations. Therefore, the application of the CFT results in an unchanged magnitude spectrum (see also figure 3.5).

Let be $L = \boldsymbol{v}(\boldsymbol{x})\nabla_{\boldsymbol{x}}$ where $\boldsymbol{v}(\boldsymbol{x}) = (v_1(\boldsymbol{x}), v_2(\boldsymbol{x}), \ldots, v_n(\boldsymbol{x}))$ and $\nabla_{\boldsymbol{x}} = (\partial_{x_1}, \ldots, \partial_{x_n})^T$. The aspired transformation of coordinates is denoted by $\boldsymbol{\xi}(\boldsymbol{x}) = (\xi_1(\boldsymbol{x}), \ldots, \xi_n(\boldsymbol{x}))$ and the

$$
\begin{array}{c}
\boxed{\text{signal under group–operation of } G} \\
\Big\downarrow \text{canonical coordinate transform} \\
\boxed{G \text{ acts as translation}} \\
\Big\downarrow \text{Clifford Fourier transform} \\
\boxed{\text{(strong) invariant spectrum}}
\end{array}
$$

Figure 3.5: Idea for an invariant transform

group G is transformed into $\bar{G}$. The generator $\bar{L}$ of $\bar{G}$ in the new coordinates is obtained by a substitution ($\nabla_{\boldsymbol{\xi}} = (\partial_{\xi_1}, \ldots, \partial_{\xi_n})^T$):

$$
\begin{aligned}
\bar{L} &= (\boldsymbol{v}(\boldsymbol{x})\nabla_{\boldsymbol{x}}\boldsymbol{\xi})\nabla_{\boldsymbol{\xi}} \\
&= \left(v_1 \frac{\partial \xi_1}{\partial x_1} + \ldots + v_n \frac{\partial \xi_1}{\partial x_n}\right) \partial_{\xi_1} + \ldots + \left(v_1 \frac{\partial \xi_n}{\partial x_1} + \ldots + v_n \frac{\partial \xi_n}{\partial x_n}\right) \partial_{\xi_n}
\end{aligned}
\tag{3.12}
$$

Assuming that $\bar{G}$ is a translation of the first coordinate we can derive its generator:

$$
\begin{aligned}
\xi_1' &= \xi_1 + \tau \\
\xi_i' &= \xi_i \quad \forall i \in \{2, \ldots, n\}
\end{aligned}
$$

and the derivative of $\boldsymbol{\xi}'$ is evaluated by

$$
\left.\frac{\partial \boldsymbol{\xi}'}{\partial \tau}\right|_{\tau=0} = \left.\begin{bmatrix} \frac{\partial(\xi_1+\tau)}{\partial \tau} \\ \frac{\partial \xi_2}{\partial \tau} \\ \vdots \\ \frac{\partial \xi_n}{\partial \tau} \end{bmatrix}\right|_{\tau=0} = \begin{bmatrix} 1 \\ 0 \\ \vdots \\ 0 \end{bmatrix}
$$

which yields the generator

$$
\bar{L} = \partial_{\xi_1}. \tag{3.13}
$$

Consequently, from (3.12) and (3.13) we obtain the following system of partial differential equations which need to be solved:

$$
\begin{aligned}
\left(v_1 \frac{\partial \xi_1}{\partial x_1} + \ldots + v_n \frac{\partial \xi_1}{\partial x_n}\right) &= 1 \\
\left(v_1 \frac{\partial \xi_i}{\partial x_1} + \ldots + v_n \frac{\partial \xi_i}{\partial x_n}\right) &= 0 \quad \forall i \in \{2, \ldots, n\}
\end{aligned}
\tag{3.14}
$$

Let $\mathbb{D} \subseteq \mathbb{R}^n$ be the domain so that $\boldsymbol{\xi}(\boldsymbol{x})$ is defined for all $\boldsymbol{x} \in \mathbb{D}$ and $\bigcup_{\boldsymbol{x}\in\mathbb{D}} \boldsymbol{\xi}(\boldsymbol{x}) = \mathbb{R}^n$. Furthermore, let f be a signal which is defined on $\mathbb{D}$ ($f(\boldsymbol{x}) = 0 \; \forall \boldsymbol{x} \in \mathbb{R}^n \setminus \mathbb{D}$). In the new coordinates a new signal is defined by

$$\bar{f}(\boldsymbol{\xi}(\boldsymbol{x})) = f(\boldsymbol{x}). \tag{3.15}$$

Starting from the Fourier transform of this new signal $\bar{f}$ in the changed coordinates the invariant kernel $K_G(\boldsymbol{u}, \boldsymbol{x})$ can be derived:

$$\begin{aligned} & \int_{\mathbb{R}^n} \bar{f}(\boldsymbol{\xi}) e^{-2\pi \boldsymbol{u} I_n \boldsymbol{\xi}} d\boldsymbol{\xi} \\ \overset{\text{in old coordinates}}{=} & \int_{\mathbb{D}} f(\boldsymbol{x}) e^{-2\pi \boldsymbol{u} I_n \boldsymbol{\xi}(\boldsymbol{x})} J(\boldsymbol{x}) d\boldsymbol{x} \\ = & \int_{\mathbb{D}} f(\boldsymbol{x}) K_G(\boldsymbol{u}, \boldsymbol{x}) d\boldsymbol{x} \end{aligned} \tag{3.16}$$

where $J(\boldsymbol{x})$ is the Jacobian which is given by

$$J(\boldsymbol{x}) = \left| \det \begin{bmatrix} \frac{\partial \xi_1}{\partial x_1} & \frac{\partial \xi_1}{\partial x_2} & \cdots & \frac{\partial \xi_1}{\partial x_n} \\ \frac{\partial \xi_2}{\partial x_1} & \frac{\partial \xi_2}{\partial x_2} & \cdots & \frac{\partial \xi_2}{\partial x_n} \\ \vdots & \vdots & & \vdots \\ \frac{\partial \xi_n}{\partial x_1} & \frac{\partial \xi_n}{\partial x_2} & \cdots & \frac{\partial \xi_n}{\partial x_n} \end{bmatrix} \right| = \left| \frac{\partial \boldsymbol{\xi}}{\partial \boldsymbol{x}} \right|. \tag{3.17}$$

Applying the shift theorem (theorem 2.51) to the transform in new coordinates yields an additional factor $e^{-i_1 2\pi u_1 \tau}$ which is not changed if the coordinate system is switched to the old one. Consequently, the magnitude spectrum is invariant with respect to the group G:

$$\mathcal{T}_K\{f\}(\boldsymbol{u}) = e^{-i_1 2\pi u_1 \tau} \mathcal{T}_K\{f_G\}(\boldsymbol{u}) \tag{3.18}$$

For the sake of better understanding the invariant kernel for one example group is developed. Consider a two–dimensional signal $f(x_1, x_2)$ which is rotated by an angle of φ. The group of rotations has the generator $L = -x_2 \partial_{x_1} + x_1 \partial_{x_2}$ (see (3.9)). Consequently, the differential equations read:

$$-x_2 \frac{\partial \xi_1}{\partial x_1} + x_1 \frac{\partial \xi_1}{\partial x_2} = 1 \tag{3.19}$$

$$-x_2 \frac{\partial \xi_2}{\partial x_1} + x_1 \frac{\partial \xi_2}{\partial x_2} = 0 \tag{3.20}$$

and they are solved by

$$\xi_1(x_1, x_2) = \arctan\left(\frac{x_2}{x_1}\right) \tag{3.21}$$

and every monotonous function of $x_1^2 + x_2^2$, e.g.

$$\xi_2(x_1, x_2) = \sqrt{x_1^2 + x_2^2}. \tag{3.22}$$

The derivatives of (3.21) are

$$\begin{aligned} \frac{\partial \xi_1(x_1, x_2)}{\partial x_1} &= \frac{x_1^2}{x_1^2 + x_2^2}\left(-\frac{x_2}{x_1^2}\right) = \frac{-x_2}{x_1^2 + x_2^2} \qquad \text{and} \\ \frac{\partial \xi_1(x_1, x_2)}{\partial x_2} &= \frac{x_1^2}{x_1^2 + x_2^2}\frac{1}{x_1} = \frac{x_1}{x_1^2 + x_2^2} \end{aligned}$$

so equation (3.19) holds true, just as for the derivatives of (3.22):

$$\begin{aligned} \frac{\partial \xi_2(x_1, x_2)}{\partial x_1} &= \frac{1}{2\sqrt{x_1^2 + x_2^2}} 2x_1 = \frac{x_1}{\sqrt{x_1^2 + x_2^2}} \qquad \text{and} \\ \frac{\partial \xi_2(x_1, x_2)}{\partial x_2} &= \frac{1}{2\sqrt{x_1^2 + x_2^2}} 2x_2 = \frac{x_2}{\sqrt{x_1^2 + x_2^2}}. \end{aligned}$$

So equation (3.20) is satisfied as well.

The Jacobian in this case reads:

$$J(x_1, x_2) = \left| \det \begin{bmatrix} \frac{-x_2}{x_1^2+x_2^2} & \frac{x_1}{x_1^2+x_2^2} \\ \frac{x_1}{\sqrt{x_1^2+x_2^2}} & \frac{x_2}{\sqrt{x_1^2+x_2^2}} \end{bmatrix} \right| = \frac{1}{\sqrt{x_1^2 + x_2^2}}. \tag{3.23}$$

Eventually, we obtain the aspired kernel

$$K_{SO(2)}(u_1, u_2, x_1, x_2) = e^{-2\pi\left(i_1 u_1 \arctan\left(\frac{x_2}{x_1}\right) + i_2 u_2 \sqrt{x_1^2+x_2^2}\right)} \frac{1}{\sqrt{x_1^2 + x_2^2}}. \tag{3.24}$$

Consider now the rotated signal $f(x_1', x_2')$ with $x_1' = x_1 \cos\varphi + x_2 \sin\varphi$ and $x_2' = -x_1 \sin\varphi + x_2 \cos\varphi$). Note that the coordinate system is rotated by $-\varphi$. Consequently, the signal is rotated by $+\varphi$. Since

$$\arctan\left(\frac{x_2'}{x_1'}\right) = \arctan\left(\frac{x_2}{x_1}\right) - \varphi \tag{3.25}$$

and

$$\sqrt{{x_1'}^2 + {x_2'}^2} = \sqrt{x_1^2 + x_2^2} \tag{3.26}$$

the equation

$$\mathcal{T}_K\{f(x_1', x_2')\}(u_1, u_2) = e^{-i_1 2\pi u_1 \varphi} \mathcal{T}_K\{f(x_1, x_2)\}(u_1, u_2) \tag{3.27}$$

is satisfied.

3.2.2 Invariant Kernels for n–Parameter Groups

Consider a solution of the equations (3.14). Besides the given one–parameter group which acts as a translation on the first component there are $n-1$ groups which act as translation groups on the other $n-1$ components of $\boldsymbol{x}$. So far, this feature has not been used, but it is possible to choose the solutions the homogeneous equations of (3.14) so that the transform is invariant to a group with more than one parameter. This n–parameter group is restricted to be commutative, i.e. it must be an Abelian group. Therefore, the Lie bracket of the generators must be zero:

$$[L_i, L_j] = 0 \qquad \forall i \neq j \in \{1, \dots, n\} \tag{3.28}$$

Furthermore, the following two definitions are used in the sequel:

Definition 20 (Invariant curve) *A curve $a(\boldsymbol{x}) = c$ is said to be invariant under a group G if*

$$La = 0 \tag{3.29}$$

where L is the generator of G.

Such a curve is also called an *orbit* of the group. The group operation on a point which lies on an orbit yields a point which still lies on the same orbit.

Example: Consider circles in the plane around the origin and rotations of the coordinate system. Obviously, a point which lies on a circle remains on the same circle if the coordinate system is rotated.

Definition 21 (Unconnectedness) *Consider k functions $\phi_1, \dots, \phi_k$. They are called* unconnected *if they are linearly independent in the vector space of functions, i.e. there is no functional relation Ψ so that*

$$\Psi(\phi_1, \dots, \phi_k) \equiv 0. \tag{3.30}$$

Similarly k generators $L_1, \dots, L_k$ are unconnected if there is no set of functions $\phi_1, \dots, \phi_k$ so that

$$\phi_1(\boldsymbol{x})L_1 + \dots + \phi_k(\boldsymbol{x})L_k \equiv 0. \tag{3.31}$$

In the subsequent paragraphs a method is described which creates an unconnected coordinate system $\boldsymbol{\xi}$ from $k \in \{1, \dots, n\}$ unconnected, permutable generators so that the following equation is satisfied:

$$L_i\xi_j = \delta_{ij} = \begin{cases} 1 & \text{if } i = j \\ 0 & \text{else} \end{cases} \tag{3.32}$$

where $i \in \{1, \dots, k\}$ and $j \in \{1, \dots, n\}$. Let A_i be the set of $n-1$ unconnected invariant curves[1] of L_i and B_i the set of the common invariants of all generators except for L_i:

$$B_i = \bigcap_{j \in \{1,\dots,k\} \setminus \{i\}} A_j. \tag{3.33}$$

Each set B_i contains $n-k+1$ invariants $b_{i1}, \dots, b_{i(n-k+1)}$. The set of the common invariants of all generators is called Z; it contains $n-k$ unconnected invariants:
$Z = \{\varphi_1, \dots, \varphi_{n-k}\}$. A set of functions $\{\phi_1, \dots, \phi_n\}$ must be found which satisfies equation (3.32) where ξ_j is defined in the following way:

$$\begin{aligned} \xi_1 &= \phi_1(B_1) \\ &\vdots \\ \xi_k &= \phi_k(B_k) \\ \xi_{k+1} &= \phi_{k+1}(\varphi_1) \\ &\vdots \\ \xi_n &= \phi_n(\varphi_{n-k}) \end{aligned} \tag{3.34}$$

Due to the commutativity of the generators a new set of functions can be defined by

$$\zeta_{il}(B_i) = L_i b_{il} \tag{3.35}$$

where $i \in \{1, \dots, k\}$, $l \in \{1, \dots, n-k+1\}$, and $b_{il} \in B_i$. If we use the term (3.34) and (3.35) in equation (3.32) we obtain the following set of partial differential equations:

$$\sum_{l=1}^{n-k+1} \frac{\partial \phi_i}{\partial b_{il}} \zeta_{il}(B_i) = 1 \tag{3.36}$$

where $i \in \{1, \dots, k\}$. The functions $\phi_{k+1}, \dots, \phi_n$ can be chosen as arbitrary monotonous functions.

[1] They span an $(n-1)$–dimensional subspace of $\mathbb{R}^n$.

3.2.3 Two Parameter Groups and Fourier–Mellin Transform

To facilitate the understanding of the preceeding section, the two–dimensional case dealing with a two–parameter group is considered in more detail.

Obviously, the sets A_1, A_2, B_1 and B_2 consist of only one invariant each. Furthermore, $A_1 = B_2 = \{a_1\}$, $A_2 = B_1 = \{a_2\}$, and $Z = \emptyset$. Consequently, $\xi_1 = \phi_1(a_2)$, $\xi_2 = \phi_2(a_1)$, $\zeta_{11}(a_2) = L_1 a_2$, and $\zeta_{21}(a_1) = L_2 a_1$; and the equations (3.36) read

$$\frac{\partial \phi_1}{\partial a_2}\zeta_{11}(a_2) = 1 \qquad \text{and}$$
$$\frac{\partial \phi_2}{\partial a_1}\zeta_{21}(a_1) = 1.$$

These equations are solved by

$$\xi_1 = \phi_1(a_2) = \int \frac{1}{\zeta_{11}(a_2)} da_2 = \int \frac{1}{L_1 a_2} da_2 \qquad \text{and} \tag{3.37}$$
$$\xi_2 = \phi_2(a_1) = \int \frac{1}{\zeta_{21}(a_1)} da_1 = \int \frac{1}{L_2 a_1} da_1. \tag{3.38}$$

Typical groups of pattern distortions are rotations and change in scale (dilation). These groups are commutative and their generators are

$$L_1 = -x_2\partial_{x_1} + x_1\partial_{x_2}$$
$$L_2 = x_1\partial_{x_1} + x_2\partial_{x_2}$$

and the Lie bracket reads

$$[L_1, L_2] = -x_2\partial_{x_1} + x_1\partial_{x_2} - (x_1\partial_{x_2} - x_2\partial_{x_1}) = 0. \tag{3.39}$$

Consider a point in polar coordinates. Obviously, the rotation does not change the radius and the dilation does not change the angle of the point. Consequently, $a_1 = \sqrt{x_1^2 + x_2^2}$, $a_2 = \arctan\left(\frac{x_2}{x_1}\right)$, and $L_1 a_1 = L_2 a_2 = 0$. The functions ζ_{11} and ζ_{21} are calculated by:

$$\begin{aligned}
\zeta_{11}(a_2) &= (-x_2\partial_{x_1} + x_1\partial_{x_2}) \arctan\left(\frac{x_2}{x_1}\right) \\
&= -x_2 \frac{\partial \arctan\left(\frac{x_2}{x_1}\right)}{\partial x_1} + x_1 \frac{\partial \arctan\left(\frac{x_2}{x_1}\right)}{\partial x_2} \\
&= -x_2 \frac{x_1^2}{x_1^2 + x_2^2}\frac{-x_2}{x_1^2} + x_1 \frac{x_1^2}{x_1^2 + x_2^2}\frac{1}{x_1} \\
&= \frac{x_2^2}{x_1^2 + x_2^2} + \frac{x_1^2}{x_1^2 + x_2^2} \\
&= 1
\end{aligned} \tag{3.40}$$

and

$$
\begin{aligned}
\zeta_{21}(a_1) &= (x_1\partial_{x_1} + x_2\partial_{x_2})\sqrt{x_1^2+x_2^2} \\
&= x_1\frac{\partial\sqrt{x_1^2+x_2^2}}{\partial x_1} + x_2\frac{\partial\sqrt{x_1^2+x_2^2}}{\partial x_2} \\
&= x_1\frac{1}{2\sqrt{x_1^2+x_2^2}}2x_1 + x_2\frac{1}{2\sqrt{x_1^2+x_2^2}}2x_2 \\
&= \sqrt{x_1^2+x_2^2} \\
&= a_1.
\end{aligned}
\tag{3.41}
$$

Consequently, the partial differential equations are solved by

$$
\xi_1 = \phi_1(a_2) = \int da_2 = a_2 = \arctan\left(\frac{x_2}{x_1}\right) \tag{3.42}
$$

and

$$
\xi_2 = \phi_2(a_1) = \int \frac{1}{a_1}da_1 = \ln(a_1) = \ln\left(\sqrt{x_1^2+x_2^2}\right). \tag{3.43}
$$

These transformations of coordinates yield the Fourier–Mellin transform. Their Jacobian reads

$$
J(x_1,x_2) = \left|\det\begin{bmatrix} \frac{-x_2}{x_1^2+x_2^2} & \frac{x_1}{x_1^2+x_2^2} \\ \frac{x_1}{x_1^2+x_2^2} & \frac{x_2}{x_1^2+x_2^2} \end{bmatrix}\right| = \frac{1}{x_1^2+x_2^2} \tag{3.44}
$$

and the transform is calculated by

$$
\iint_{\mathbb{R}^2} f(x_1,x_2)e^{-2\pi\left(i_1u_1\arctan\left(\frac{x_2}{x_1}\right)+i_2u_2\ln\left(\sqrt{x_1^2+x_2^2}\right)\right)}\frac{1}{x_1^2+x_2^2}dx_1dx_2. \tag{3.45}
$$

Since the Fourier–Mellin transform is considered in many articles about image processing (e.g. [RSZ91, CDD94, FC94]) no examples have been worked out here. However, in the context of the cross group correlation in section 4.1 there will be some examples.

Instead of the Fourier–Mellin transform we consider another example in the sequel.

3.3 Application of the Invariant Kernels

3.3.1 The Projective Group

One of the most important groups which are of interest in image processing is the projective group. This group is constructed in the following way: take a three–dimensional scene and consider its projection on a two–dimensional screen (figure 3.6). The Y–coordinate on the

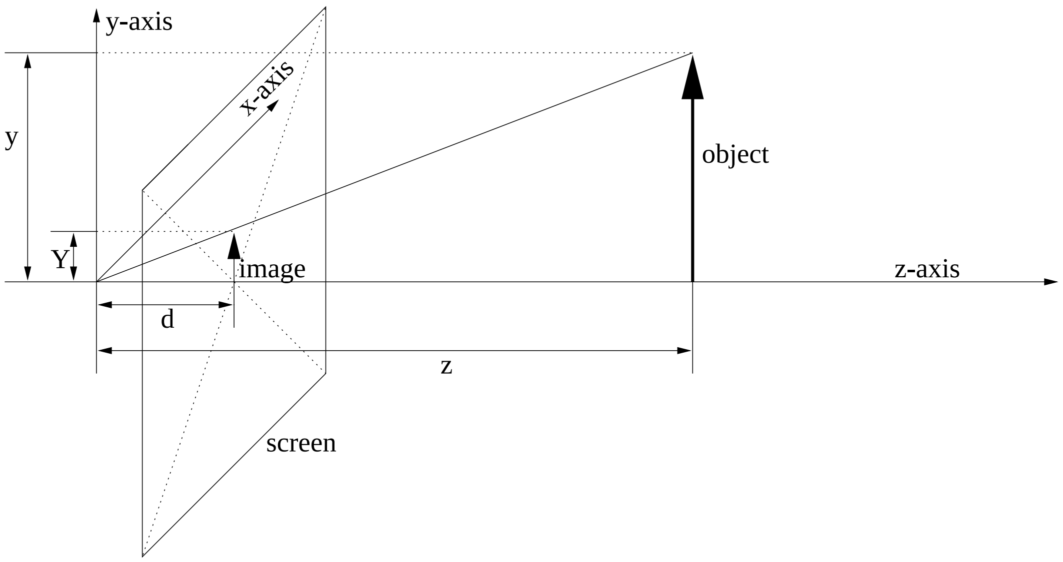

Figure 3.6: Projection of a scene on a screen

screen is calculated by

$$Y = d\frac{y}{z} \tag{3.46}$$

and the X–coordinate analogously reads

$$X = d\frac{x}{z}. \tag{3.47}$$

The effect of an arbitrary isometric group which is applied to a three–dimensional object can be calculated in the projective plane but there are groups which are more interesting than others. It depends on the application which group is considered most important. A commonly considered group is the projective group of SO(3). It describes the distortion of images taken by a camera which rotates around its projective centre (e.g. [SZ93]). For this model it is assumed that the objects do not move in the scene but only the camera.

This assumption is not always justified, of course. For example, in face–recognition, the camera is usually fixed and the head of the person is rotated with respect to the spine.

From this problem arises a projective mapping which no longer is a group. Using the concept of the previous sections, an approximation can be developed and is presented in the following.

Consider a plane[2] $p_z(x, y)$ which is rotated around a parallel to the y–axis at z (see figure 3.7). This group operation can be described in the following way:

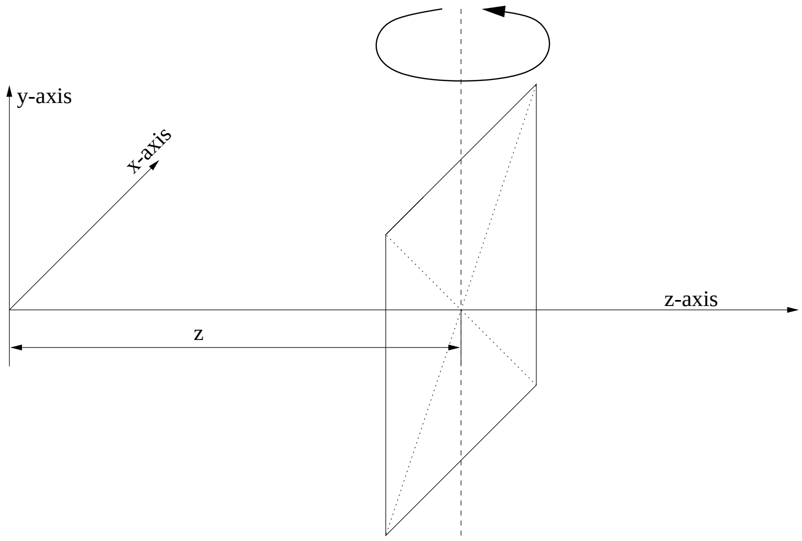

Figure 3.7: Rotation around a parallel to the y–axis

1. Move the object to the origin.
2. Rotate the object by the given angle.
3. Move the object to its original place.

These steps can be expressed by the following formula:

$$\begin{pmatrix} x' \\ y' \\ z' \end{pmatrix} = \begin{bmatrix} \cos\varphi & 0 & \sin\varphi \\ 0 & 1 & 0 \\ -\sin\varphi & 0 & \cos\varphi \end{bmatrix} \begin{pmatrix} x \\ y \\ z - z \end{pmatrix} + \begin{pmatrix} 0 \\ 0 \\ z \end{pmatrix} \tag{3.48}$$

So the new coordinates read:

$$\begin{aligned} x' &= x\cos\varphi \\ y' &= y \\ z' &= -x\sin\varphi + z \end{aligned} \tag{3.49}$$

[2]Obviously, it is a rather poor approximation to consider a face as a plane, but since the angle of rotation is bound it can be assumed. Besides, in other publications faces are treated as planes as well (e.g. Eigenfaces in [TP91]).

In the projective plane we obtain:

$$X' = d\frac{x'}{z'} = d\frac{x\cos\varphi}{-x\sin\varphi + z} = d\frac{X\cos\varphi}{-X\sin\varphi + d} \tag{3.50}$$

and

$$Y' = d\frac{y'}{z'} = d\frac{y}{-x\sin\varphi + z} = d\frac{Y}{-X\sin\varphi + d}. \tag{3.51}$$

Note that this mapping is not a group anymore, because the plane is not parallel to the projective plane if it is rotated. Nevertheless, the derivatives at the identity can be calculated:

$$\begin{aligned}
\left.\frac{\partial X'}{\partial\varphi}\right|_{\varphi=0} &= d\left(\frac{-X\sin\varphi}{-X\sin\varphi + d} - \frac{X\cos\varphi}{(-X\sin\varphi + d)^2}(-X\cos\varphi)\right)\Bigg|_{\varphi=0} = \frac{X^2}{d} \\
\left.\frac{\partial Y'}{\partial\varphi}\right|_{\varphi=0} &= -d\frac{Y}{(-X\sin\varphi + d)^2}(-X\cos\varphi)\Bigg|_{\varphi=0} = \frac{XY}{d}
\end{aligned} \tag{3.52}$$

These terms can be interpreted as coefficients of a generator of a group that is obtained by Taylor series expansion:

$$\begin{aligned}
\begin{pmatrix} X' \\ Y' \end{pmatrix} &= \exp\left(t\left(\frac{X^2}{d}\partial_X + \frac{XY}{d}\partial_Y\right)\right)\begin{pmatrix} X \\ Y \end{pmatrix} \\
&= \begin{pmatrix} X \\ Y \end{pmatrix} + \frac{t}{d}\begin{pmatrix} X^2 \\ XY \end{pmatrix} + \frac{t^2}{d^2 2}\begin{pmatrix} 2X^3 \\ X^2Y + X^2Y \end{pmatrix} + \frac{t^3}{d^3 6}\begin{pmatrix} 6X^4 \\ 4X^3Y + 2X^3Y \end{pmatrix}\cdots \\
&= \sum_{i=0}^{\infty}\left(\frac{t^i}{d^i i!}\begin{pmatrix} i!X^{i+1} \\ i!X^iY \end{pmatrix}\right) \\
&= \begin{pmatrix} X \\ Y \end{pmatrix}\sum_{i=0}^{\infty}\left(\frac{tX}{d}\right)^i \\
&\overset{\left|\frac{tX}{d}\right|<1}{=} \begin{pmatrix} X \\ Y \end{pmatrix}\frac{d}{d - tX}
\end{aligned} \tag{3.53}$$

Obviously, the calculated group (3.53) is an approximation of the transformations (3.50 and 3.51) for small angles φ. Assuming that $x, y < z$ and $d = 1$ the error of Y' is less than 5% if $\varphi < 0.52$ and the error of X' is less than 5% if $\varphi < 0.29$. Therefore, the overall error is less than 5% if the angle is less than $\pm 16.5°$. In these cases, the constraint $\left|\frac{tX}{d}\right| < |t| < 1$ is satisfied.

Finally, the projection of the considered transformation is well approximated by the group (3.53) in a wide range of the parameter. An invariant transform for that group can be applied in practical tasks as is shown in the experiments at the end of the next section.

3.3.2 Experiments

The transform which is invariant under group operations of (3.53) is derived and tested in this section. Note that it is not necessary to design a special transform. Instead, the image can be transformed into the canonical coordinates and a classical Fourier transform can be applied afterwards.

In order to obtain the canonical coordinates, the following partial differential equations have to be solved:

$$\frac{X^2}{d}\frac{\partial\xi}{\partial X} + \frac{XY}{d}\frac{\partial\xi}{\partial Y} = 1 \tag{3.54}$$

and

$$\frac{X^2}{d}\frac{\partial\eta}{\partial X} + \frac{XY}{d}\frac{\partial\eta}{\partial Y} = 0. \tag{3.55}$$

The equations are solved by

$$\xi(X,Y) = -\frac{d}{X} \tag{3.56}$$

and

$$\eta(X,Y) = \frac{Y}{X} \tag{3.57}$$

where $\eta(X,Y)$ is only one possible solution. These solutions can easily be verified by applying them to the differential equations:

$$\begin{aligned} \frac{X^2}{d}\frac{\partial\xi}{\partial X} + \frac{XY}{d}\frac{\partial\xi}{\partial Y} &= \frac{X^2}{d}\frac{d}{X^2} + \frac{XY}{d}0 = 1 \\ \frac{X^2}{d}\frac{\partial\eta}{\partial X} + \frac{XY}{d}\frac{\partial\eta}{\partial Y} &= \frac{X^2}{d}\frac{-Y}{X^2} + \frac{XY}{d}\frac{1}{X} = 0 \end{aligned} \tag{3.58}$$

In order to obtain the kernel of the transform the Jacobi–determinant must be evaluated:

$$J(X,Y) = \left|\det\begin{bmatrix} \frac{d}{X^2} & 0 \\ \frac{-Y}{X^2} & \frac{1}{X} \end{bmatrix}\right| = \left|\frac{d}{X^3}\right| \tag{3.59}$$

and hence, the kernel reads

$$K_P(X,Y,u,v) = e^{-2\pi(i_2 u_2 Y X^{-1} - i_1 u_1 d X^{-1})}\left|\frac{d}{X^3}\right|. \tag{3.60}$$

This kernel is invariant under the operation of a two–dimensional group. Consequently, we can find a second group besides (3.53) that does not change the magnitude spectrum.

In general, its generator reads $L = a(X,Y)\partial_X + b(X,Y)\partial_Y$ with a, b so that the following equations are satisfied:

$$a(X,Y)\frac{d}{X^2} + b(X,Y)0 = a(X,Y)\frac{d}{X^2} = 0 \tag{3.61}$$

$$a(X,Y)\frac{-Y}{X^2} + b(X,Y)\frac{1}{X} = 1 \tag{3.62}$$

The first equation implies that $a(X,Y) \equiv 0$. Hence, $b(X,Y) = X$ and

$$\exp(tX\partial_Y)\begin{pmatrix} X \\ Y \end{pmatrix} = \begin{pmatrix} X \\ Y \end{pmatrix} + \begin{pmatrix} 0 \\ tX \end{pmatrix} = \begin{pmatrix} X \\ Y + tX \end{pmatrix} \tag{3.63}$$

is the to–be–found group.

In order to show that the presented concept is working and that the approximation is correct for a wide range of parameters we have performed some experiments which are illustrated in the sequel. Consider a rectangular plane which is located parallel to the projective plane. This plane is rotated around the x–axis for five different angles. The projection of the plane can be seen in figure 3.8.

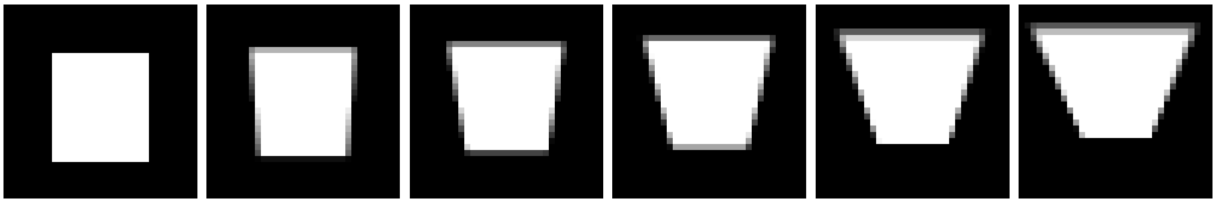

(a) Plane 0 (b) Plane 1 (c) Plane 2 (d) Plane 3 (e) Plane 4 (f) Plane 5

Figure 3.8: A plane manipulated by (3.50/3.51)

Assuming that the viewing distance in the experiments has been 1.0 the fraction $\frac{x_{max}}{z}$ is 1.6 which explains the enormous distortion. The plane seems to slide upwards with the angle increasing but this is only due to the perspective effect. The rotation angles of the planes can be found in table 3.1.

Plane no.	0	1	2	3	4	5
Angle	0°	5.7°	11.5°	17.2°	22.9°	28.6°

Table 3.1: Rotation angles of the planes

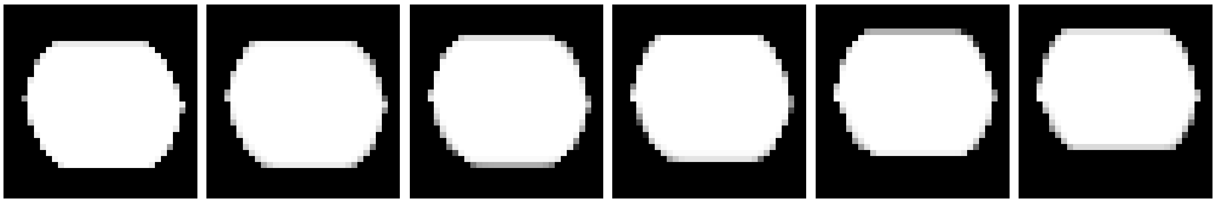

(a) Plane 0 (b) Plane 1 (c) Plane 2 (d) Plane 3 (e) Plane 4 (f) Plane 5

Figure 3.9: The planes from figure 3.8 in canonical coordinates according to (3.56/3.57)

The images are transformed into canonical coordinates by use of formulae (3.56) and (3.57). The resulting images are represented in figure 3.9.

These new signals are Fourier transformed. The so resulting magnitude spectra can be found in figure 3.10.

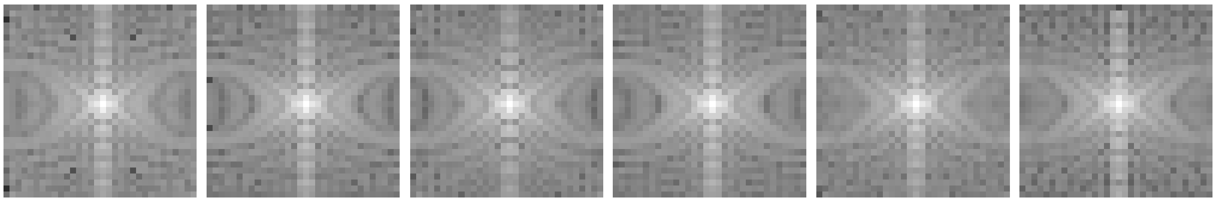

(a) Plane 0 (b) Plane 1 (c) Plane 2 (d) Plane 3 (e) Plane 4 (f) Plane 5

Figure 3.10: The magnitude spectra of the signals from figure 3.9

All the magnitude spectra are supposed to be identical, but due to the poor resolution and the approximation error they are only similar. In the following pictures (figure 3.11) those pixels are coloured white where the difference between the spectrum of plane 0 and

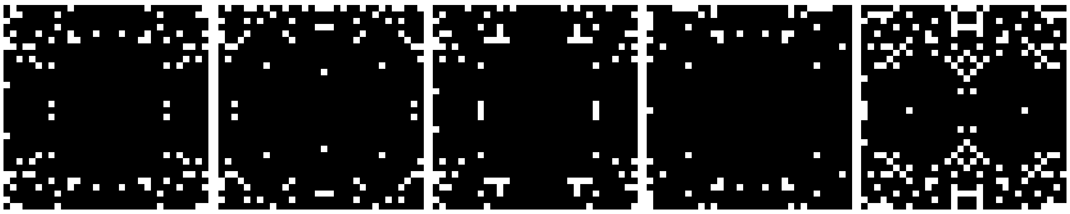

(a) Plane 0-1 (b) Plane 0-2 (c) Plane 0-3 (d) Plane 0-4 (e) Plane 0-5

Figure 3.11: The points which are different in the spectra from figure 3.10

plane i is greater than 8% of the maximum brightness. Obviously, the fifth plane shows quite a high error rate. The reason for the increase of the error rate is established in the approximation which becomes worse the wider the angle.

In order to show that other group operations result in different magnitude spectra the plane is scaled and the whole procedure is repeated for this new image (see figure 3.12). Obviously, the difference between the spectrum of the original plane and the new one is bigger than the differences illustrated in figure 3.11.

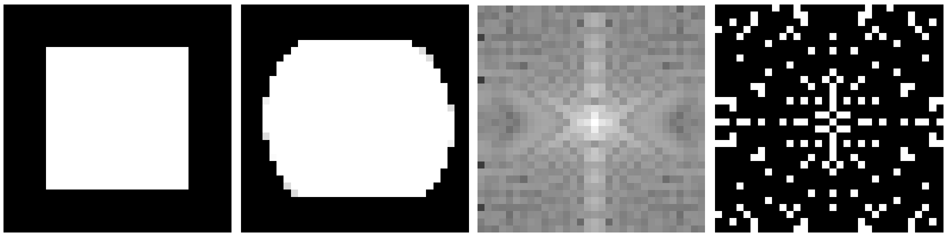

(a) Scaled plane (b) Canonical coordinates (c) Magnitude spectrum (d) Difference to 3.10(a)

Figure 3.12: A plane with different size has a much greater error in the spectrum

Note that the error rate in figure 3.11 rises with high frequencies. The bilinear approximation of the edges of the plane might be the reason for this error. The error rate in figure 3.12(d) instead is almost equally distributed across the whole frequency domain.

Finally, we have verified that the concept of canonical coordinates works correctly even if we use the approximation of a mapping instead of the mapping itself.

3.3.3 Non–Commutative Groups

The presented concept of canonical coordinates has one great disadvantage: the groups under which the transform is invariant must commute. Unfortunately, in most cases the groups of interest are not commutative (e.g. shifting and rotations). Segman and Zeevi proposed a solution of the problem of affine transforms in their article [SZ93]. In a first step, the complex Fourier spectrum of the signal is calculated. Then, the magnitude spectrum is transformed by the Fourier–Mellin transform. Due to the affine theorem the spectrum of a rotated and scaled signal is transformed in a reciprocal manner. Therefore, the Fourier–Mellin transform of such a magnitude spectrum is invariant. Note that this approach (which is often referred to as Fourier–Mellin invariant, *FMI*, see [CDD94]) is only a weak invariance concept. By the way, the affine theorem for Clifford spectra is different from that one of complex spectra (see e.g. [Bül98]).

Consequently, another approach has to be developed for solving the problem of the non–commutativity with a strong invariance concept.

Chapter 4

Concepts for Pattern Matching

In this chapter, the concept of canonical coordinates is applied to the cross correlation of two signals, which yields a generalised correlation that is called *cross group correlation*. This new correlation function can be calculated via the frequency domain as the classical cross correlation. Hence, a correlation theorem is obtained. The theoretical results are underpinned by experiments.

The second part deals with a concept which enhances the results of correlations. This concept is called *(symmetric) phase only matched filtering* and is abbreviated (S)POMF. The POMF, and especially the SPOMF, yield sharp correlation peaks which are independent of signal energy. Again, the theoretical results are verified by experiments.

In the last part, the dimension of the parameter space of the correlation functions is extended. Beginning with classical cross correlations, a correlation with parameter space of doubled dimension is derived for the combination of an n–dimensional translation and an n–dimensional linear group (*double parametric cross group correlation*). Just as for the cross group correlation, a correlation theorem is formulated and verified by an experiment.

4.1 The Generalised Cross Correlation

In this first part, we generalise the cross correlation by substituting shifting with an arbitrary group within the correlation integral. This integral is called *cross group correlation* (CGC) in the following sections. Furthermore, we state and prove a correlation theorem for the CGC and verify it in an experiment.

4.1.1 The Cross Group Correlation

In their article [SZ93], Segman and Zeevi suggested to consider the convolution or cross correlation[1] in such a way that the shifting inside the integrand is a group operation. So they generalised the cross correlation to arbitrary groups. Due to the change of the volume of each infinitesimal interval of the coordinate system an additional measure which acts as a weighting function must be introduced.

The measure which is needed can be calculated easily by the Jacobian for "nice" groups, i.e. groups for which the Jacobian of the canonical coordinate transform exists. The introduction of the measure can be justified by using the classical correlation in canonical coordinates (see [GMPO95]). When the integration variable is substituted the Jacobian must be multiplied with the integrand. For the following derivation let $\boldsymbol{x}(\boldsymbol{\xi})$ be the inverse of the transformation to canonical coordinates which lets the group G act as the translation group and let $f(\boldsymbol{t}, \boldsymbol{x})$ be the group operation with parameter vector $\boldsymbol{t}$ at point $\boldsymbol{x}$. In contrast to the classical correlation function (which is a function of the same variable as the original functions) our group correlations are functions of a new variable $\boldsymbol{t}$. The new variable is justified by the fact that the domain on which it is defined is generally different from the spatial domain.

$$v_1(\boldsymbol{x}(-\boldsymbol{\xi})) * v_2(\boldsymbol{x}(\boldsymbol{\xi})) = \int v_1(\boldsymbol{x}(\boldsymbol{\eta}))v_2(\boldsymbol{x}(\boldsymbol{t}+\boldsymbol{\eta}))d\boldsymbol{\eta} \overset{\tau=x(\eta)}{=} \int v_1(\boldsymbol{\tau})v_2(f(\boldsymbol{t},\boldsymbol{\tau}))\left(\frac{\partial\boldsymbol{\tau}}{\partial\boldsymbol{\eta}}\right)^{-1} d\boldsymbol{\tau} \tag{4.1}$$

The derivation (4.1) is illustrated in the following graph:

$$\begin{tikzcd}
\boxed{\text{two signals } v_1, v_2} \arrow[d, "\text{canonical coordinate transform}"'] \\
\boxed{v_1, v_2 \text{ in canonical coordinates}} \arrow[d, "\text{cross correlation}"'] \\
\boxed{\text{cross group correlation function } C_G^{v_1 v_2}}
\end{tikzcd}$$

Figure 4.1: The construction of the cross group correlation

[1] Note that the cross correlation of two signals is the convolution of one signal with the reflected version of the other one.

Consider, for example, the group of dilations on the one–dimensional Euclidean space: $x \longrightarrow e^t x$ where $t, x \in \mathbb{R}$. The canonical coordinates are obtained by the logarithm, hence the inverse transform is the exponential function, and equation (4.1) reads

$$v_1(x(-\xi)) * v_2(x(\xi)) = \int_{\mathbb{R}+} v_1(e^\eta) v_2(e^{(t+\eta)}) d\eta \overset{\tau = e^\eta}{=} \int_{\mathbb{R}+} v_1(\tau) v_2(e^t \tau) \frac{1}{\tau} d\tau. \tag{4.2}$$

Consequently, the cross correlation is defined in the following way, where $\mathbb{D}$ is defined as in section 3.2.1 and v_1, v_2 are defined on $\mathbb{D}$:

Definition 22 (Cross group correlation) *Let G be an arbitrary n–dimensional group of transformations of the n–dimensional Euclidean space, let $f(\boldsymbol{t}, \boldsymbol{x})$ be the operation of this group with the parameter vector $\boldsymbol{t}$, and let $J(\boldsymbol{\tau})$ be the Jacobian of the canonical coordinate transform. The function*

$$C_G^{v_1 v_2}(\boldsymbol{t}) = \int_{\mathbb{D}} v_1(\boldsymbol{\tau}) v_2(f(\boldsymbol{t}, \boldsymbol{\tau})) J(\boldsymbol{\tau}) d\boldsymbol{\tau} \tag{4.3}$$

is called the cross group correlation of v_1 and v_2.

If G is the group of translations (4.3) yields the classical cross correlation.

$$C^{v_1 v_2}(t) = \int_{\mathbb{R}} v_1(\tau) v_2(t + \tau) d\tau = v_1(-x) * v_2(x)|_{x=t} \tag{4.4}$$

If $n = 1$ and G is the group of dilation (4.3) yields formula (4.2).

In the example (4.2) the generalised correlation (4.3) scales one of the two signals to every size and multiplies them afterwards. The maximum is reached if they are scaled to the same size. In canonical coordinates the signal is not scaled but shifted, so the correlation is maximal if the offsets of both signals are identical as in the classical correlation. Note that there are some problems concerning the singularities of the canonical coordinate transform and the sampling theorem. They are considered shortly in section 4.3.4.

4.1.2 The Cross Group Correlation Theorem

In order to calculate the cross group correlation more rapidly it is useful to have a theorem which makes it possible to calculate it in the frequency domain. This theorem is called the *cross group correlation theorem.* It can be proved in several ways. One possible way is to use the classical correlation theorem in canonical coordinates as in the derivation of the cross group correlation.

$$\begin{tikzcd}
\boxed{\text{two signals } v_1, v_2} \arrow[d, "\text{canonical coordinate transform}"'] \\
\boxed{v_1, v_2 \text{ in canonical coordinates}} \arrow[d, "\text{Fourier transform}"'] \\
\boxed{\text{invariant spectra of } v_1, v_2} \arrow[d, "\text{pointwise multiplication}"'] \\
\boxed{\text{Fourier transform of CGC function } C_G^{v_1 v_2}}
\end{tikzcd}$$

Figure 4.2: The construction of the cross group correlation

In this section the theorem will be proved in a more basic manner. Therefore, we prove the following auxiliary theorem before the cross group correlation theorem can be formulated .

Theorem 9 (Jacobian identity) *Let G be an $n-$parameter group, L its Lie algebra and $\boldsymbol{\xi} : \mathbb{D} \longrightarrow \mathbb{R}^n$ the transformation of coordinates so that G acts as the translation group G'. Furthermore, we estimate $\boldsymbol{x}$ by the group operation $f(\boldsymbol{t}, \boldsymbol{x}_0) = \boldsymbol{x}$ using the parameter vector $\boldsymbol{t}$ and an arbitrary original point $\boldsymbol{x}_0$. Then the following equation is satisfied:*

$$\left| \frac{\partial \boldsymbol{t}}{\partial \boldsymbol{x}} \right| = \left| \frac{\partial \boldsymbol{\xi}}{\partial \boldsymbol{x}} \right| = J(\boldsymbol{x}). \tag{4.5}$$

Proof:

From the conditions (3.32) we get the following group operations of G' in canonical coordinates:

$$\boldsymbol{\xi}(\boldsymbol{x}) = \boldsymbol{\xi}(f(\boldsymbol{t}, \boldsymbol{x}_0)) = \boldsymbol{t} + \boldsymbol{\xi}(\boldsymbol{x}_0) = \boldsymbol{t} + \boldsymbol{\xi}_0. \tag{4.6}$$

Hence, the partial derivations of $\boldsymbol{\xi}(\boldsymbol{t})$ form the identity matrix:

$$\begin{bmatrix} \frac{\partial \xi_1}{\partial t_1} & \frac{\partial \xi_1}{\partial t_2} & \cdots & \frac{\partial \xi_1}{\partial t_n} \\ \frac{\partial \xi_2}{\partial t_1} & \ddots & & \vdots \\ \vdots & & \ddots & \frac{\partial \xi_{n-1}}{\partial t_n} \\ \frac{\partial \xi_n}{\partial t_1} & \cdots & \frac{\partial \xi_n}{\partial t_{n-1}} & \frac{\partial \xi_n}{\partial t_n} \end{bmatrix} = \begin{bmatrix} 1 & 0 & \cdots & 0 \\ 0 & \ddots & & \vdots \\ \vdots & & \ddots & 0 \\ 0 & \cdots & 0 & 1 \end{bmatrix} = \mathrm{Id}_n\,. \tag{4.7}$$

On the other hand, due to the determinant theorem[2] we have

$$1 = \left|\frac{\partial \boldsymbol{\xi}}{\partial \boldsymbol{t}}\right| = \left|\frac{\partial \boldsymbol{\xi}}{\partial \boldsymbol{x}}\right| \left|\frac{\partial \boldsymbol{x}}{\partial \boldsymbol{t}}\right| = J(\boldsymbol{x}) \left|\frac{\partial \boldsymbol{x}}{\partial \boldsymbol{t}}\right|. \tag{4.8}$$

Finally, we obtain

$$J(\boldsymbol{x}) = \left|\frac{\partial \boldsymbol{x}}{\partial \boldsymbol{t}}\right|^{-1} = \left|\frac{\partial \boldsymbol{t}}{\partial \boldsymbol{x}}\right| \tag{4.9}$$

(see e.g. [BHW92]) and thus the theorem is proved.

□

Example: Consider the projection of the two–dimensional rotations onto a line (i.e. PSO(2)). Let the projective line be located at $x = 1$. Consequently, we obtain the projective coordinate $z = \frac{y}{x}$, and the projection of a rotated point

$$\begin{pmatrix} x \\ y \end{pmatrix} = \begin{bmatrix} \cos t & -\sin t \\ \sin t & \cos t \end{bmatrix} \begin{pmatrix} x_0 \\ y_0 \end{pmatrix} \tag{4.10}$$

reads

[2]The determinant of the product of two matrices is equal to the product of the determinants of the two matrices.

$$z = \frac{y}{x} = \frac{x_0 \sin t + y_0 \cos t}{x_0 \cos t - y_0 \sin t} = \frac{\sin t + z_0 \cos t}{\cos t - z_0 \sin t} \tag{4.11}$$

and we obtain its derivative in terms of z as

$$\frac{dz}{dt} = \frac{\cos t - z_0 \sin t}{\cos t - z_0 \sin t} - \frac{\sin t + z_0 \cos t}{(\cos t - z_0 \sin t)^2}(-\sin t - z_0 \cos t) = 1 + z^2. \tag{4.12}$$

On the other hand, we derive the canonical transform as

$$\xi(z) = \arctan z \tag{4.13}$$

and its derivative reads

$$\frac{d\xi(z)}{dz} = \frac{1}{1 + z^2} \tag{4.14}$$

so that theorem 9 is satisfied.

Now the cross group correlation theorem is formulated and proved. It is derived directly from the classical convolution theorem applied to the signals in canonical coordinates. Consequently, this theorem makes it possible to calculate the cross group correlation via the frequency domain which is quite advantageous because the Fourier transform can be performed with less complexity using FFT–algorithms.

Theorem 10 (Cross group correlation theorem) *The Fourier transform of the cross group correlation is equal to the product of the invariant spectrum of the second signal and the reflected invariant spectrum of the first one.*

$$\mathcal{F}\{C_G^{v_1 v_2}(\boldsymbol{t})\} = \mathcal{T}_G\{v_1\}(-\boldsymbol{u})\mathcal{T}_G\{v_2\}(\boldsymbol{u}) \tag{4.15}$$

Proof:

Using the previous definitions the theorem can directly be derived:

$$\begin{aligned}
\mathcal{F}\{C_G^{v_1 v_2}(\boldsymbol{t})\} &= \int_{\mathbb{R}^n} C_G^{v_1 v_2}(\boldsymbol{t}) e^{-2\pi \boldsymbol{t} I_n \boldsymbol{u}^T} d\boldsymbol{t} \\
&= \int_{\mathbb{R}^n} \int_{\mathbb{D}} v_1(\boldsymbol{\tau}) v_2(f(\boldsymbol{t}, \boldsymbol{\tau})) J(\boldsymbol{\tau}) d\boldsymbol{\tau} e^{-2\pi \boldsymbol{t} I_n \boldsymbol{u}^T} d\boldsymbol{t} \\
&= \int_{\mathbb{R}^n} \int_{\mathbb{D}} v_1(\boldsymbol{\tau}) v_2(f(\boldsymbol{t}, \boldsymbol{\tau})) e^{-2\pi(\boldsymbol{\xi}(\boldsymbol{\tau}) + \boldsymbol{t} - \boldsymbol{\xi}(\boldsymbol{\tau})) I_n \boldsymbol{u}^T} J(\boldsymbol{\tau}) d\boldsymbol{\tau} d\boldsymbol{t}
\end{aligned}$$

where $\boldsymbol{\xi}(\boldsymbol{\tau})$ lets G act as the translation group

$$\begin{aligned}
&= \int_{\mathbb{R}^n} \int_{\mathbb{D}} v_1(\boldsymbol{\tau}) v_2(f(\boldsymbol{t}, \boldsymbol{\tau})) e^{-2\pi(\boldsymbol{\xi}(f(\boldsymbol{t},\boldsymbol{\tau})) - \boldsymbol{\xi}(\boldsymbol{\tau})) I_n \boldsymbol{u}^T} J(\boldsymbol{\tau}) d\boldsymbol{\tau} d\boldsymbol{t} \\
&\overset{\boldsymbol{z}=f(\boldsymbol{t},\boldsymbol{\tau})}{=} \int_{\mathbb{D}} v_1(\boldsymbol{\tau}) \int_{\mathbb{D}} v_2(\boldsymbol{z}) e^{-2\pi \boldsymbol{\xi}(\boldsymbol{z}) I_n \boldsymbol{u}^T} \left| \frac{\partial \boldsymbol{t}}{\partial \boldsymbol{z}} \right| d\boldsymbol{z} e^{-2\pi \boldsymbol{\xi}(\boldsymbol{\tau}) I_n (-\boldsymbol{u})^T} J(\boldsymbol{\tau}) d\boldsymbol{\tau} \\
&\overset{\text{theorem 9}}{=} \int_{\mathbb{D}} v_1(\boldsymbol{\tau}) e^{-2\pi \boldsymbol{\xi}(\boldsymbol{\tau}) I_n (-\boldsymbol{u})^T} J(\boldsymbol{\tau}) d\boldsymbol{\tau} \int_{\mathbb{D}} v_2(\boldsymbol{z}) e^{-2\pi \boldsymbol{\xi}(\boldsymbol{z}) I_n \boldsymbol{u}^T} J(\boldsymbol{z}) d\boldsymbol{z} \qquad (4.16) \\
&= \int_{\mathbb{D}} v_1(\boldsymbol{\tau}) e^{-2\pi \boldsymbol{\xi}(\boldsymbol{\tau}) I_n (-\boldsymbol{u})^T} J(\boldsymbol{\tau}) d\boldsymbol{\tau} \mathcal{T}_G\{v_2\}(\boldsymbol{u}) \\
&= \mathcal{T}_G\{v_1\}(-\boldsymbol{u}) \mathcal{T}_G\{v_2\}(\boldsymbol{u})
\end{aligned}$$

so that the theorem is proved.

□

In the following experiments we check theorem 10 and show that the magnitudes of the maxima of the cross group correlation functions are independent of the group parameter. This is an important fact because the absolute value of the maximum is a measure of how similar the signals are. The value of the maximum is constant because scaling in the original coordinates is changed to shifting in canonical coordinates, so that the energy is not changed. Furthermore, the cross group correlation function can be normalised, referring to the energy of the first signal (the one that is not scaled in the correlation integral).

4.1.3 Experiments on 1–D Cross Group Correlation

In order to check theorem 10 under practical application we have performed some experiments using the Khoros system. The Khoros environment used is illustrated in figure 4.3.

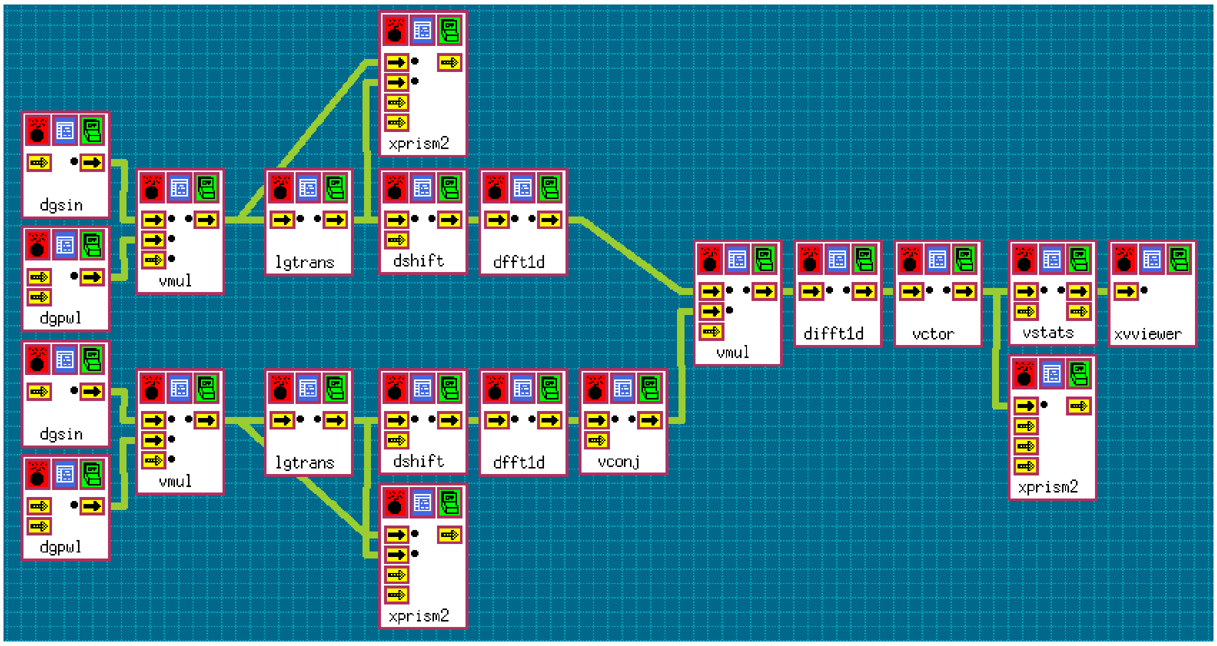

Figure 4.3: Khoros environment for the following experiments

On the left hand side the test signals are generated which are then transformed to canonical coordinates by `lgtrans` which performs the following mapping:

$$g(x) = v((N-1)^{\frac{x}{N-1}}) \tag{4.17}$$

where v is the input signal, g is the output signal and N is the size of the domain.

For the glyph `lgtrans` we assume that the signal v is a sampled continuous signal, so that values between the sampling points must be interpolated. Although the theoretically correct interpolation would be sinc–interpolation the results are more accurate and calculated faster if linear interpolation is used. After mapping the signals they are transformed into the frequency domain and the second spectrum is flipped (conjugated). After multiplying and transforming them back into the spatial domain the correlation functions and the maxima are put out.

In figure 4.4(a)–(d) the signals which have been generated to test the applicability of the cross group correlation are represented. The signals themselves are plotted in solid lines; the signals in canonical coordinates are plotted in dotted lines.

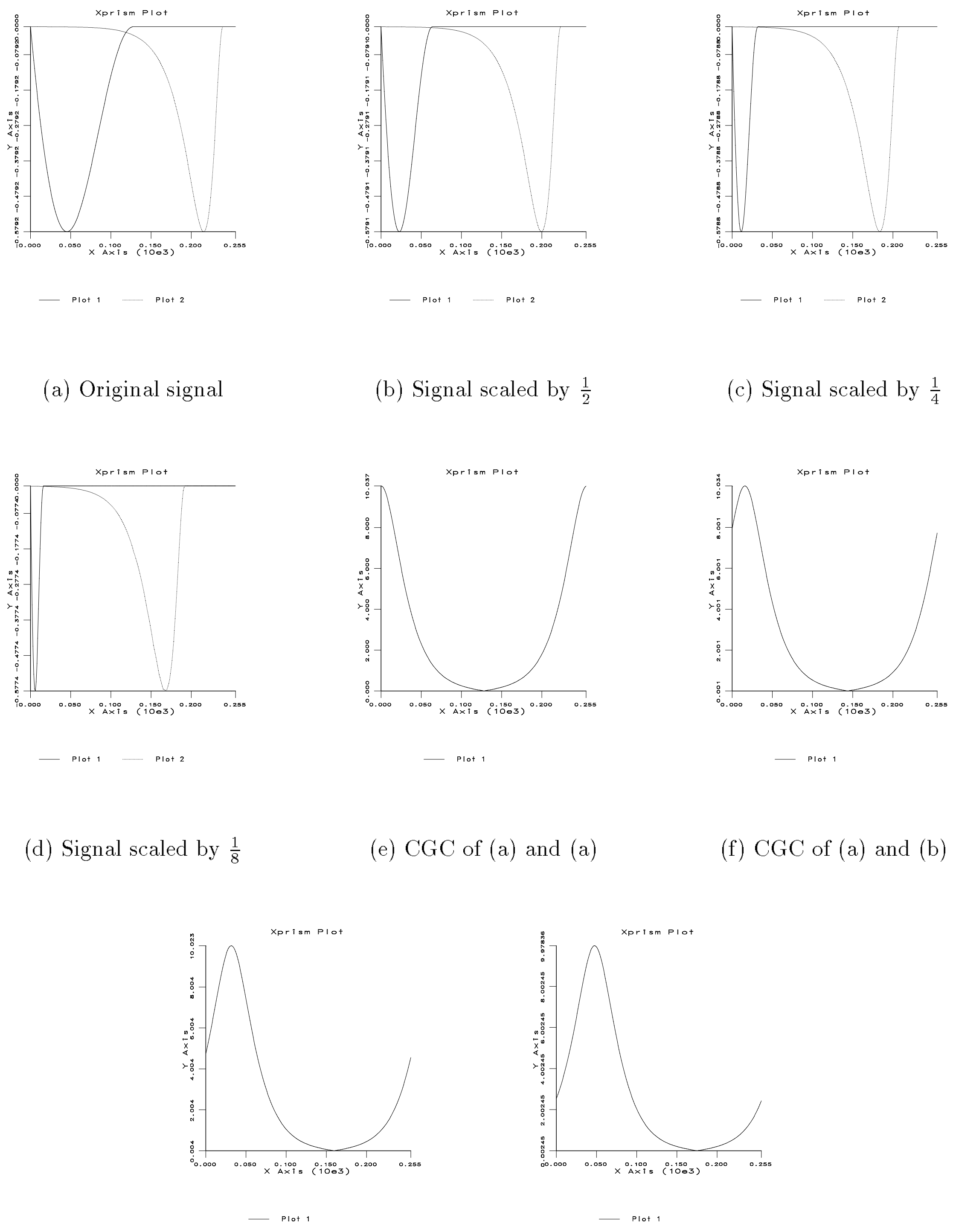

(a) Original signal

(b) Signal scaled by $\frac{1}{2}$

(c) Signal scaled by $\frac{1}{4}$

(d) Signal scaled by $\frac{1}{8}$

(e) CGC of (a) and (a)

(f) CGC of (a) and (b)

(g) CGC of (a) and (c)

(h) CGC of (a) and (d)

Figure 4.4: The generated signal in different scales and the corresponding CGC

The images in figure 4.4(e)–(h) show the result of the cross group correlation (CGC). It is obvious that the positions of the maxima of the correlation functions describe a linear dependency from the scaling parameter.

If we consider the scaling of the coordinate system instead of the scaling of the signal we obtain the inverse scale parameter. These parameters can be calculated from the correlation functions by

$$t = \ln(N-1)\frac{x_{max}}{N-1}. \tag{4.18}$$

The results can be found in the following table 4.1. The signal length is $N = 256$.

Experiment no.	1	2	3	4
Scaling parameter t	0	ln 2	ln 4	ln 8
Scaled by (e^t)	1	2	4	8
Maximum at	0	32	64	96
Calculated scaling	1	2.004	4.018	8.054
Error	±0.011	±0.022	±0.044	±0.087

Table 4.1: Experimental results

Note that we simply take the position of the highest value as the maximum. Hence, the real maximum might be located at $x_{max} \pm 0.5$. The error which results from this inaccuracy can be found in the last line of table 4.1. Obviously, all calculated parameters are situated between the bounds of the calculated error.

4.2 Phase–Only Matched Filtering

Phase–only matched filtering (POMF) has already been proposed in 1984 by J. L. Horner and P. D. Gianino [HG84]. This concept utilises the fact that the structure of a signal is mainly contained in the phase of its spectrum but not in its magnitude. The authors made experiments which show that the correlation peak is much sharper if only the phase is used. Even noisy signals produce more significant correlation functions if the magnitude information is omitted.

Q. Chen, M. Defrise and F. Deconinck applied the concept of POMF and of symmetric phase–only matched filtering (SPOMF) for the comparison of Fourier–Mellin invariants [CDD94]. They performed experiments with both concepts and noisy signals. According to these experiments the peaks of correlations using SPOMF are even sharper than those employing POMF.

4.2.1 Derivation

Consider the classical correlation theorem. The cross correlation function of two signals can be calculated by multiplying the flipped spectrum of the first signal with the second spectrum (see theorem 10). Assume that the first signal is a filter and the other one is the signal which is to be manipulated or recognised. If the spectrum of the filter is divided by its magnitude spectrum we obtain its phase spectrum[3]. Instead of multiplying the spectrum of the second spectrum with the flipped spectrum of the first signal we only multiply it with the phase spectrum. Hence, POMF is linear only with respect to the signal but it is not bilinear as classical filtering.

Definition 23 (Phase–only matched filtering) *Let $v(\boldsymbol{x})$ be an arbitrary n–dimensional signal, $V(\boldsymbol{u})$ its spectrum, $h(\boldsymbol{x})$ an arbitrary filter, and $H(\boldsymbol{u})$ the corresponding transfer function. Then, the result $w(\boldsymbol{x})$ of the POMF is calculated by:*

$$w(\boldsymbol{x}) = \mathcal{F}^{-1}\left\{ V(\boldsymbol{u}) \frac{H(-\boldsymbol{u})}{|H(-\boldsymbol{u})|} \right\}. \tag{4.19}$$

The symmetric POMF which is mentioned above is defined analogously. We do not only divide the transfer function by its magnitude spectrum but also the spectrum of the signal. Hence, SPOMF is a nonlinear filtering.

[3]The term phase spectrum usually means the function of the phase φ but in this thesis we refer to the function $e^{i\varphi}$ if we use this term.

Definition 24 (Symmetric phase–only matched filtering) *Let $v(\boldsymbol{x})$ be an arbitrary n–dimensional signal, $V(\boldsymbol{u})$ its spectrum, $h(\boldsymbol{x})$ an arbitrary filter, and $H(\boldsymbol{u})$ the corresponding transfer function. Then, the result $w(\boldsymbol{x})$ of the SPOMF is calculated by:*

$$w(\boldsymbol{x}) = \mathcal{F}^{-1}\left\{\frac{V(\boldsymbol{u})}{|V(\boldsymbol{u})|}\frac{H(-\boldsymbol{u})}{|H(-\boldsymbol{u})|}\right\}. \tag{4.20}$$

Consider the following example. Let $v(\boldsymbol{x})$ be the translated version of the signal $h(\boldsymbol{x})$. Then, the product of equation (4.20) results in a difference of the phases, where the difference at each point $\boldsymbol{u}$ is just the modulation term which corresponds to the translation vector $\boldsymbol{t}$. Consequently, we calculate the following Fourier transform:

$$w(\boldsymbol{x}) = \mathcal{F}^{-1}\left\{e^{-2\pi \boldsymbol{t} I_n \boldsymbol{u}^T}\right\}. \tag{4.21}$$

This transform is well known:

$$w(\boldsymbol{x}) = \delta_0(\boldsymbol{x} - \boldsymbol{t}) \tag{4.22}$$

Hence, SPOMF ends up in a (theoretically) perfect Dirac impulse. In practical applications, however, the results of SPOMF are quite different. The correlation becomes very noisy because of the noise contained in the signal and in particular because of the sampling error. If the Dirac impulse is not exactly placed on any of the sample points, its amplitude is decreased due to its little spatial extension. Hence, under real conditions the POMF is more stable, as shown in the experiments.

The POMF can also be interpreted from another point of view: let a noiseless filter and a noisy signal be correlated and do not divide the spectrum of the filter by its magnitude spectrum, but instead the spectrum of the signal. In general, the part of the spectrum which is created by the noise is located at other (higher) frequencies then the structural information. The transfer function still contains its magnitude information and hence, those parts of the spectrum which are typical of the filter have great magnitude. Consequently, they also have more weight in the correlation. Compared to the SPOMF the product of the spectra is the same except for the additional weighting by the magnitude spectrum of the transfer function. This interpretation is only correct if the filter is noiseless, because noise would distort the magnitude spectrum of the transfer function in such a way, that noise of the signal would be increased instead of being decreased. This is the reason why a POMF does not work as accurately as described above if it is linear with respect to the signal because the magnitude spectrum of the signal would increase the noisy part of the resulting correlation function.

4.2.2 Experiments on 1–D CGC Using (S)POMF

The concepts of the (S)POMF and the cross group correlation can also be combined. Based on the experiments on cross group correlation (figure 4.3 on page 77) the modified Khoros workspace (as illustrated in figure 4.5) has been constructed (POMF version).

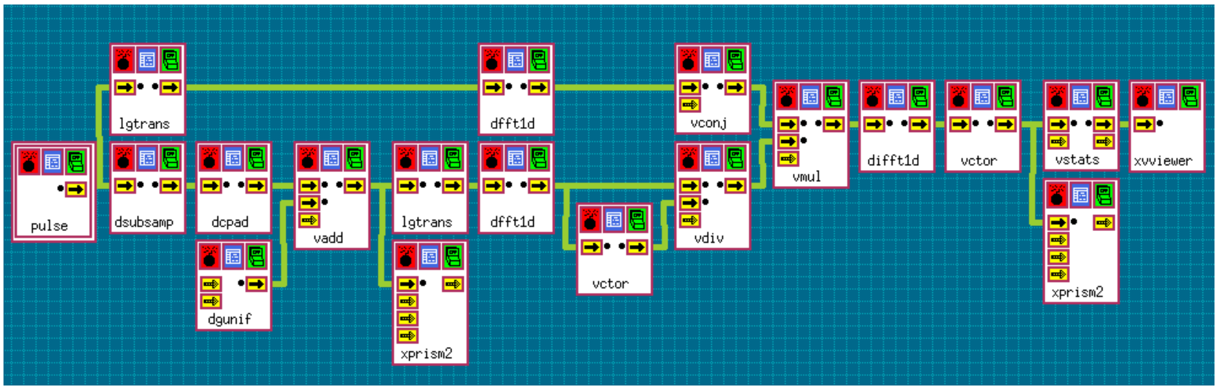

Figure 4.5: Khoros workspace for 1–D cross group correlation (POMF)

The input signals are now periodic pulses which have maximum spatial and frequency extension. One signal (the filter) is noiseless (see figure 4.6(a)) and the other one is superposed by additive uniform noise. The signal to noise ratio for the signal in figure 4.6(b) amounts to

$$SNR = 10 \log_{10} \frac{E_f}{E_n} \, \mathrm{dB} = 10 \log_{10} 23.3 \, \mathrm{dB} = 13.7 \, \mathrm{dB} \tag{4.23}$$

with E_f, E_n being the energy of the signal and the noise respectively. This noisy signal is shrunk by the factors 2 and 4 respectively (see figure 4.6) so that the SNR decreases by 3dB and 6dB respectively. For the signal in figure 4.6(e) which is scaled by $\frac{1}{2}$ we have

$$SNR = 10 \log_{10} \frac{E_f}{E_n} \, \mathrm{dB} = 10 \log_{10} 3.16 \, \mathrm{dB} = 5.0 \, \mathrm{dB}. \tag{4.24}$$

In the first four experiments the correlation functions are calculated using POMF. The spectrum of the noisy pulses is divided by its magnitude spectrum and multiplied by the transfer function. The inverse Fourier transform yields the correlation functions which can be found in figure 4.7(a)–(d) on page 84.

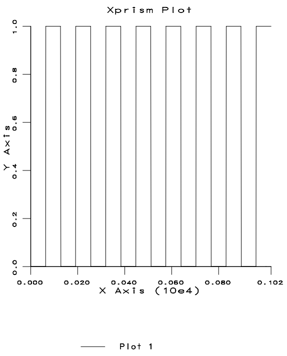

(a) Pulse signal

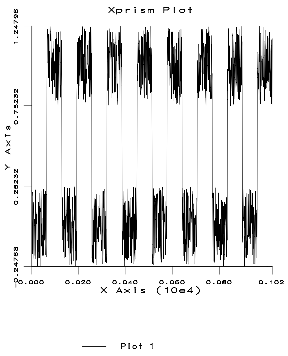

(b) Noisy pulse signal scale 1

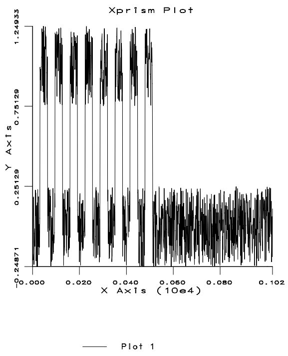

(c) Noisy pulse signal scale $\frac{1}{2}$

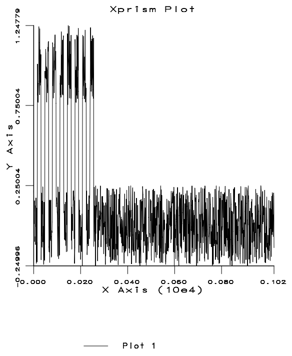

(d) Noisy pulse signal scale $\frac{1}{4}$

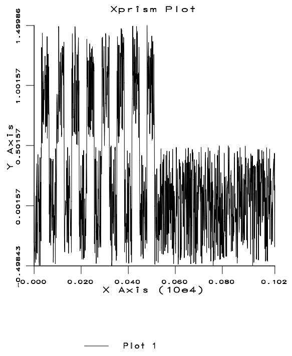

(e) Noisier pulse signal scale $\frac{1}{2}$

Figure 4.6: Pulse signals

Obviously, the peaks are very sharp and the distortion in the correlation function is less than the noise in the original signals. The increase of noise in the signal in figure 4.6(e) compared to the one in figure 4.6(c) yields only little distortion in the correlation signals (see figure 4.7(b) and (d)).

In the last two experiments the correlation is calculated by SPOMF. Hence, both spectra are divided by their magnitude spectra. The resulting correlation functions are represented in figure 4.7(e) and (f). These correlation functions show that the increase of noise is more critical if SPOMF is used.

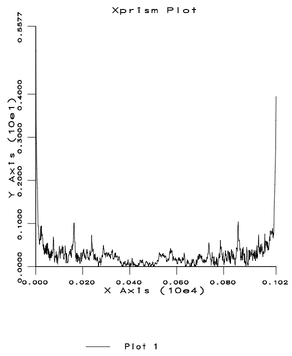

(a) POMF (a)-(b)

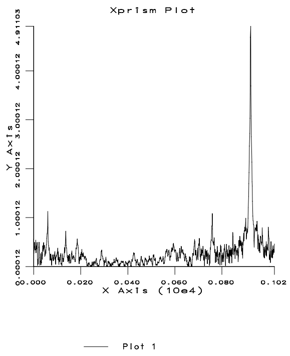

(b) POMF (a)-(c)

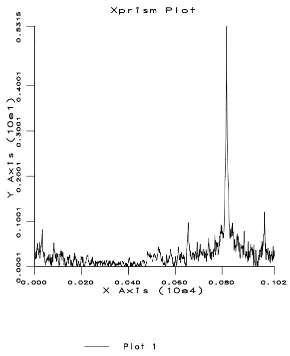

(c) POMF (a)-(d)

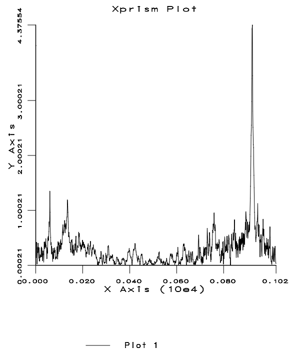

(d) POMF (a)-(e)

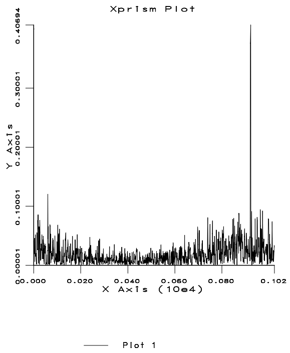

(e) SPOMF (a)-(c)

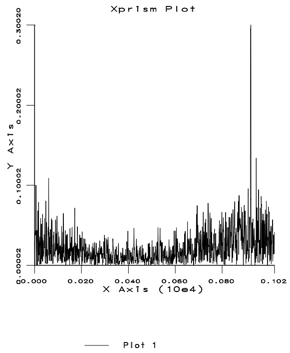

(f) SPOMF (a)-(e)

Figure 4.7: Correlation functions corresponding to figure 4.6

In all experiments the shrinking factor (scaling of the coordinate system) can be calculated from the position of the maximum by

$$t = \frac{1024 - x_{max}}{1023} \ln 1023. \tag{4.25}$$

All results are summarised in table 4.2. In the last row the error is stated which occurs due to sampling like in the previous tables.

Experiment no.	1	2	3	4	5	6
POMF	x	x	x	x		
SPOMF					x	x
Scaling parameter t	0	ln 2	ln 4	ln 2	ln 2	ln 2
Scaled by (e^t)	1	2	4	2	2	2
Maximum at	1024	922	819	921	922	922
Calculated scaling	1	1.996	4.010	2.009	1.996	1.996
Sampling error $\pm \cdot 10^{-3}$	3.4	6.8	13.6	6.8	6.8	6.8

Table 4.2: Experimental results

Again, we feed an entirely different signal into the system (see figure 4.8(a)). As expected, the correlation function differs completely from that of the previous ones. Especially the height of the maximum has decreased (see figure 4.8(b)).

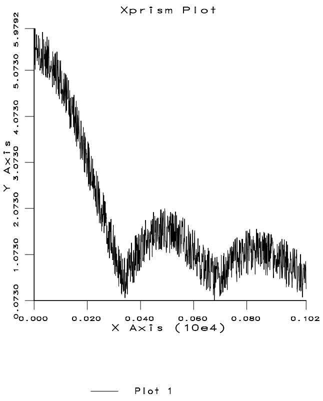

(a) New signal

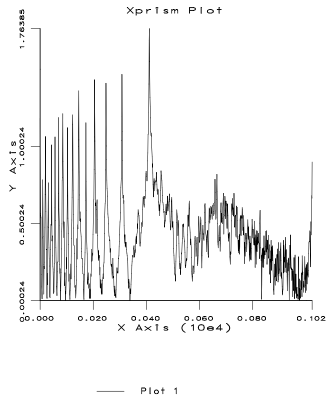

(b) Flat correlation function

Figure 4.8: New signal and the corresponding correlation function

4.2.3 Experiments on 2–D CGC Using (S)POMF

So far we have not performed experiments on the two–dimensional group correlations. In this section we present such an experiment in combination with POMF and SPOMF. In figure 4.9 the Khoros environment for the experiments is illustrated. Obviously, it is very

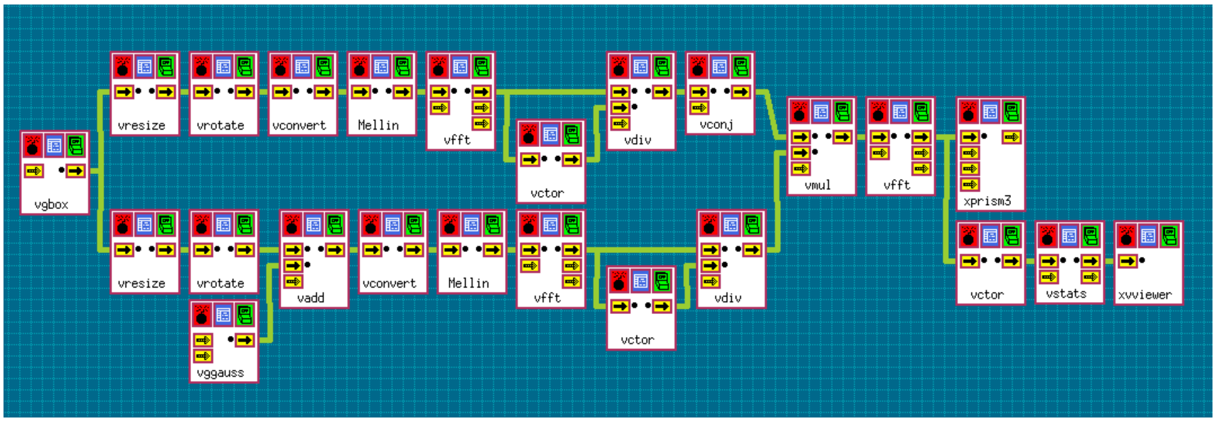

Figure 4.9: Khoros workspace for Fourier–Mellin correlation

similar to that in figure 4.5 except for the second division by the magnitude spectrum (SPOMF version) and the different canonical transform: `Mellin` transforms the image into log–polar coordinates by using the formulae

$$x = \frac{\frac{N}{2}-1}{N-1}(N-1)^{\frac{r}{N-1}} \cos\left(\frac{2\pi\varphi}{N}\right) + \frac{N}{2} \tag{4.26}$$

$$y = \frac{\frac{N}{2}-1}{N-1}(N-1)^{\frac{r}{N-1}} \sin\left(\frac{2\pi\varphi}{N}\right) + \frac{N}{2} \tag{4.27}$$

(see also [CDD94]). In our experiments we have $N = 256$. Contrary to the theoretical derivation we have not used quaternionic spectra because the results are identical in this case (as verified) and the arithmetic operations are performed faster in the complex algebra.

The two signals that are fed into the system are a) a rectangular without noise (see figure 4.10(a)) and b) scaled and rotated variants of the image in figure 4.10(b), which is the same rectangular as under a) but with noise.

The signal to noise ratio of the unscaled noisy signal amounts to

$$SNR = 10 \log_{10} \frac{E_f}{E_n} \,\mathrm{dB} = 10 \log_{10} 0.65 \,\mathrm{dB} = -1.9 \,\mathrm{dB}. \tag{4.28}$$

In the experiments, both POMF and SPOMF have been applied. The correlation function is calculated for several scales, angles, and combinations of both. The results

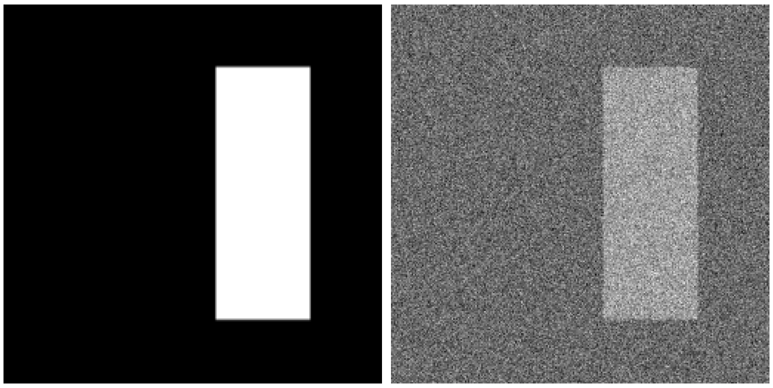

(a) Rectangular without noise (b) Rectangular with noise

Figure 4.10: Signals for Fourier–Mellin correlation

of the first four tests can be found in figure 4.11 on page 88. The remainder of the tests is illustrated in figure 4.12 on page 89. We have already mentioned that SPOMF is more sensitive with regard to noise. Obviously, the results of SPOMF become worse with increasing parameters (see experiment no. 1–3). Therefore, we have performed more experiments using POMF instead (experiment no. 4, 7, and 8). The results are more stable concerning the height of the correlation peak but less exact concerning the parameter identification (e.g. experiment no. 8).

The subsequent table 4.3 on page 90 summarises the parameters for each experiment and the results from the correlation functions.

The parameter of the distortion of the coordinate system can be obtained from the maximum (r_{max}, φ_{max}) of the correlation function by using the following formulae:

$$t = \frac{r_{max}}{N-1} \ln(N-1) \tag{4.29}$$

$$\theta = \frac{\varphi_{max}}{N} 360^\circ \tag{4.30}$$

with $N = 256$. The error of the sampling can be found in the rows below the estimated parameters. Note that not all parameters are situated inside the error intervals. The inaccuracy amounts to one pixel.

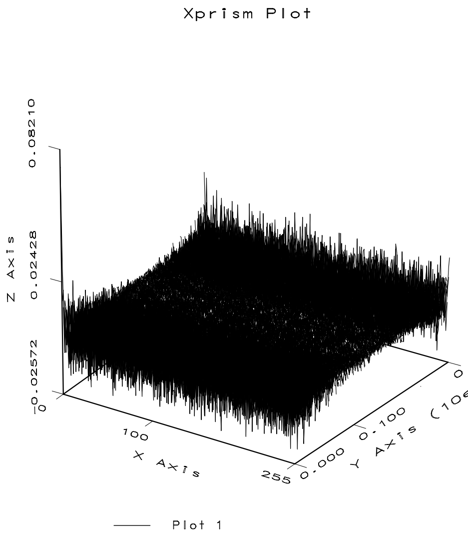

(a) Auto correlation, SPOMF (no. 1)

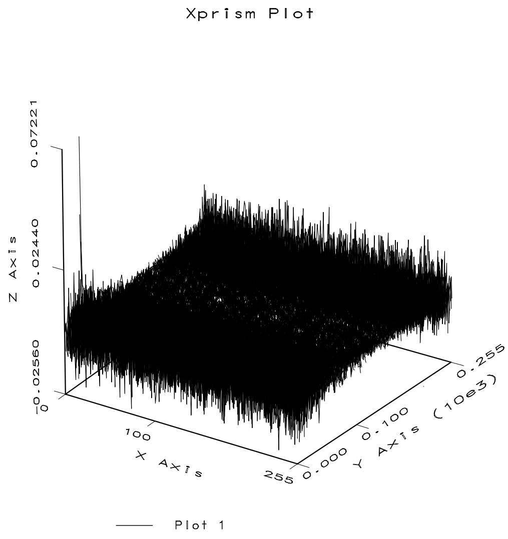

(b) Scaled by 2, SPOMF (no. 2)

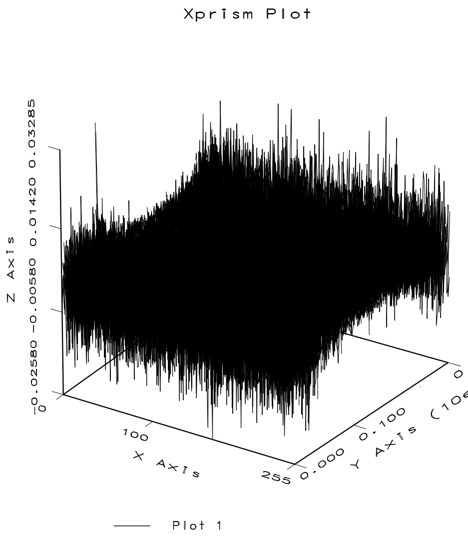

(c) Scaled by 4, SPOMF (no. 3)

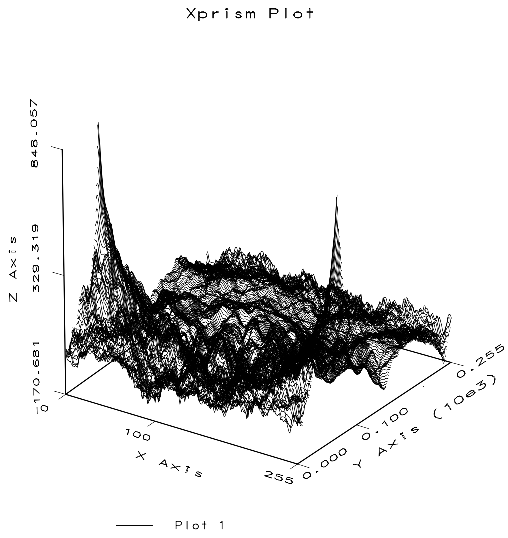

(d) Scaled by 4, POMF (no. 4)

Figure 4.11: Correlation functions of scaled signals

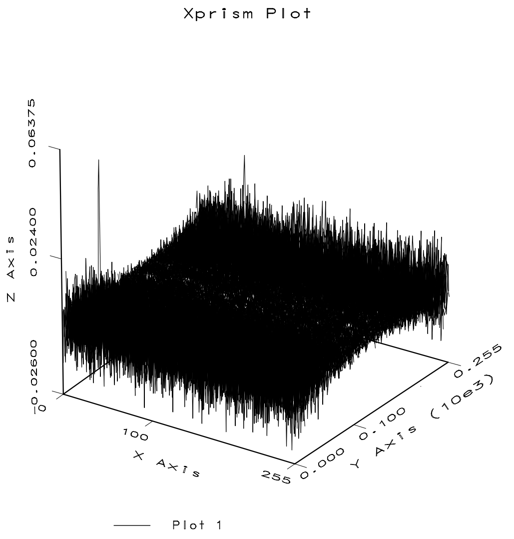

(a) Rotated by 60°, SPOMF (no. 5)

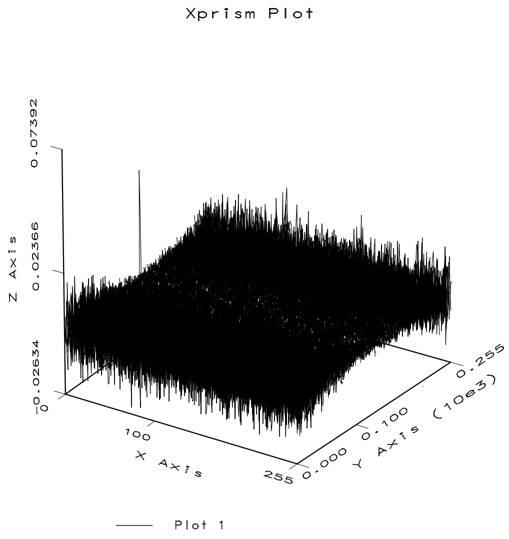

(b) Rotated by 120°, SPOMF (no. 6)

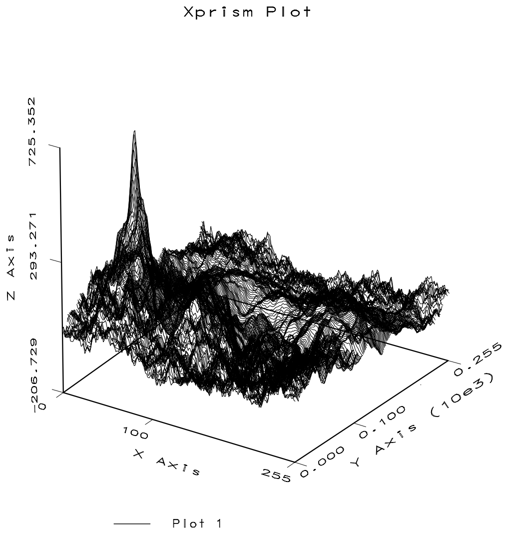

(c) Rotated by 60°, scaled by 4, POMF (no. 7)

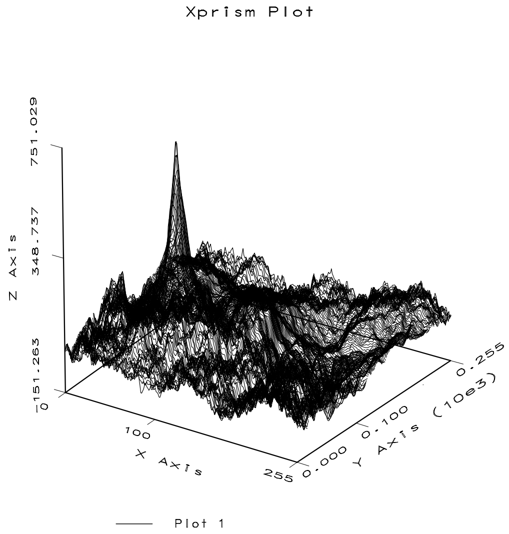

(d) Rot. by 120°, scaled by 4, POMF (no. 8)

Figure 4.12: Correlation functions of rotated and scaled signals

Experiment no.	1	2	3	4	5	6	7	8
SPOMF	x	x	x		x	x		
POMF				x			x	x
Scaling param. t	0	ln 2	ln 4	ln 4	0	0	ln 4	ln 4
Scaled by (e^t)	1	2	4	4	1	1	4	4
Rotated by	0°	0°	0°	0°	60°	120°	60°	120°
Maximum at	(0,0)	(0,32)	(0,64)	(0,65)	(43,0)	(86,0)	(43,65)	(86,64)
Calculated scale	1	2.004	4.018	4.106	1	1	4.106	4.018
Sampling error ±	0.011	0.022	0.044	0.044	0.011	0.011	0.044	0.044
Calculated angle	0°	0°	0°	0°	60.47°	120.94°	60.47°	120.94°
Sampling error ±	0.7°	0.7°	0.7°	0.7°	0.7°	0.7°	0.7°	0.7°

Table 4.3: Experimental results

Again we feed a completely different signal (see figure 4.13(a)) into the system in order to show that the graph of the correlation function (figure 4.13(b)) is less significant than those in the figures 4.11(d), 4.12(c) and 4.12(d).

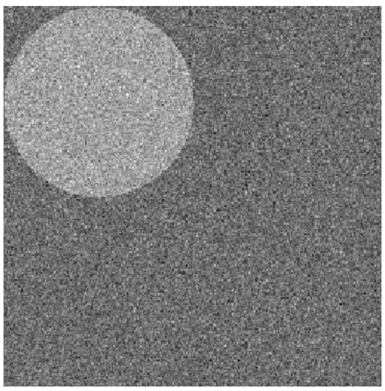

(a) Different signal

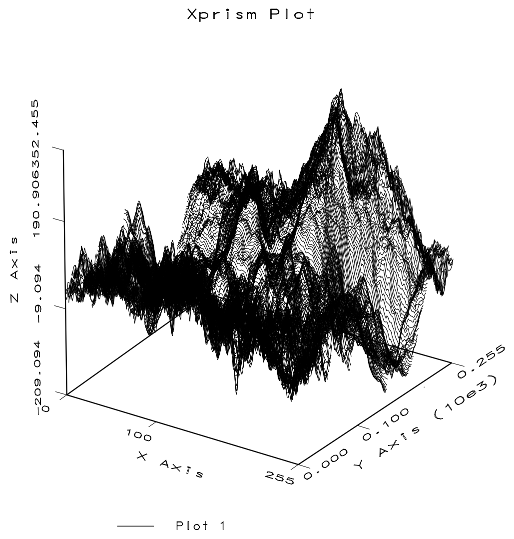

(b) Flat correlation function

Figure 4.13: Different signal and corresponding correlation function

4.3 An Extension to the Affine Group

In this chapter a possible solution for matching two n–dimensional signals which are distorted by the n–dimensional affine group is presented. The affine group of dimension n consists of the n–dimensional linear group and the n–dimensional translation group. These groups do not commute. Hence, an invariant transform cannot be obtained by applying the concept of canonical coordinates.

The classical example of affine distortion is the matching of shifted, rotated and scaled images. A straight forward solution is to sample the pattern for different scales and angles. For each of these instances of the pattern the correlation is calculated. Performing this procedure requires a lot of time and memory resources.

In our investigation we try to use the cross group correlation to express the proceeding concept in a closed mathematical form for the sake of a deeper understanding.

4.3.1 The Double Parametric Cross Correlation

Similar to the theory of Volterra filters (see e.g. [KZ96, KP85]) the method which is described below constructs a generalised cross correlation which creates a double–dimensional parameter space. In contrast to the Volterra binom where a $2n$–dimensional filter and the signal are convoluted, our approach constructs a $2n$–dimensional correlation signal. Hence, our concept is something like a mathematical inverse of the Volterra convolution term of second order with regard to the operations on the signals.

In this section we only consider translations. Hence, the calculation of such a correlation is nothing else but the dyadic product of the cross correlation by itself. Consequently, the definition of the double cross correlation is not useful in itself and it becomes only interesting if a linear group is involved. Exactly this is done in section 4.3.2.

To start with, the trivial case is considered:

Definition 25 (The double parametric cross correlation) *The double parametric cross correlation of two n–dimensional signals is defined as:*

$$C^{v_1 v_2}(\boldsymbol{t}_1, \boldsymbol{t}_2) = \int_{\mathbb{R}^n} v_1(\boldsymbol{t}_1 + \boldsymbol{\eta}) v_2(\boldsymbol{t}_2 + \boldsymbol{\eta}) d\boldsymbol{\eta}. \tag{4.31}$$

The double cross correlation theorem can be derived from calculating the Fourier transform of $C^{v_1v_2}(\boldsymbol{t}_1,\boldsymbol{t}_2)$:

$$\begin{aligned}\mathcal{F}\{C^{v_1v_2}(\boldsymbol{t}_1,\boldsymbol{t}_2)\} &= \int_{\mathbb{R}^{3n}} v_1(\boldsymbol{t}_1+\boldsymbol{\eta})v_2(\boldsymbol{t}_2+\boldsymbol{\eta})d\boldsymbol{\eta}e^{-2\pi(\boldsymbol{t}_1 I_n^1\boldsymbol{u}_1^T+\boldsymbol{t}_2 I_n^2\boldsymbol{u}_2^T)}d\boldsymbol{t}_1 d\boldsymbol{t}_2\\ &\overset{\boldsymbol{\tau}=\boldsymbol{t}_2+\boldsymbol{\eta}}{=} \int_{\mathbb{R}^{2n}} v_1(\boldsymbol{t}_1+\boldsymbol{\eta})\int_{\mathbb{R}^n} v_2(\boldsymbol{\tau})e^{-2\pi\boldsymbol{\tau} I_n^2\boldsymbol{u}_2^T}d\boldsymbol{\tau}e^{-2\pi(-\boldsymbol{\eta})I_n^2\boldsymbol{u}_2^T}d\boldsymbol{\eta}e^{-2\pi\boldsymbol{t}_1 I_n^1\boldsymbol{u}_1^T}d\boldsymbol{t}_1\\ &\overset{\boldsymbol{\chi}=\boldsymbol{t}_1+\boldsymbol{\eta}}{=} \int_{\mathbb{R}^{2n}} v_1(\boldsymbol{\chi})e^{-2\pi\boldsymbol{\chi} I_n^1\boldsymbol{u}_1^T}d\boldsymbol{\chi}e^{-2\pi(-\boldsymbol{\eta})I_n^1\boldsymbol{u}_1^T}e^{-2\pi(-\boldsymbol{\eta})I_n^2\boldsymbol{u}_2^T}d\boldsymbol{\eta}\mathcal{F}\{v_2(\boldsymbol{x})\}(\boldsymbol{u}_2)\end{aligned}$$

By substituting $\boldsymbol{u}_1^T$ with $I_n^1 I_n^2\boldsymbol{v}^T$, $I_n^1\boldsymbol{u}_1^T$ yields $I_n^2(-\boldsymbol{v}^T)$ and hence, we get

$$\begin{aligned}&= \mathcal{F}\{v_1(\boldsymbol{x})\}(-\boldsymbol{v})\mathcal{F}\{K(\boldsymbol{x},-\boldsymbol{v})\}(\boldsymbol{u}_2)\mathcal{F}\{v_2(\boldsymbol{x})\}(\boldsymbol{u}_2)\\ &= \mathcal{F}\{v_1(\boldsymbol{x})\}(-\boldsymbol{u}_1 I_n^1 I_n^2)\mathcal{F}\{K(\boldsymbol{x},-\boldsymbol{u}_1 I_n^1 I_n^2)\}(\boldsymbol{u}_2)\mathcal{F}\{v_2(\boldsymbol{x})\}(\boldsymbol{u}_2)\end{aligned} \tag{4.32}$$

where $K(\boldsymbol{a},\boldsymbol{b}) = e^{-2\pi\boldsymbol{a}I_n^2\boldsymbol{b}^T}$ is the kernel of the Clifford Fourier transform and its Fourier transform reads

$$\begin{aligned}\mathcal{F}\{K(\boldsymbol{x},-\boldsymbol{u}_1 I_n^1 I_n^2)\}(\boldsymbol{u}_2) &= \mathcal{F}\{K(\boldsymbol{x},-\boldsymbol{u}_2)\}(\boldsymbol{u}_1 I_n^1 I_n^2)\\ &= \mathcal{F}\{1\}(\boldsymbol{u}_1 I_n^1 I_n^2-\boldsymbol{u}_2) = \delta(\boldsymbol{u}_1 I_n^1 I_n^2-\boldsymbol{u}_2).\end{aligned} \tag{4.33}$$

Therefore, equation (4.32) yields

$$\mathcal{F}\{C^{v_1v_2}(\boldsymbol{t}_1,\boldsymbol{t}_2)\}(\boldsymbol{u}_1,\boldsymbol{u}_2) = \mathcal{F}\{v_1(\boldsymbol{x})\}(-\boldsymbol{u}_2)\mathcal{F}\{v_2(\boldsymbol{x})\}(\boldsymbol{u}_2)\delta(\boldsymbol{u}_1 I_n^1 I_n^2-\boldsymbol{u}_2). \tag{4.34}$$

Note that if instead of $\boldsymbol{u}_1$ $\boldsymbol{u}_2$ were substituted in equation 4.32, the spectra of v_1 and v_2 would have been mirrored. So swapping of the projective axis yields the same result as exchanging the two signals for each other.

Hence, the double cross correlation is intrinsically n–dimensional because it is projective. The projected elements are exactly the same as if the classical cross correlation were calculated. Consequently, the double cross correlation is useless unless it is combined with the cross group correlation (using a linear group) so that the spectrum of the kernel is intrinsically $2n$–dimensional.

4.3.2 The Double Parametric Cross Group Correlation

Following from 4.3.1, the double parametric cross group correlation is defined by substituting one translation of the double parametric cross correlation with a linear group:

Definition 26 (Double parametric cross group correlation) *Let G be an arbitrary linear group and v_1, v_2 two n–dimensional signals which are defined on $\mathbb{D}$. The group operation of G with the parameter vector $\boldsymbol{t}_2$ on $\boldsymbol{x}$ is denoted as $f(\boldsymbol{t}_2, \boldsymbol{x})$ and $J(\boldsymbol{t}_2)$ is the Jacobian of the canonical coordinate transform. The double parametric cross group correlation is defined as*

$$C_G^{v_1 v_2}(\boldsymbol{t}_1, \boldsymbol{t}_2) = \frac{1}{\sqrt{kJ(\boldsymbol{t}_2)}} c_G^{v_1 v_2}(\boldsymbol{t}_1, \boldsymbol{t}_2) \tag{4.35}$$

and $c_G^{v_1 v_2}(\boldsymbol{t}_1, \boldsymbol{t}_2)$ is defined by

$$c_G^{v_1 v_2}(\boldsymbol{t}_1, \boldsymbol{t}_2) = \int_{\mathbb{D}} v_1(\boldsymbol{t}_1 + \boldsymbol{\eta}) v_2(f(\boldsymbol{t}_2, \boldsymbol{\eta})) d\boldsymbol{\eta} \tag{4.36}$$

where $1/\sqrt{kJ(\boldsymbol{t}_2)}$ is an additional factor which normalises the energy.

The additional factor is necessary because the $\boldsymbol{t}_2$ projection does not yield the cross group correlation according to formula (4.3), since the Jacobian is missing. Hence, the energy of the signal is changed by the group G. Consequently, the maximum of the double parameter cross group correlation might be displaced because the correlation peak becomes higher with increasing energy. The absolute height of the peak which is a criterion of matching is changed, too. Both problems can be avoided by normalising the energy of the signals.

Consider, for example, the dilation of a one–dimensional signal. If a signal is scaled by a factor k (i.e. $v(\frac{x}{k})$) the energy will increase by k:

$$E\left(v\left(\frac{x}{k}\right)\right) = \int v\left(\frac{x}{k}\right) v^*\left(\frac{x}{k}\right)\, dx \overset{\frac{x}{k}=t}{=} \int v(t) v^*(t) k\, dt = kE(v(x)) \tag{4.37}$$

Therefore, the signal values must be divided by $\sqrt{k}$ in order to keep the energy constant. Or, more generally, we must divide the signal by $\sqrt{J}$, where J is the Jacobian of the transformation group.

Note that the position of the maximum of the resulting correlation function is located correctly if the function is multiplied by $\sqrt{J^{-1}}$ but the absolute value of the maximum still depends on the group parameter.

Consider the dilation again. The double parametric cross group correlation should contain shifted versions of the auto group correlation but if the unknown signal is dilated by a factor of, e.g., 2, the value of the maximum would be multiplied by $\sqrt{2}$. This problem cannot be solved by simply multiplying the correlation function with J^{-1} instead of $\sqrt{J^{-1}}$ because the position of the maximum would also be changed.

For the sake of better understanding consider the following example. Two rectangular

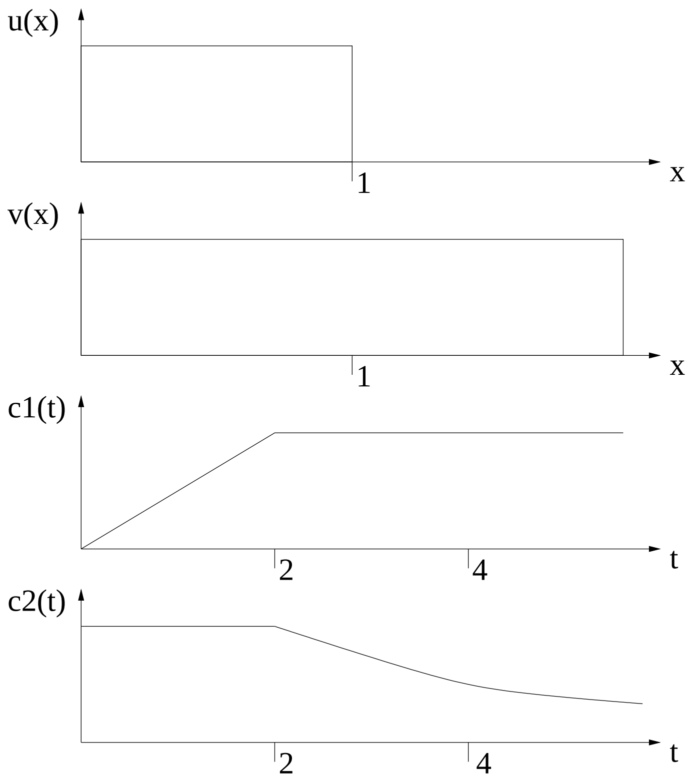

Figure 4.14: Two wrong norming factors

signals are compared (figure 4.14): if no norming factor is used at all, the correlation function increases until the signals are of same length. At this point the correlation function ($c1(t)$) stays constant. If $J^{-1} = t^{-1}$ is used as norming factor the correlation function ($c2(t)$) is constant until $u(x)$ is as long as $v(x)$ and decreases by t^{-1} after that point.

In order to get a constant maximum at the correct position the integrand is multiplied by $\sqrt{J(t)^{-1}}$ and the resulting function is divided by the square root of the peak value of the auto correlation function of the signal which is to be recognised. It is also possible to divide it by $\sqrt{J(t_{max})}$ where t_{max} is the position of the maximum. Therefore, we prefer to use $k = J(t_{max})$ in definition 26.

The normalisation of the energy is the reason why the double parameter cross group correlation can only be applied to subgroups of the affine group. The energy of a signal which is transformed by a non–linear group depends on its absolute position in the spatial domain.

Consider, for example, a subgroup of the one–dimensional projective group. Let the corresponding two–dimensional group be the rotations with respect to the origin, so that the projective subgroup is the PSO(2) (see also section 4.1.2). If the projective line is placed at $x = 1$ the projective coordinate is obtained by $z = \frac{y}{x}$. Consider now two signals v and w which have the value 1 in the dark areas in figure 4.15. Obviously, the signals

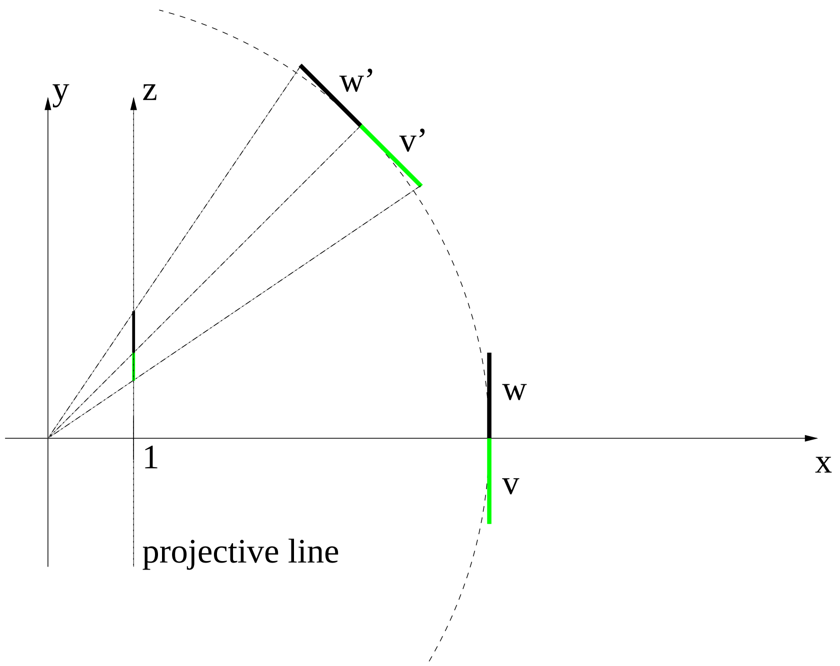

Figure 4.15: Two signals of the same energy are rotated and projected

have the same energy in the plane and on the projective line. Let v' and w' be the rotated signals. Though they are rotated by the same angle and have the same energy in the plane their energy on the projective line now differs. Consequently, there is no function which is constant with respect to the z–coordinate and which normalises the energy of the projections of v' and w'.

In the sequel we refer to the double parametric cross group correlation as DPCG correlation.

4.3.3 The DPCG Correlation Theorem

Since the DPCG correlation doubles the dimension of the signal it should be calculated as fast as possible. At least the DPCG correlation theorem must be formulated in order to make it possible to calculate the DPCG correlation via the frequency domain using FFT–algorithms.

Theorem 11 (DPCG correlation theorem) *Using the former terms the equation*

$$\mathcal{F}\{c_G^{v_1 v_2}(\boldsymbol{t}_1,\boldsymbol{t}_2)\}(\boldsymbol{u}_1,\boldsymbol{u}_2) = \mathcal{F}\{v_1(\boldsymbol{x})\}(\boldsymbol{u}_1)\mathcal{F}\{K_G(\boldsymbol{x},-\boldsymbol{u}_2)\}(-\boldsymbol{u}_1)\mathcal{T}_G\{v_2(\boldsymbol{x})\}(\boldsymbol{u}_2) \tag{4.38}$$

is satisfied.

Proof:

Let $\boldsymbol{\xi}$ be the coordinate transform so that G acts as the translation group. In analogy to the proofs of the previous theorems we get the following derivation:

$$\begin{aligned}
&\mathcal{F}\{c_G^{v_1 v_2}(\boldsymbol{t}_1,\boldsymbol{t}_2)\}(\boldsymbol{u}_1,\boldsymbol{u}_2)\\
&= \int_{\mathbb{R}^{2n}}\int_{\mathbb{D}} v_1(\boldsymbol{t}_1+\boldsymbol{\tau})v_2(f(\boldsymbol{t}_2,\boldsymbol{\tau}))d\boldsymbol{\tau}\, e^{-2\pi(\boldsymbol{t}_1 I_n^1 \boldsymbol{u}_1^T + \boldsymbol{t}_2 I_n^2 \boldsymbol{u}_2^T)} d\boldsymbol{t}_1 d\boldsymbol{t}_2\\
&= \int_{\mathbb{R}^{2n}}\int_{\mathbb{D}} v_1(\boldsymbol{t}_1+\boldsymbol{\tau})v_2(f(\boldsymbol{t}_2,\boldsymbol{\tau}))e^{-2\pi((\boldsymbol{t}_1+\boldsymbol{\tau}-\boldsymbol{\tau})I_n^1\boldsymbol{u}_1^T + (\boldsymbol{\xi}(\boldsymbol{\tau})+\boldsymbol{t}_2-\boldsymbol{\xi}(\boldsymbol{\tau})))I_n^2\boldsymbol{u}_2^T)} d\boldsymbol{\tau} d\boldsymbol{t}_1 d\boldsymbol{t}_2
\end{aligned}$$

where $\boldsymbol{\xi}(\boldsymbol{\tau})$ lets G act as the translation group

$$= \int_{\mathbb{R}^{2n}}\int_{\mathbb{D}} v_1(\boldsymbol{t}_1+\boldsymbol{\tau})v_2(f(\boldsymbol{t}_2,\boldsymbol{\tau}))e^{-2\pi((\boldsymbol{t}_1+\boldsymbol{\tau}-\boldsymbol{\tau})I_n^1\boldsymbol{u}_1^T + (\boldsymbol{\xi}(f(\boldsymbol{t}_2,\boldsymbol{\tau}))-\boldsymbol{\xi}(\boldsymbol{\tau}))I_n^2\boldsymbol{u}_2^T)} d\boldsymbol{\tau} d\boldsymbol{t}_1 d\boldsymbol{t}_2$$

substitute $\boldsymbol{z}_1 = \boldsymbol{t}_1 + \boldsymbol{\tau}$ and $\boldsymbol{z}_2 = f(\boldsymbol{t}_2,\boldsymbol{\tau})$

$$\begin{aligned}
&= \int_{\mathbb{D}}\int_{\mathbb{R}^n} v_1(\boldsymbol{z}_1)v_2(\boldsymbol{z}_2)e^{-2\pi(\boldsymbol{z}_1 I_n^1\boldsymbol{u}_1^T + \boldsymbol{\xi}(\boldsymbol{z}_2)I_n^2\boldsymbol{u}_2^T)}\left|\frac{\partial \boldsymbol{t}_2}{\partial \boldsymbol{z}_2}\right| d\boldsymbol{z}_1 d\boldsymbol{z}_2 \int_{\mathbb{D}} e^{-2\pi(-\boldsymbol{\tau} I_n^1\boldsymbol{u}_1^T - \boldsymbol{\xi}(\boldsymbol{\tau})I_n^2\boldsymbol{u}_2^T)} d\boldsymbol{\tau}\\
&\overset{\text{th.9}}{=} \int_{\mathbb{R}^n} v_1(\boldsymbol{z}_1)e^{-2\pi \boldsymbol{z}_1 I_n^1 \boldsymbol{u}_1^T} d\boldsymbol{z}_1 \int_{\mathbb{D}} v_2(\boldsymbol{z}_2)e^{-2\pi\boldsymbol{\xi}(\boldsymbol{z}_2)I_n^2\boldsymbol{u}_2^T} J(\boldsymbol{z}_2) d\boldsymbol{z}_2 \int_{\mathbb{D}} e^{-2\pi(\boldsymbol{\xi}(\boldsymbol{\tau})I_n^2(-\boldsymbol{u}_2^T) + \boldsymbol{\tau} I_n^1(-\boldsymbol{u}_1^T))} d\boldsymbol{\tau}
\end{aligned}$$

using $K_G(\boldsymbol{x},-\boldsymbol{u}_2) = e^{-2\pi\boldsymbol{\xi}(\boldsymbol{x})I_n^2(-\boldsymbol{u}_2^T)}$ which is only defined on $\mathbb{D}$ we get

$$= \mathcal{F}\{v_1(\boldsymbol{x})\}(\boldsymbol{u}_1)\mathcal{F}\{K_G(\boldsymbol{x},-\boldsymbol{u}_2)\}(-\boldsymbol{u}_1)\mathcal{T}_G\{v_2(\boldsymbol{x})\}(\boldsymbol{u}_2) \tag{4.39}$$

Therefore, the theorem 11 is finally proved to be correct. □

In the sequel the term $\mathcal{F}\{K_G(\boldsymbol{x}, -\boldsymbol{u}_2)\}(-\boldsymbol{u}_1)$ will be considered more closely. Firstly, it can be interpreted in an inverse way:

$$\mathcal{K}(\boldsymbol{u}_1, \boldsymbol{u}_2) = \mathcal{F}\{K_G(\boldsymbol{x}, -\boldsymbol{u}_2)\}(-\boldsymbol{u}_1) = \mathcal{T}_G\{e^{-2\pi \boldsymbol{x} I_n^1 - \boldsymbol{u}_1^T}\}(-\boldsymbol{u}_2). \tag{4.40}$$

Consider further a signal v and its representation in canonical coordinates g. It is easy to obtain g from v and v from g by the canonical coordinate transform and its inverse transform respectively. But how can we get the spectrum of v from the spectrum of g and vice versa? Exactly this question is answered by the next theorem. We use the term (4.40) to formulate a correspondence.

Theorem 12 (Correspondence of the invariant spectrum) *The spectrum of a signal can be obtained from the spectrum of the signal in canonical coordinates with regard to the group G:*

$$\mathcal{F}\{v(\boldsymbol{x})\}(-\boldsymbol{u}_1) = \int_{\mathbb{R}^n} \mathcal{T}_G\{v(\boldsymbol{x})\}(\boldsymbol{u}_2)\mathcal{K}(\boldsymbol{u}_1, \boldsymbol{u}_2)d\boldsymbol{u}_2 \tag{4.41}$$

where $\mathcal{K}(\boldsymbol{u}_1, \boldsymbol{u}_2)$ is defined in equation (4.40).

Proof:

The theorem can be proved by calculating the integral in a straightforward way:

$$\begin{aligned}
&\int_{\mathbb{R}^n} \mathcal{T}_G\{v(\boldsymbol{x})\}(\boldsymbol{u}_2)\mathcal{K}(\boldsymbol{u}_1, \boldsymbol{u}_2)d\boldsymbol{u}_2 \\
&= \int_{\mathbb{R}^n}\int_{\mathbb{D}} v(\boldsymbol{x})e^{-2\pi\boldsymbol{\xi}(\boldsymbol{x})I_n^2\boldsymbol{u}_2^T} J(\boldsymbol{x})d\boldsymbol{x} \int_{\mathbb{D}} e^{2\pi\boldsymbol{\xi}(\boldsymbol{\tau})I_n^2\boldsymbol{u}_2^T} e^{2\pi\boldsymbol{\tau} I_n^1\boldsymbol{u}_1^T} d\boldsymbol{\tau} d\boldsymbol{u}_2 \\
&= \int_{\mathbb{D}}\int_{\mathbb{D}} v(\boldsymbol{x}) \int_{\mathbb{R}^n} e^{2\pi(\boldsymbol{\xi}(\boldsymbol{\tau})-\boldsymbol{\xi}(\boldsymbol{x}))I_n^2\boldsymbol{u}_2^T} d\boldsymbol{u}_2 J(\boldsymbol{x})e^{2\pi\boldsymbol{\tau} I_n^1\boldsymbol{u}_1^T} d\boldsymbol{\tau} d\boldsymbol{x} \\
&= \int_{\mathbb{D}}\int_{\mathbb{D}} v(\boldsymbol{x})\delta_0(\boldsymbol{\xi}(\boldsymbol{\tau}) - \boldsymbol{\xi}(\boldsymbol{x}))J(\boldsymbol{x})e^{2\pi\boldsymbol{\tau} I_n^1\boldsymbol{u}_1^T} d\boldsymbol{\tau} d\boldsymbol{x} \\
&= \int_{\mathbb{D}}\int_{\mathbb{D}} v(\boldsymbol{x})\delta_0(\boldsymbol{\tau} - \boldsymbol{x})e^{2\pi\boldsymbol{\tau} I_n^1\boldsymbol{u}_1^T} d\boldsymbol{\tau} d\boldsymbol{x} \\
&= \int_{\mathbb{D}} v(\boldsymbol{x})e^{-2\pi\boldsymbol{x} I_n^1(-\boldsymbol{u}_1^T)} d\boldsymbol{x} \overset{v \text{ is defined on } \mathbb{D}}{=} \mathcal{F}\{v(\boldsymbol{x})\}(-\boldsymbol{u}_1).
\end{aligned} \tag{4.42}$$

Therefore, the correspondence between the spectra is proved.

□

Hence, the term (4.40) enables us to obtain the spectrum of a signal from the spectrum of an invariant transform. Consider, for example, the scale invariant transform. The spectrum is calculated by

$$\mathcal{T}_D\{v(x)\} = \int_{\mathbb{R}^+} v(x) e^{-i2\pi u \ln x} x^{-1} dx \tag{4.43}$$

and theorem 12 yields

$$\begin{aligned}
&\int_{\mathbb{R}} \int_{\mathbb{R}^+} v(x) e^{-i2\pi u \ln x} x^{-1} dx \int_{\mathbb{R}^+} e^{i2\pi u \ln \tau} e^{j2\pi v \tau} d\tau du \\
=&\int_{\mathbb{R}^+} \int_{\mathbb{R}^+} v(x) \int_{\mathbb{R}} e^{-i2\pi u(\ln x - \ln \tau)} du x^{-1} e^{j2\pi v\tau} dx d\tau \\
=&\int_{\mathbb{R}^+} \int_{\mathbb{R}^+} v(x) \delta_0(\ln x - \ln \tau) x^{-1} e^{j2\pi v \tau} dx d\tau \\
=&\int_{\mathbb{R}^+} \int_{\mathbb{R}^+} v(x) \delta_0(x - \tau) e^{j2\pi v\tau} dx d\tau \\
=&\int_{\mathbb{R}^+} v(x) e^{j2\pi v x} dx = \mathcal{F}\{v(x)\}(-v).
\end{aligned} \tag{4.44}$$

There still exists one more interesting property of the term (4.40). In order to make it explicit we calculate the Fourier transform of the $\mathcal{K}$ term of the example:

$$\begin{aligned}
&\mathcal{F}\left\{\int_{\mathbb{R}^+} e^{i2\pi u \ln \tau} e^{j2\pi v\tau} d\tau\right\} \\
=&\int_{\mathbb{R}^2} \int_{\mathbb{R}^+} e^{i2\pi u \ln \tau} e^{j2\pi v \tau} e^{-2\pi(ixu + jyv)} d\tau du dv \\
=&\int_{\mathbb{R}} \int_{\mathbb{R}^+} e^{i2\pi u \ln \tau} \int_{\mathbb{R}} e^{-j2\pi v(y-\tau)} dv e^{-i2\pi x u} d\tau du \\
=&\int_{\mathbb{R}} \int_{\mathbb{R}^+} e^{-i2\pi u(x - \ln \tau)} \delta_0(y-\tau) d\tau du \\
=&\int_{\mathbb{R}} e^{-i2\pi u(x - \ln y)} du \\
=&\delta_0(x - \ln y)
\end{aligned} \tag{4.45}$$

This result is not surprising if theorem 12 is considered as a correlation. Referring to the cross group correlation theorem (theorem 10) the corresponding operation in the spatial domain is the multiplication and in the discrete case equation (4.45) is exactly the characteristic function of the monge patch (1D: of the graph) of the canonical coordinate transform! So we obtain the signal in canonical coordinates by multiplying the signal by $\delta_0(x - \ln y)$. Of course that property could be proved for the general case but since this is a direct result of theorem 10 and 12, it makes the proof redundant. Nevertheless, we formulate a theorem to conclude this section.

Theorem 13 (Spatial image of the $\mathcal{K}$ term) *The Fourier transform of the term (4.40) yields $\delta_0(\boldsymbol{x}-\boldsymbol{\xi}(\boldsymbol{y}))$ (where $\boldsymbol{y}$ are the new n coordinates) which is the characteristic function of the monge patch of the canonical coordinate transform in the discrete case.*

Proof:

Theorem 10 and 12.

□

4.3.4 Singularities and Sampling Theorem

New problems arise if the invariant transforms and the new theorems are used. Signals which can be Fourier transformed need not have a corresponding invariant spectrum. Especially the transform of a kernel may be critical. For example, consider the Fourier–Mellin transform: at the point $(x, y) = 0$ the term $\ln(\sqrt{x^2 + y^2})$ diverges and hence the phase is not defined. This behaviour of the transform is ingenious because if $(x, y) = 0$ the signal is scaled to zero and does not exist any more. The question is how to handle these problems in practical applications, because the transform need to be calculated. One possible solution is to use an aperture filter on the parameter space in order to exclude the singularity. For dilation e.g. the results are very poor for very large or very small scales. Hence, the scaling is effectively described by an interval $[a, b]$ (see also [MS94]).

The second problem which needs to be considered is the sampling theorem which yields the reciprocal problem concerning the Siemens star: the sampling is done with a constant angle increment but the data is given in a regular lattice. So when the coordinate system is transformed some data have great influence on the result and some data have no effect. This problem can be attenuated by interpolating the data. Certainly, there is an optimal interpolation formula for each coordinate transformation but we only use the performant (bi–) linear interpolation in this thesis because the difference to an optimal technique is minimal.

The last problem concerning the coordinate transformations is the noise which increases if not all points of data have the same influence on the result. In particular, the spectrum of the noise is heavily distorted. Noise is a signal that usually consists of high frequencies. After a canonical coordinate transform this property is lost. Noise is now distributed across the whole spectrum. Consequently, the classical methods for noise reduction do not work anymore.

4.3.5 Experiments on 1–D DPCGC

Consider a one–dimensional signal $v(x)$ which is compared to some patterns $p_1(x), \ldots, p_k(x)$. This signal is scaled and shifted. In which way can we use the previous theorems to solve the problems of matching and parameter identification?

Obviously, the signal can be compared to each pattern by rotating it to any angle (by a certain increment), shifting it to any position (by a certain increment), and then calculating the deviation. This is exactly what is done by the (sampled) double cross group correlation:

$$c_D^{vp_i}(t_1, t_2) = \int_{\mathbb{R}^+} v(x + t_1) p_i(e^{t_2} x) dx \tag{4.46}$$

The function $C_D^{vp_i}(t_1, t_2) = \sqrt{t_{2max}^{-1} t_2^{-1}} c_D^{vp_i}(t_1, t_2)$ has a maximum at the point (parameter configuration) where the signals v and p_i match best[4]. Hence, both aspired results are obtained: a measure for the matching and the parameters of the transformations.

Using theorem 11 the matching can be done with less complexity by

$$c_D^{vp_i}(t_1, t_2) = \mathcal{F}^{-1}\{\mathcal{F}\{v(x)\}(u_1) \mathcal{F}\{e^{i_2 2\pi u_2 \ln(x)}\}(-u_1) \mathcal{T}_D\{p_i(x)\}(u_2)\} \tag{4.47}$$

because the Fourier transform of the dilation invariant kernel and the transforms of the p_is can be calculated once at the beginning. If a new signal v is recorded, it must be transformed first. After that the spectra are multiplied pointwise and the result is transformed back into the spatial domain. Hence, the complexity is decreased from N^3 to $N^2 \log N$. For each correlation the maximum and its coordinates are searched. The overall maximum indicates the best matching pattern. Its position depends linearly on the parameter of the shifting and the scaling of the signal v relative to the pattern p_i.

In our experiments we use two instances of a signal (figure 4.17) which are scaled and shifted with regard to each other.

All signals are of length 256. The Khoros workspace in figure 4.16 models the formula (4.47). According to the theorem 13 all experiments were further performed using the image 4.18 and the workspace in figure 4.19 on page 102.

[4] This statement is not always true — in this case we have the same restriction as for the classical cross correlation matching.

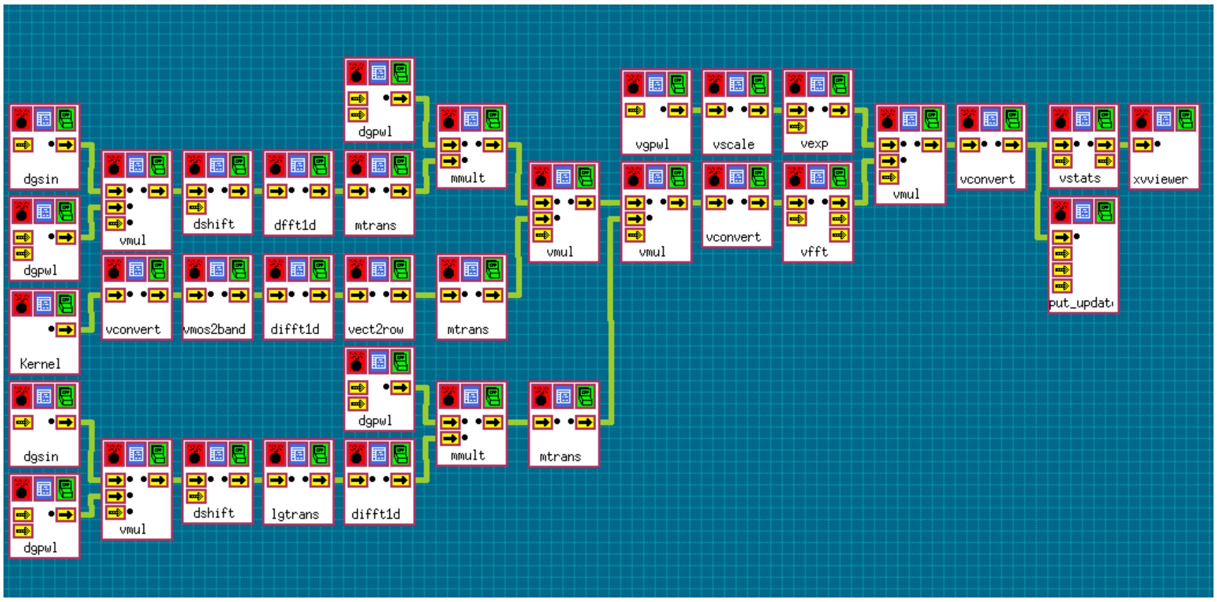

Figure 4.16: The Khoros workspace which corresponds to formula 4.47

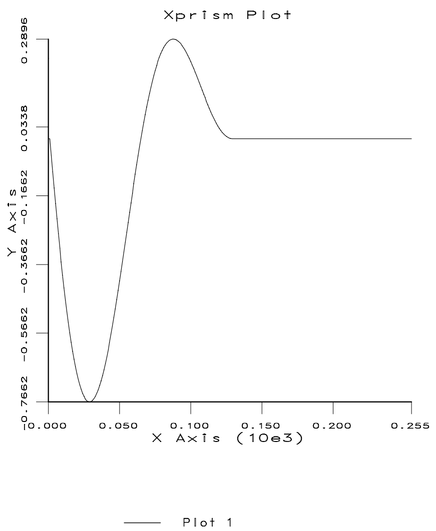

Figure 4.17: Original signal for the following experiments

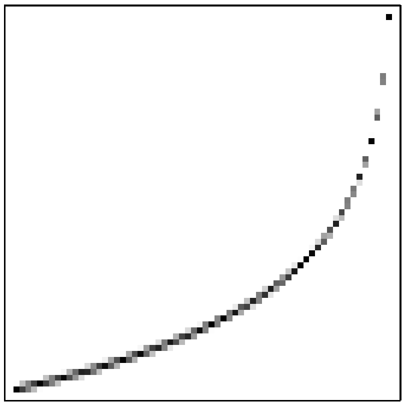

Figure 4.18: Characteristic function of the monge patch of the logarithm transform

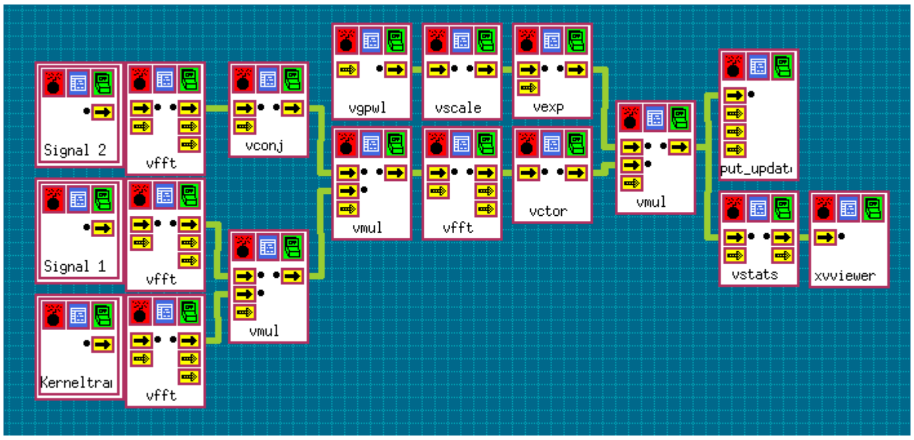

Figure 4.19: DPCG correlation in the spatial domain

In the experiment the original signal is scaled and shifted for some specific values and the maxima are detected in the resulting correlation signals. The applied parameters, the reconstructed parameters, and the corresponding images are summarised in table 4.4 and in figure 4.20 (page 104) respectively. The shift parameter is centred, the scale parameter

Experiment no.	1	2	3	4	5	6	7	8	9
Signal 1 shrunk by	1	1	1	1	1	1	1	1	0.5
Signal 2 shrunk by	1	1	1	1	2	2	2	4	1
Signal 1 shifted by	0	10	10	10	0	10	10	0	0
Signal 2 shifted by	0	0	10	20	0	0	10	0	0
Shift parameter from fig. 4.20	0	10	0	-10	0	10	-11	0	0
Scale parameter from fig. 4.20	1	1	1	1	1.96	1.96	2.01	3.93	2.01
Error by sampling ($\pm$)	0.01	0.01	0.01	0.01	0.02	0.02	0.02	0.04	0.02
Experiments in worksp. 4.19									
Shift parameter	0	10	0	-10	0	10	-10	0	0
Scale parameter	1	1	1	1	2.01	2.01	2.01	4.02	2.01
Error by sampling ($\pm$)	0.01	0.01	0.01	0.01	0.02	0.02	0.02	0.04	0.02

Table 4.4: Parameters and results of the experiment

is not centred, so that the parameter vector $(0, 0)$ is located at the position $(128, 0)$ in the images. Note that the signal two is shifted after it was scaled. Consequently, the translation must be multiplied by the shrinking factor in order to obtain the correct offset. (Cfg. experiment number seven: the signal two is shrunk by two and shifted by ten. Hence, the other signal must be shifted by -20 to be at the same position relative to the origin. Consequently, the position of the maximum is (nearly) correct, because $128-20+10 = 118$.)

The scaling parameter is obtained from formula (4.18) as in the previous chapter. The maximum is detected as the pixel with the highest value. According to this procedure we obtain an error for the shift parameter of ± 0.5 for all experiments. The error of the scale parameter can be found in the rows below the estimated scale parameters. Obviously, the results of workspace 4.19 are more exact than those of workspace 4.16. We suppose that numerical inaccuracies are the reason for the higher error rate. Note that the maximum error is a displacement of only one pixel in the correlation image.

So far we have only investigated if the parameter can be extracted correctly from the correlation function. The second interesting property of a correlation function is the height of the maximum which indicates whether the compared signal is similar to the pattern or not. In figure 4.21(a) on page 105 a new, quite different signal is represented. Due to the difference between this new signal and the signal in figure 4.17 the maximum of the correlation function is not as significant as the maximum of the auto correlation function. The difference is more obvious in the 3D–patches (figure 4.21(c) and (d)) than in the correlation images (figure 4.20(a) and 4.21(b)).

(a) Experiment no. 1 (b) Experiment no. 2 (c) Experiment no. 3

(d) Experiment no. 4 (e) Experiment no. 5 (f) Experiment no. 6

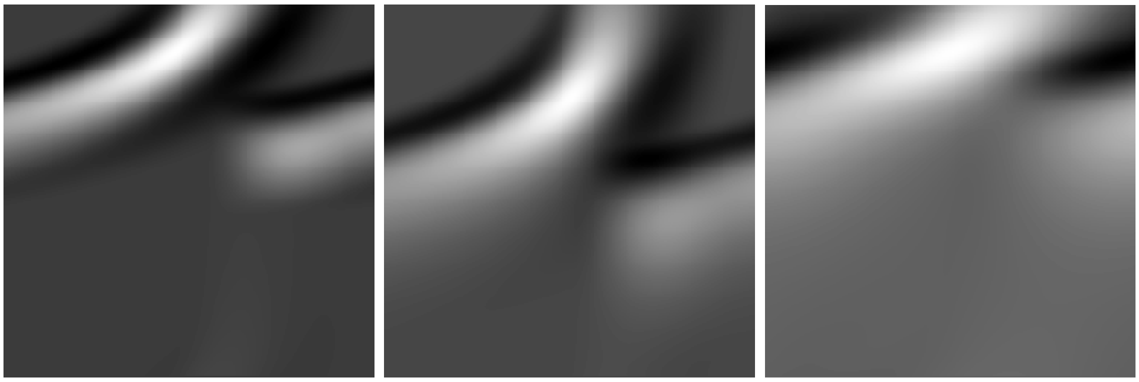

(g) Experiment no. 7 (h) Experiment no. 8 (i) Experiment no. 9

Figure 4.20: Correlation images corresponding to table 4.4

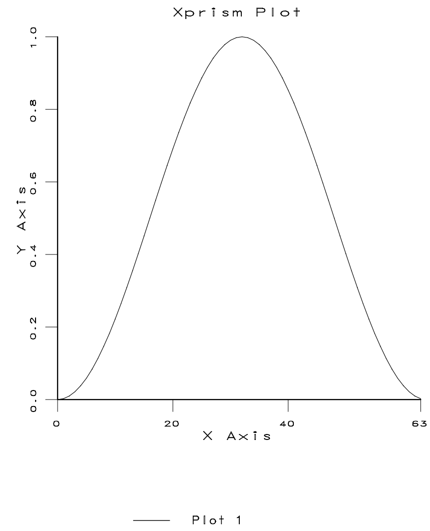

(a) New, different signal

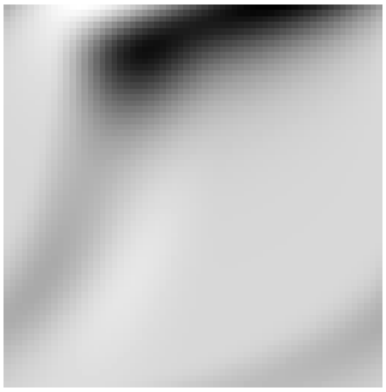

(b) Correlation image

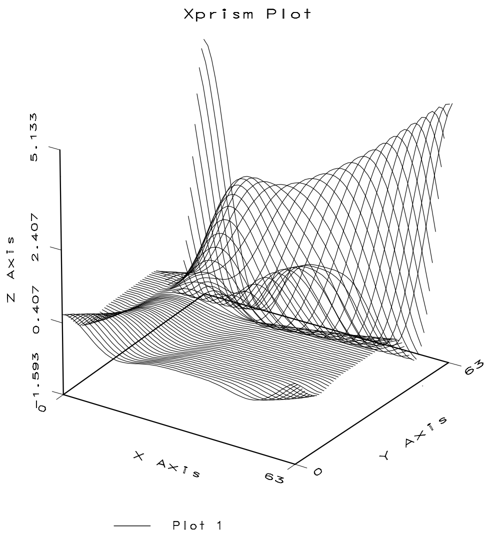

(c) Auto correlation patch of 4.17

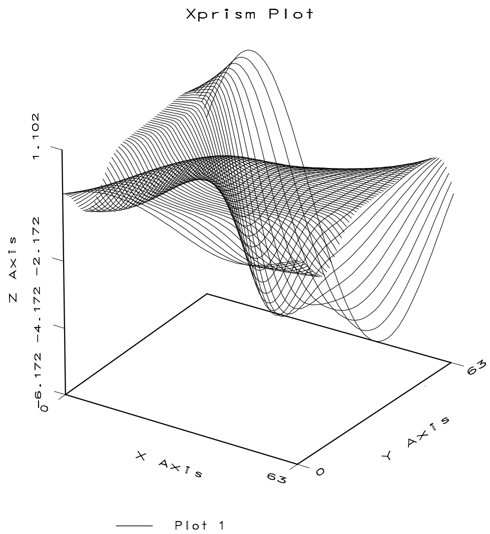

(d) Correlation patch

Figure 4.21: Experiments with a different signal

Chapter 5

Conclusion

In this chapter the results of the previous three chapters are reviewed, discussed, and further investigations are encouraged.

The most important result of the second chapter is the fact that the Clifford spectrum of a real signal can be calculated from its complex spectrum. This amazing fact implies that the Clifford spectrum is obtained nearly as fast as the complex one. Because of the possibility to calculate the spectrum of a Clifford valued signal in a component–wise fashion, no specific fast Clifford Fourier transform is needed. With regard to both, the computational complexity and the effort of programming, this method is superior to specific fast algorithms.

Nevertheless, it has been shown that quite fast specific algorithms can be developed. In addition, the correspondence between the Clifford spectrum and the HCA spectrum would not have been found if the commutative algebra was not needed for the derivation of the FCFTb, and without this commutative algebra the connection to the $\mathbb{C}^m$ would not have been found either. Consequently, it would not have been discovered, that the Clifford spectrum can be obtained from the complex spectrum.

The commutative algebra offers a lot of advantages: some frequently used theorems (shift theorem and convolution theorem) for the CFT can be formulated more easily in HCA. The isomorphism to the $\mathbb{C}^m$ gives rise to new possibilities of how to interpret and illustrate the spectrum. Future research will have to show if the Clifford algebra or the $\mathbb{C}^m$ is the better choice for an intrinsic multidimensional signal analysis. The representation of the spectrum in $\mathbb{C}^m$ has the advantage that the classical complex spectrum is contained in one of the components of the spectrum in $\mathbb{C}^m$ and, consequently, the latter spectrum is an extension in the form of a vector.

The concept of Lie algebras and canonical coordinates for estimating strong invariant integral transforms is a very powerful tool for spectral approaches. Though the concept is restricted to commutative groups it can be used in many practical applications. In combination with local methods, new possibilities arise which will be the target of further investigations.

The concept of cross correlation in the representation of canonical coordinates yields an efficient method for recognising distorted patterns and for reconstructing parameters. Conceptually speaking, this method cannot deal with non–commutative groups, however, an extension will certainly be found — for linear groups it is proposed in this thesis. The cross group correlation can also be applied locally.

The extension of the classical cross correlation to the cross group correlation including the corresponding correlation theorem seems to be a logical consequence. The signals which are to be processed are hardly ever distorted by mere translations. Consequently, the Lie algebra approach is the most powerful one, though it has not made use of the properties of the Clifford spectrum so far.

Nevertheless, all presented methods are formulated in terms of Clifford Fourier transforms because this is the representation which should be used for multidimensional signal processing in future. Furthermore, there might be opportunities when only Clifford spectra can be used.

Consider, for example, the two–dimensional case: if each spectral value (which is a quaternion) is identified with a rotation, three rotation angles can be extracted. Two angles correspond to the first two phases; the third angle yields a new phase [Bül98]. This third phase is zero if the spectra of two shifted versions of the same signal are multiplied; and it is not zero if the signals are different. Unfortunately, the third phase highly depends on the noise, so this feature has not been used for signal comparison so far. However, different applications will possibly be found in future.

Probably, connections between Clifford spectra and canonical coordinates will be found during the investigation of Gabor–filters in canonical coordinates. Gabor–filters are more powerful in Clifford algebras which has been shown by T. Bülow in his PhD Thesis [Bül98]. Hence, local approaches might profit from the Clifford representation.

Last but not least, an investigation of filters with specific symmetries in the frequency domain (representation in $\mathbb{C}^m$) will also be very interesting. However, the idea of a direct coherence between Clifford spectra and the geometric product becomes rather improbable: the non–commutativity of CA is not used in the spectra of real signals.

All these considerations are meant to be suggestions for future research within the rapidly evolving domain of computer vision and multi–dimensional signal processing.

Bibliography

[BHW92] Burg, Haf, and Wille. *Höhere Mathematik für Ingenieure, Band I Analysis*, chapter 7, page 571. Teubner Stuttgart, 1992.

[Bül98] T. Bülow. *Global and Local Hypercomplex Spectral Signal Representations for Image Processing and Analysis*. PhD thesis, Christian–Albrechts–University of Kiel, 1998.

[Bra86] R. N. Bracewell. *The Fourier transform and its applications*. McGraw Hill, 1986.

[BS97a] T. Bülow and G. Sommer. Algebraically Extended Representation of Multi–Dimensional Signals. In *Proceedings of the 10th Scandinavian Conference on Image Analysis*, pages 559–566, 1997.

[BS97b] T. Bülow and G. Sommer. Multi–Dimensional Signal Processing Using an Algebraically Extended Signal Representation. In *Proceedings of the AFPAC Workshop*, pages 148–163, 1997.

[CDD94] Q. Chen, M. Defrise, and F. Deconinck. Symmetric Phase–Only Matched Filtering of Fourier–Mellin Transforms for Image Registration and Recognition. *Transactions on Pattern Analysis and Machine Intelligence*, 16(12):1156–1168, December 1994.

[Che95] V. M. Chernov. Discrete orthogonal transforms with data representation in composition algebras. In *Proceedings of the 9th Scandinavian Conference on Image Analysis*, pages 357–364, 1995.

[CP97] M. A. Chichyeva and M. V. Pershina. On Various Schemes of 2D–DFT Decomposition with Data Representation in the Quaternion Algebra. *Image Processing & Communications*, 2(1):13–20, 1997.

[Dav96] Clyde M. Davenport. A Commutative Hypercomplex Algebra with Associated Function Theory. In R. Ablamowicz, editor, *Clifford Algebras with Numeric and Symbolic Computations*, pages 213–227. Birkhäuser Bosten, 1996.

[Ell92] T. A. Ell. *Hypercomplex Spectral Transformations.* PhD thesis, University of Minnesota, 1992.

[FC94] M. Ferraro and T. M. Caelli. Lie transformation groups, integral transforms, and invariant pattern recognition. *Spatial Vision*, 8(4):33–44, 1994.

[Fel97] M. Felsberg. Fast Quaternion Fourier Transform. Student project, Christian–Albrechts–University of Kiel, 1997.

[Gil74] R. Gilmore. *Lie Groups, Lie Algebras and Some of Their Applications.* John Wiley & Sons New York, 1974.

[GM91] J. E. Gilbert and M. A. M. Murray. *Clifford algebras and Dirac operators in harmonic analysis.* Cambridge University Press, 1991.

[GMPO95] L. van Gool, T. Moons, E. Pauwels, and A. Oosterlinck. Vision and Lie's approach to invariance. *Image and Vision Computing*, 13(4):259–277, May 1995.

[HG84] J. L. Horner and P. D. Gianino. Phase–only matched filtering. *Applied Optics*, 23(6):812–816, 15 March 1984.

[KP85] T. Koh and E. Powers. Second–Order Volterra Filtering and Its Application to Nonlinear System Identification. *IEEE Transactions on Acoustics, Speech, and Signal Processing*, 33(6):1445–1455, December 1985.

[KZ96] G. Krieger and C. Zetzsche. Nonlinear Image Operators for the Evaluation of Local Intrinsic Dimensionality. *IEEE Transactions on Image Processing*, 5(6):1026–1041, June 1996.

[MS94] M. Michaelis and G. Sommer. A Lie group approach to steerable filters. Technical Report 9415, Institute of Computer Science and Applied Mathematics, Christian–Albrechts–University of Kiel, September 1994.

[Nee91] J. Hilgert & K.-H. Neeb. *Lie–Gruppen und Lie–Algebren.* Vieweg Verlag Braunschweig, 1991.

[Olv86] P. J. Olver. *Application of Lie–Groups to Differential Equations.* Springer Verlag, New York, 1986.

[Por95] I. R. Porteous. *Clifford Algebras and the Classical Groups.* Cambridge University Press, 1995.

[RSZ91] J. Rubinstein, J. Segman, and Y. Y. Zeevi. Recognition of Distorted Patterns by Invariance Kernels. *Pattern Recognition*, 24(10):959–967, 1991.

[San96] S. J. Sangwine. Fourier–Transforms of Color Images using Quaternion of Hypercomplex, Numbers. *Electronic Letters*, 32(21):1979–1980, October 1996.

[Sol89] I. L. Kantor & A. S. Solodovnikov. *Hypercomplex Numbers.* Springer Verlag, New–York, 1989.

[SRZ92] J. Segman, J. Rubinstein, and Y. Y. Zeevi. The Canonical Coordinates Method for Pattern Deformation: Theoretical and Computational Considerations. *IEEE Transactions on Pattern Analysis and Machine Intelligence*, 14(12):1171–1183, December 1992.

[SZ93] J. Segman and Y. Y. Zeevi. Image Analysis by Wavelet–Type Transforms: Group Theoretic Approach. *Journal of Mathematical Imaging and Vision*, 3:51–77, 1993.

[TP91] M. Turk and A. Pentland. Eigenfaces for Recognition. *Journal of Cognitive Neuroscience*, 3(1):71–86, 1991.